Light-controlled bacteria-surface and bacteria-bacteria adhesions

Dissertation

Zur Erlangung des Grades

Doktor der Naturwissenschaften

Chemie, Pharmazie, Geographie und Geowissenschaften (FB 09)

der Johannes Gutenberg-Universität Mainz

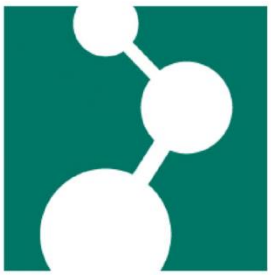

vorgelegt von

Fei Chen

geboren in Hubei, P.R. China

Mainz, 2019

The thesis was carried out from March 2016 until July 2019 at the Max Planck Institute for Polymer Research, Mainz.

Dekan:

Prodekan:

Gutachter 1:

Gutachter 2:

Date of oral examination: 23.08.2019

Affidavit

I hereby declare that I wrote the dissertation submitted without any unauthorized external assistance and used only sources acknowledged in the work. All textual passages which are appropriated verbatim or paraphrased from published and unpublished texts as well as all information obtained from oral sources are duly indicated and listed in accordance with bibliographical rules. In carrying out this research, I complied with the rules of standard scientific practice as formulated in the statutes of Johannes Gutenberg-University Mainz to insure standard scientific practice.

Fei Chen

"Insight must precede application."

- Max Planck

Publications

1. **Chen, F.**; Wegner, S. V., Photoswitchable bacteria-bacteria adhesions enable the control of multicellular bacterial communities by using blue light. *ACS Synthetic Biology* **2020**, *9 (5)*, 1169-1180.

2. **Chen, F.**; Ricken, J.; Xu, D.; Wegner, S. V., Bacterial Photolithography: Patterning Escherichia coli Biofilms with High Spatial Control Using Photocleavable Adhesion Molecules. *Advanced Biosystems* **2019,** *3* (3), 1800269.

3. **Chen, F.**; Wegner, S. V., Implementation of Blue Light Switchable Bacterial Adhesion for Design of Biofilms. *Bio-protocol* **2018,** *8* (12), e2893.

4. **Chen, F.**; Wegner, S. V., Blue Light Switchable Bacterial Adhesion as a Key Step toward the Design of Biofilms. *ACS Synthetic Biology* **2017,** *6* (12), 2170-2174.

5. Xu, D.; Bartelt, S. M.; Rasoulinejad, S.; **Chen, F.**; Wegner, S. V., Green light lithography: a general strategy to create active protein and cell micropatterns. *Materials Horizons* **2019**, DOI: 10.1039/C9MH00170K.

Contents

Abstract

In bacterial biofilms, collective functions arise from the social interactions and spatial organization of bacteria. Controlling bacterial adhesion as key steps in biofilm formation with high spatial and temporal precision is essential for controlling the formation, organization and microstructure of biofilms. Light as a trigger provides unique advantages to dynamically manipulate bacterial interactions, including high spatiotemporal resolution and non-invasive, biocompatible and tunability remote control.

In this thesis, different methods to control bacterial adhesions using light have been developed to control biofilm formation with high spatiotemporal precision and to study how the spatial organization of bacteria influences their collective functions. In chapter 2, I developed a method named bacterial photolithography that allows photopatterning biofilms with complicated geometries. In bacterial lithography, α-D-mannoside, which is recognized by the FimH surface receptor *of Escherichia coli* (*E.coli*), was linked to a non-adhesive poly(ethylene glycol) (PEG) surface through a photocleavable 2-nitrobenzyl linker. When a pattern of UV light in a desired shape was projected onto these surfaces, the light-exposed areas become non-adhesive and bacteria only adhered to the unexposed areas in the photopattern. This approach enabled bacterial patterning with high spatial resolution down to 10 μm without mechanical interference and the investigation of how microscale spatial organization affects collective bacterial interactions such as quorum sensing.

In the following chapters photoswitchable proteins were used to control bacterial adhesions in an optogenetic approach. In particular, the protein pair nMag and pMag, which heterodimerizes under blue light and dissociates from each other in the dark were used as optogenetic building blocks. In chapter 3, I engineered bacteria to adhere specifically to substrates with high spatiotemporal control under blue light, but not in the dark, by using the nMag and pMag proteins as adhesins. For this, I expressed pMag proteins on the surface of *E.coli* so that these bacteria adhered to substrates with immobilized nMag protein under blue light. These adhesions were reversible in the dark and could be repeatedly turned on and off.

Further, the number of bacteria that adhered to the substrate as well as their attachment and detachment kinetics were adjustable by using different point mutants of pMag and altering light intensities. Overall, this approach overcomes the problem of using UV light for photoregulation and chemically modifying the bacteria surface.

Multi-bacterial communities are of fundamental importance and have great biotechnological potentials. However, controlling the assembly and organization of multicellular structures and therefore their function remains challenging. In chapter 4, I developed the first photoswitchable bacteria-bacteria adhesions and used these to regulate multicellularity and associated bacterial behavior. For this purpose, the proteins nMag and pMag were expressed on bacterial surfaces as adhesins. This allowed to trigger the assembly of multicellular clusters under blue light and reversibly disassemble them in the dark. These photoswitchable adhesions made it possible to regulate collective bacterial functions using light including aggregation, quorum sensing, biofilm formation and metabolic cross-feeding between auxotrophic bacteria.

In a summary, light-responsive bacteria-surface and bacteria-bacteria adhesions allow controlling them with high spatiotemporal precision. While in a chemical approach bacterial lithography was used to pattern stable biofilms through irreversible light response, the photoswitchable proteins implemented in an optogenetic approach provide reversible and dynamic control over bacterial adhesions. All these tools open new possibilities for engineering multicellular communities, understand fundamental bacterial behavior in biofilms and design biofilms with new functions for biotechnological applications.

Zusammenfassung

In bakteriellen Biofilmen entstehen kollektive Funktionen durch soziale Interaktionen und räumliche Organisation von Bakterien. Die Kontrolle der Bakterienadhäsion als Schlüsselschritte bei der Bildung von Biofilmen mit hoher räumlicher und zeitlicher Präzision ist für die Kontrolle der Bildung, Organisation und Mikrostruktur von Biofilmen unerlässlich. Licht als Auslöser bietet einzigartige Vorteile für die dynamische Manipulation bakterieller Interaktionen, einschließlich einer hohen räumlich-zeitlichen Auflösung und einer nicht-invasiven, biokompatiblen und abstimmbaren Fernbedienung.

In dieser Arbeit wurden verschiedene Methoden zur Kontrolle von Bakterienadhäsionen unter Verwendung von Licht entwickelt, um die Bildung von Biofilmen mit hoher räumlich-zeitlicher Präzision zu kontrollieren und zu untersuchen, wie die räumliche Organisation von Bakterien ihre kollektiven Funktionen beeinflusst. In Kapitel 2 habe ich eine Methode der bakteriellen Fotolithografie entwickelt, mit der Biofilme mit komplizierten Geometrien fotostrukturiert werden können. In der Bakterienlithographie wurde α-D-Mannoside, das vom FimH-Oberflächenrezeptor von Escherichia coli (*E. coli*) erkannt wird, über einen photospaltbaren 2-Nitrobenzyl-Linker an eine nichtklebende Polyethylenglykol (PEG) - Oberfläche gebunden. Wenn ein Muster von UV-Licht in einer gewünschten Form auf diese Oberflächen projiziert wurde, werden die belichteten Bereiche nicht-haftend und Bakterien haften nur an den unbelichteten Bereichen in dem Fotomuster. Dieser Ansatz ermöglichte die Strukturierung von Bakterien mit einer hohen räumlichen Auflösung von bis zu 10 µm ohne mechanische Interferenz und die Untersuchung, wie sich die mikroskalige räumliche Organisation auf kollektive bakterielle Interaktionen wie Quorum Sensing auswirkt.

In den folgenden Kapiteln wurden photoschaltbare Proteine verwendet, um bakterielle Adhäsionen in einem optogenetischen Ansatz zu kontrollieren. Als optogenetische Bausteine dienten insbesondere das unter Blaulicht heterodimerisierende und im Dunkeln voneinander dissoziierende Proteinpaar nMag und pMag. In Kapitel 3 habe ich Bakterien so konstruiert, dass sie spezifisch an Substraten mit hoher räumlicher und zeitlicher Kontrolle unter blauem Licht, jedoch nicht im Dunkeln, haften, indem ich die nMag- und pMag-Proteine als Adhäsine verwendete. Dazu habe ich pMag-Proteine auf der Oberfläche von *E. coli*

exprimiert, so dass diese Bakterien mit immobilisiertem nMag-Protein unter blauem Licht an Substraten hafteten. Diese Adhäsionen waren im Dunkeln reversibel und konnten wiederholt ein- und ausgeschaltet werden. Die Anzahl der Bakterien, die an dem Substrat anhafteten, sowie ihre Anheftungs- und Ablösekinetik waren durch Verwendung verschiedener Punktmutanten von pMag und durch Veränderung der Lichtintensität einstellbar. Insgesamt überwindet dieser Ansatz das Problem der Verwendung von UV-Licht zur Photoregulierung und chemischen Modifizierung der Bakterienoberfläche.

Multibakterielle Gemeinschaften sind von grundlegender Bedeutung und verfügen über ein großes biotechnologisches Potenzial. Die Kontrolle des Aufbaus und der Organisation mehrzelliger Strukturen und damit ihrer Funktion bleibt jedoch eine Herausforderung. In Kapitel 4 habe ich die ersten photoschaltbaren Bakterien-Bakterien-Adhäsionen entwickelt und diese verwendet, um die Mehrzelligkeit und das damit verbundene Bakterienverhalten zu regulieren. Zu diesem Zweck wurden die Proteine nMag und pMag als Adhäsine auf Bakterienoberflächen exprimiert. Dies ermöglichte es, die Anordnung von mehrzelligen Clustern unter blauem Licht auszulösen und diese im Dunkeln reversibel zu zerlegen. Diese photoschaltbaren Adhäsionen ermöglichten die Regulierung kollektiver Bakterienfunktionen unter Verwendung von Licht, einschließlich Aggregation, Quorum Sensing, Biofilmbildung und metabolischer Kreuzfütterung zwischen auxotrophen Bakterien.

Zusammenfassend lässt sich sagen, dass lichtempfindliche Bakterienoberflächen- und Bakterien-Bakterien-Adhäsionen es ermöglichen, sie mit hoher räumlich-zeitlicher Präzision zu kontrollieren. Während in einem chemischen Ansatz Bakterienlithographie verwendet wurde, um stabile Biofilme durch irreversible Lichtantwort zu strukturieren, stellen die in einem optogenetischen Ansatz implementierten photoschaltbaren Proteine eine reversible und dynamische Kontrolle über Bakterienadhäsionen bereit. Alle diese Werkzeuge eröffnen neue Möglichkeiten für die Entwicklung von mehrzelligen Gemeinschaften, das Verständnis des grundlegenden Bakterienverhaltens in Biofilmen und das Design von Biofilmen mit neuen Funktionen für biotechnologische Anwendungen.

Chapter 1. Introduction

1.1 Bacterial biofilms

Bacteria in nature usually do not only exist as free-floating cells but predominantly live in a biofilm.[1] From bacteria's point of view, they are exposed to environments with rapid and frequent changes. The biofilm is a survival strategy of bacteria to stabilize the local environment of cells and overcome the stresses in adverse conditions.

The discovery of biofilms dates back to the year 1684 when Antonie Van Leeuwenhoek, the inventor of the microscope, first observed the accumulation of microorganism (now known as biofilms) in dental plaque from his own teeth.[2] Actually, biofilms are omnipresent, not just on teeth. However, it was not until the late decades of the 20th century that the study of biofilms began to be a serious and important scientific topic. With the help of developed technology such as molecular biology and electron microscopy, scientists could effectively study microbial communities and began to understand the significance of biofilms. Bill Costerton is recognized as the founding father of the field of biofilms for the pioneered development of the biofilm theory.[3] In 1978, he stated that most bacteria grew in a glycocalyx-enclosed biofilm that adhered to surfaces or to other cells and that these sessile bacterial populations become predominant in natural, industrial and medical ecosystems.[4] Moreover, the cells in biofilms are physiologically different from the free-floating planktonic cells.

Biofilms are defined as "aggregates of microorganisms in which cells are frequently embedded in a self-produced matrix of extracellular polymeric substances (EPS) that are adherent to each other and/or a surface".[6] EPS are a complex mixture of polysaccharides, proteins, lipid and extracellular DNA secreted by bacteria and occupy both periphery of the biofilm and the interior space between the bacteria aggregates.[7] In an analogy if the biofilm is called a "city of microbes",[8] EPS would be the "house of biofilm cells",[9] providing structural stability, mechanical strength, cohesion and adhesion, and other biological functions as a highly hydrated gel matrix.[7, 9, 10] In biofilms, bacteria interact as a coordinated functional community in order to share nutrients and resist environmental stress such as antibiotics.[11]

Biofilms can form on different surfaces including living tissues, implanted medical devices, and industrial water systems. The variable nature of biofilms can be shown by fluorescence microscopy images of biofilms on a surface in a water system (**Figure 1.1**).[5]

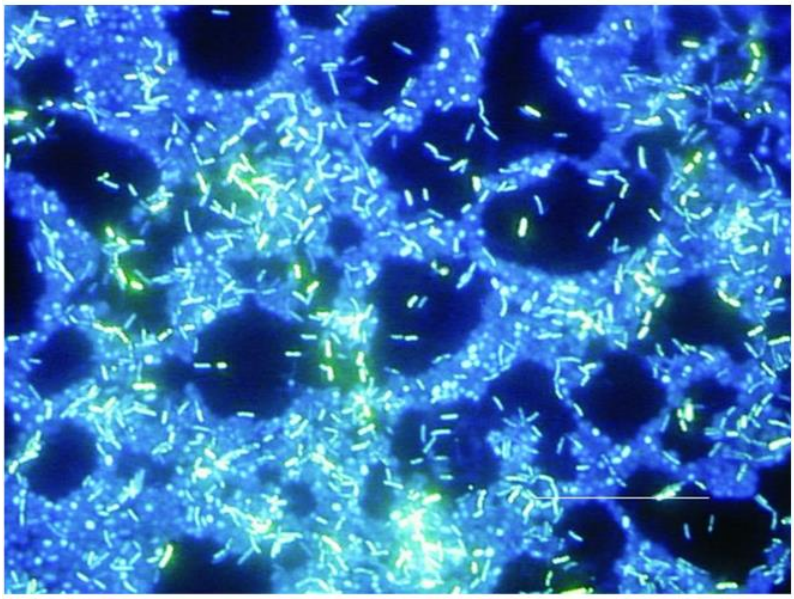

Figure 1.1 Fluorescence microscopy images of biofilms on a stainless steel surface in a laboratory potable water system. Bacteria were stained with 4, 6-diamidino-2-phenylindole (DAPI).[5] Scale bar is 20 μm. Adapted with permission from Ref. 5. Copyright 2002 Emerging Infectious Diseases journal.

1.1.1 The impact of biofilms: Detrimental and beneficial aspects

In 1978 Bill Costerton proposed the biofilm theory and reported that chronic infections in patients with implanted medical devices were caused by bacterial biofilm formation and bacteria within biofilms were resistant to antibiotic therapies and immune host defenses. Since then there was an increasing awareness of the importance of biofilms study. A better understanding of their specific properties will enable the development of effective strategies for treatment.[12] The National Institutes of Health (NIH) estimates that 80% of infectious diseases worldwide are caused by biofilms.[13] Biofilms cause severe infections in hospitalized patients. In the United States, nosocomial (hospital-acquired) infections are reported to be the leading cause of death with 1.7 million cases annually, leading to extra costs of up to $4.5

billion each year.[14, 15] The formation of biofilms on medical devices, such as indwelling catheters and wound dressings,[16] is the major reason for these infections. Biofilms are also likely to form on many household surfaces such as toilets, fridges, sinks, and kitchen. Formation of the pathogenic biofilms in the household environment increases the incidence of illnesses. It is usually difficult to get rid of the infections associated with the biofilm. The reason for this is mostly because mature biofilms are resistant to antibiotics and the host immune response. Within biofilms, bacteria are up to 1000-fold more tolerant to antibacterial agents than the same cells in the planktonic form. Therefore, the treatment of infectious diseases with currently available antibiotics cannot work effectively due to the interference from the biofilm formation.

Biofilms are also the reasons for contamination, corrosion and biofouling in industry, especially the food-processing and water-based process. In the food industry, biofilms have become problematic due to the ability to form on plants and during industrial processes of food production. Biofilm formation on the food product or the product contact surfaces leads to serious food safety problems.[17] Moreover, biofilms cause over a billion dollars' worth of damage every year in industrial settings, affecting companies' abilities to manufacture their products efficiently. They can affect installations and equipment in the industrial landscape, causing corrosion, bio-deterioration, energy loss, reduced heat transfer and product contamination.[18]

However, biofilms can also be used for beneficial purposes. For example, biofilms are widely used in the treatment of drinking water and wastewater.[19] In the natural environment, biofilms play an important role in the breakdown of organic wastes by adsorbing waste from water and removing or neutralizing contaminants in soil. As a result, biofilms are used to purify water in water treatment plants and to detoxify contaminated areas of the environment. Biofilms have been used successfully in water and wastewater treatment for over a century. The water-cleaning systems were developed by taking advantages of natural biofilm environmental activity and the first sand filter treatment methods for both water and wastewater were developed in the 1860s. In these filtration systems, the surfaces of the filter

media act as a support for biofilms formation and the organic matter in the water is used by biofilms as a carbon source. Biofilm-treated water requires less disinfectant and therefore fewer disinfection byproducts form.[7]

The applications of microbial communities are greatly expanded due to the improved understanding of natural microbial ecosystems and the development of new tools to construct synthetic bacterial consortia. The synthetic biologists have developed engineered microbial consortia for diverse applications, such as the bioproduction of drugs and other valuable compounds.[20] For example, *E. coli* and *S. cerevisiae* in a consortium can be used to produce precursors of the anti-cancer drug paclitaxel. In this consortium, *E. coli* are engineered to overproduce taxadiene, the scaffold molecule of paclitaxel, while *S. cerevisiae* are used as a host for expressing cytochrome P450s (CYPs) to functionalize taxadiene through multiple oxidation reactions. Therefore, the coculture of these two engineered organisms is essential for the overall production of the drug.[21-23]

Due to the significant impacts of biofilm, there are increasing interests in the understanding of biofilm formation and developing approaches for biofilm control. The understanding of biofilm formation, structure and properties, communication and metabolic interactions will lead to the promotion of beneficial uses and controlling the harmful impacts.

1.1.2 Biofilm formation and development

Biofilms formation on the surfaces and their development can be divided into five stages (**Figure 1.2**). These are (1) initial attachment of free-floating planktonic bacteria to a surface, (2) irreversible attachment, (3) initial maturation, (4) maturation of biofilm architecture, (5) dispersion.[3] In the stage of dispersion, detached cells return to the planktonic mode of growth, thus closing the life cycle of biofilm development.

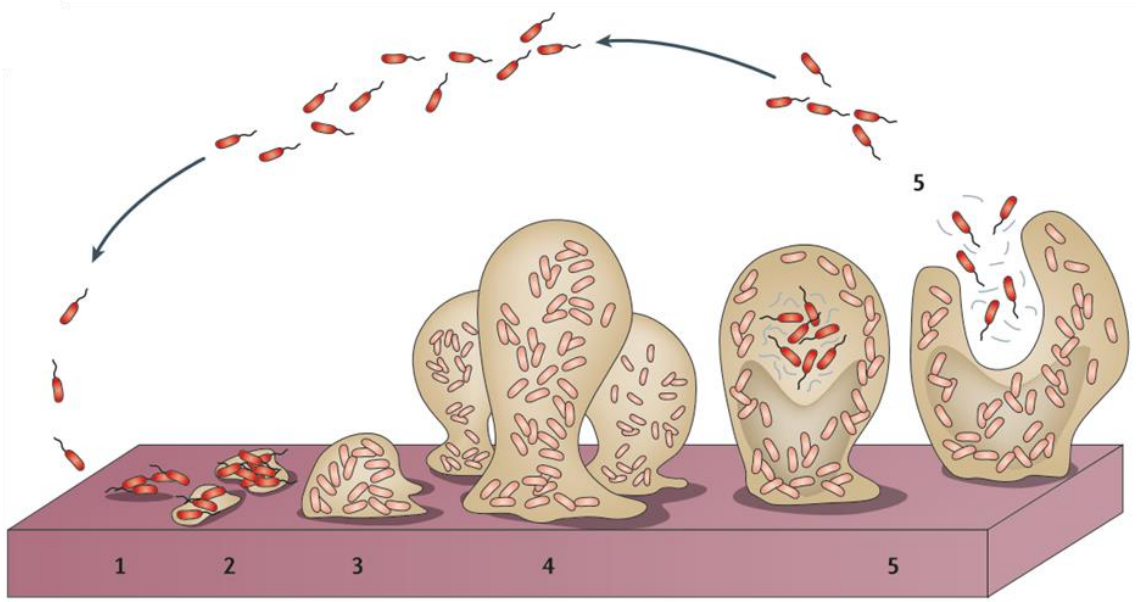

Figure 1.2 The schematic shows a conceptual model of biofilm formation as a five-stage developmental process. Stage 1: initial attachment. Stage 2: irreversible attachment. Stage 3: initial maturation. Stage 4: maturation. Stage 5: dispersion.[3] Adapted with permission from Ref. 3. Copyright 2014 Springer Nature.

Initial attachment. Biofilm formation begins with the initial attachment of free-floating planktonic bacteria to a surface, which is usually based on physical attachments including hydrogen bonds, hydrophobic interactions, *van der Waals* forces, and electrostatic interactions.[24] The individual adherent cells on a surface are capable of independent movement such as twitching or gliding which is mediated by pilus. Many of these adherent cells may actually detach from the surface and return to the planktonic lifestyle if perturbed by hydrodynamic forces, repulsive forces or in response to nutrient availability.[25-27] Therefore, the initial attachment is reversible.

Irreversible attachment. After initial attachment to a surface, bacteria must maintain the adhesion and grow in order to develop a mature biofilm. They begin to secret exopolysaccharide, form cell groups and adhere irreversibly. This transition from reversible to irreversible attachment was firstly reported by Zobel in 1943. The presence of extracellular matrix improves the interaction of the cells with the surface and induces a permanent cell-surface bonding. The formation of cell aggregates and microcolonies has also been suggested

as the mechanism for inducing irreversible and permanent attachment at a surface. In this stage, rapid colonization at a new site on the surface is possible due to the bacterial twitching motility, which is mediated by type IV pili located on the cell surface and used for propelling bacteria across a surface.[28, 29] O'Toole *et al.* suggested that the formation of microcolonies by bacteria interactions at a surface helps to strengthen the attachment.[30] Gerke *et al.* showed that the formation of microcolonies was induced by a polysaccharide intercellular adhesin which was produced by the adherent cells to bond the cells together.[31]

Maturation. In the maturation stages, many porous layers and water channels through the biofilm are developed for cells to access essential nutrients.[32] Many cells alter their physiological processes and gene expression in response to conditions in their particular surrounding such as surface contact triggers.[33] The secretion of EPS is stimulated by the chemical communication between cells and the best-characterized cell-to-cell communication system is quorum sensing (QS). QS also regulates bacteria behavior and cellular functions such as motility, which in turn could have an impact on biofilm structure. As cells replicate and the EPS accumulates, biofilms develop into three dimensional (3D) structures which are supported by EPS, allowing the transport of nutrients and removal of wastes. Additional studies showed that cellulose, polyglucosamine (PGA) and colanic acid contribute to biofilm architecture.[34, 35]

Dispersion. In the final stage of biofilm development, bacterial cells may detach from the biofilm colony and return to the environment, which enables the spreading and colonization at new sites. Enzymes such as dispersin B can degrade the biofilm extracellular matrix and release the cells from the mature biofilm.[36] The possible reasons for the biofilm dispersion are the limited nutrients present at the original sites or the physical effects such as fluid shear force.[37] The detached bacterial cells may adhere to a new surface with a plenty of nutrients and grow into a new biofilm. Overall, biofilm dispersion plays an important role in the self-renewal of bacterial communities and is an essential process for the biofilm life cycle.

1.1.3 Structure and property

Mature biofilms have complex structures with defined architectures that provide the essential living conditions for cells. Many porous layers with water channels exist in biofilms, allowing the cells in the entre of the colony to access nutrients and remove the wastes. The structures of water channels act as a circulatory system for the delivery of nutrients and wastes by diffusion and contribute to the development of biofilms.[38, 39]

EPS are considered as the primary matrix material of biofilms and the key determinant for the material properties of biofilms. The production of EPS is affected by the nutrients supply and bacterial growth. The EPS synthesis is improved when there are excess available carbon and limited nitrogen, potassium, or phosphate. EPS production can also be enhanced when bacterial growth is very slow. The physicochemical properties of EPS may vary in different biofilms but the primary components of EPS are polysaccharides. Some gram-positive bacteria such as the *staphylococci* have the cationic EPS polysaccharides. While for gram-negative bacteria, these EPS polysaccharides are primarily neutral or polyanionic. Additionally, EPS have the ability to incorporate water into the biofilm structure via hydrogen bonding due to that EPS are highly hydrated. It appears that the EPS determine b the structure and thereby cohesive strength of biofilms. The backbone structures of biofilms that contain 1, 3 - or 1, 4 - β - linked hexose residues are more rigid, less deformable and insoluble. Furthermore, EPS act as a protection to the bacterial cells living in biofilms. It has be reported protective EPS (alginate) can protect mucoid *P. aeruginosa* FRD1 biofilm cells from exposure to ultraviolet radiation.[40] EPS may also contribute to the antimicrobial resistance properties of biofilms by preventing the transfer of antibiotics through the biofilm.[41]

The structure of biofilms are also affected by the environmental factors. In an aqueous environment, shear forces from the passage of fluid over the biofilms shape the microcolonies into different morphologies within biofilms.[42, 43]

1.1.4 Quorum sensing

Cell-to-cell communication is a main ingredient of biofilm formation. Bacteria within biofilms interact with each other and function as a group for coordinated activities. Bacteria that have aggregated into biofilms can chemically communicate through quorum sensing, which was first reported and described in *Vibrio fischeri* (the marine bioluminescent bacteria) Bacteria have the ability called quorum sensing to detect the changes of cell population density and alter the gene regulation accordingly.[41, 44]

Bacteria can produce and release chemical signal molecules called autoinducers that increase in concentration as a function of cell density. The detection of a minimal threshold stimulatory concentration of an autoinducer leads to an alteration in gene expression (**Figure 1.3**). For example, the expression of genes for antibiotic resistance at high cell densities is activated through quorum sensing, providing protection for bacteria within biofilms.[45, 46] The high cell concentrations in biofilms enclosed in a matrix allows for quorum sensing even in small microcolonies as the signaling compounds are be concentrated within the microcolonies and are not degraded. Quorum sensing also plays an important role in the regulation of metabolic interaction in biofilms and influences community structure by enhancing encouraging the growth of beneficial species and inhibiting the growth of competitors.[47] The functions that can be regulated by quorum sensing include bioluminescence, nitrogen fixation and sporulation.[48, 49]

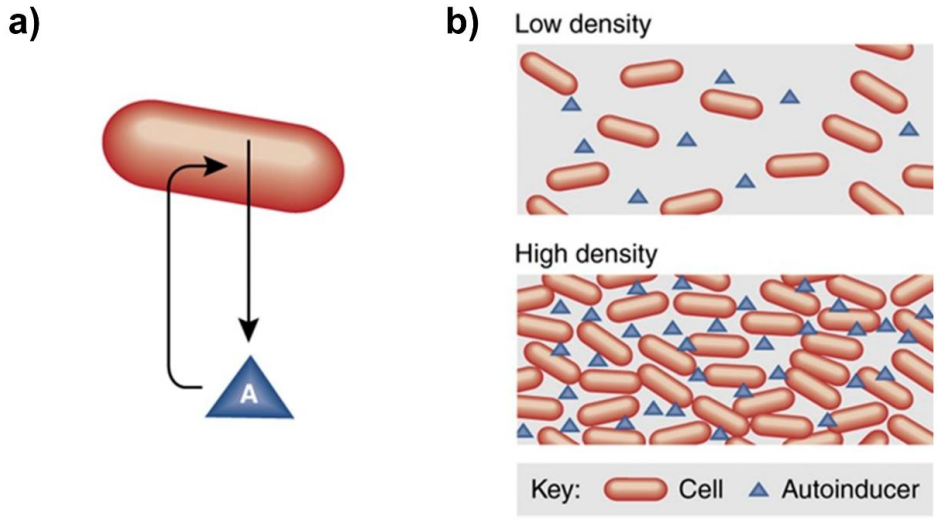

Figure 1.3 Schematic illustration of quorum sensing. **a**) Bacterial cell has the ability to produce a signaling molecule called autoinducer and sense its extracellular concentration. b). Quorum sensing is dependent on cell density.[46] Adapted with permission from Ref. 46. Copyright 2011 EMBO Press.

1.1.5 Metabolic interactions

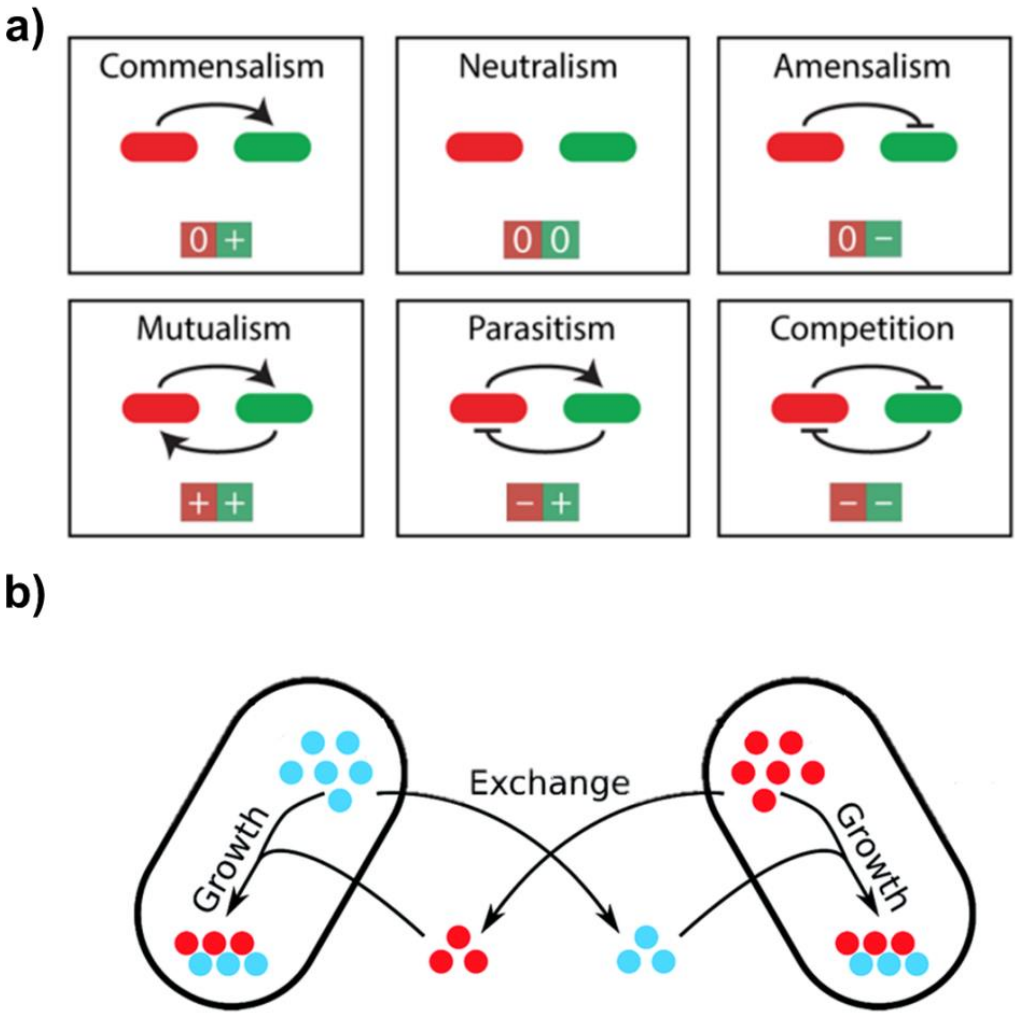

Figure 1.4 a) Six distinct types of social interactions in a two-species population.[50] Adapted with permission from Ref. 50. Copyright 2015 Springer Nature. b). Metabolic exchange between bacterial cells. Two bacteria require two metabolites (red and blue) for cell growths. Each organism is able to produce each metabolite. Metabolites are then used for both bacterial growth.[51] Adapted with permission from Ref. 51. Copyright 2018 The Royal Society of Chemistry.

Bacteria in nature usually do not exist in isolation but in complex ecosystems. In order to survive and proliferate in such complex consortia, bacteria have developed diverse social interactions with their neighboring species. The social interactions of bacteria significantly affect the dynamics and functionality of an entire community by altering the physiology, gene expression, survival of individual cells and enabling the collective behaviors of populations. These interactions can have three types of outcomes: a positive impact (win, +), a negative impact (loss, -) and no impact (neutral, 0) on the bacterial species involved.[52] For a simple ecosystem consisting of only two species, there are six possible distinct types of interaction through the possible combinations of the three outcomes, including neutralism (0, 0), commensalism (0, +), amensalism (0, -), competition (-, -), mutualism (+, +), and parasitism (-, +).[50] (**Figure 1.4a**)

Metabolic cross-feeding is one type of social interaction. Generally, there are two types of metabolic interactions: competition and cooperation. Due to the limited nutritional resources in most ecosystems, bacteria have to compete constantly for resources. The ability to compete for limiting nutrients can determine whether bacteria will be able to survive in a particular site.[53, 54] Besides the competitive metabolic interactions, cooperative metabolic interactions which allow bacteria to get benefits from each other through metabolic, are more common among bacterial species.[45, 55] Metabolic cross-feeding, also named syntrophy, is one type of cooperation in which bacteria exchange essential metabolites.[56] Cross-feeding is an important process that governs the growth and composition of microbial ecosystems.[57] Bacteria use metabolic exchanges as a strategy for group success[58] and under nutrient-poor conditions complement each other's biosynthetic capabilities.[59] Previous studies have characterized the behavior of microbes in co-culture with naturally complementary metabolism[60-62] where shared metabolites are hydrogen,[62] acetate,[61] amino acids,[63] fixed nitrogen and glucose.[64] For example, the presence of a bacterial species that actively produces beneficial molecules such as vitamins or amino acids allows both the producing bacteria and other species in the environment to use them and relaxes the metabolic burden on all species in the community.[51] (**Figure 1.4b**) Metabolic interactions are effected by the spatial structure of bacterial

community or biofilms, cost-effectiveness of biosynthesis, nutrients and diffusion.[65, 66] For example, bacterial aggregation or biofilm formation improves the efficiency of the metabolites exchange and stimulates the metabolic processes. [67]

These principles observed in natural biofilms have also been implemented into genetically engineered bacteria for biotechnological applications.[63, 68] For example, the introduction of genetic modifications into no-interacting bacterial cells could induce the persistent cooperation. Wenying Shou *et al.* constructed a synthetic synthetic cooperative system comprising a yeast pairs and each of them produce and offering the other strain an essential metabolite.[63] An example of parasitic interactions developed by Frederick *et al.*, constructed a synthetic predator-prey ecosystem consisting of two *E. coli* populations. The predator cells kill the prey by inducing expression of a killer protein in the prey, while the prey rescue the predators by eliciting expression of an antidote protein in the predator.[68] Therefore, understanding principles that govern biofilms are not just important from the standpoint of scientific understanding but also have direct implications in biotechnology.

1.2 Bacterial adhesion

1.2.1 Bacteria-surface adhesion

The biofilm formation begins from the adhesion of bacterial planktonic cells to the surface. Once a biofilm has formed, the bacteria are extremely resistant to treatment with antimicrobial agents and difficult to be removed. Therefore, controlling the initial bacterial adhesion to a surface is the most effective method to prevent the biofilm formation. Moreover, controllable bacterial adhesion allows bacterial cell patterning and engineered biofilm formation with the designed spatial organization, which are important for understanding social cell interactions and chemicals exchange within biofilms.

The bacterial adhesion can be affected by multiple factors such as bacterial surface structures, physiochemical properties of the substrate, and environmental conditions.[72]

The most important factors influencing bacteria adhesion include surface charge, hydrophobicity, topography or roughness, and the exposed functional groups.[73, 74]

In general, adhesion of bacteria is prevented on negatively charged surfaces, while it is promoted on positively charged surfaces.[75] This is because most bacteria are negatively charged on cell surfaces. Positively charged polymer surfaces have been reported to be bactericidal because the positive charge can disrupt the bacterial membrane potential or damage the membrane structure.[76, 77] Therefore, polycationic surfaces are often suggested to be efficient antibacterial coatings that bind and kill bacteria.[78]

Surface hydrophobicity is another major component that influences the bacteria–surface interaction. Hydrophobic interaction is one of the strongest noncovalent interactions in biological systems and plays a major role in bacterial adhesion to surfaces.[79] The bacterial adhesion is also affected by the hydrophobicity of the bacterial cells. Bacteria with a more hydrophobic cell surface preferentially attach to hydrophobic surfaces and vice versa.[80, 81]

Surface topography has also been found to substantially influence the interaction between bacteria and surfaces. Perera-Costa *et al.* investigated the effect of surface topography on bacterial adhesion by using the polydimethylsiloxane (PDMS) surfaces that contained microtopographic patterns in spatial organization.[82] This study showed a significant reduction in bacterial adhesion (30-45%) on microstructured surfaces compared to the control. Another important parameter for bacterial adhesion on the topographic surfaces is the spatial distribution of structures and patterns, which is relative to bacterial size and shape. It has been reported that surfaces with topographic features much smaller than bacterial cells inhibit bacterial attachment due to the decreased contact area between bacteria and surfaces.[83-85] On the contrary, for surfaces with topographic features that comparable with the bacterial size, more bacteria attach compared to smooth surfaces.[86] This is because that the microscopic structure on the surface tends to increase the overall surface roughness and therefore enhances the

adhesion of bacteria to substrates as more surface area is provided for bacterial attachment.[87, 88]

1.2.1.1 Controlling bacterial adhesion using surface chemistry

Surface modification with functional groups presents an important strategy for controlling bacterial adhesion and the formation of biofilms. For example, poly(ethylene glycol) (PEG) has been widely used for surface modification as anti-adhesive coatings cause it shows a great capacity to resist protein adsorption and cell adhesion.[89] However, adhesive surfaces with bio-specific binding properties and minimized background interferences are required for the fundamental study of bacterial cell-cell communication and biofilm formation.

1.2.1.1.1 Controlling bacterial adhesion by modifying the surface with native adhesion molecules

To construct an adhesive surface for bacteria with the ability to form a robust, specific, irreversible adhesions, native adhesive molecules have been used as exposed functional groups on surfaces. During the initial attachment in the first stage of biofilm formation, bacteria employ specific cell surface receptors, called adhesins, that bind to the substrate through specific receptor ligands for the irreversible attachment.[90, 91] Bacterial adhesins serve as anchors and act as specific surface recognition molecules, allowing the binding to specific receptor molecules on host cells or target surfaces.[92]

The best characterized bacterial adhesin is the FimH.[93] FimH is an α-D-mannoside specific lectin located at the tips of adhesive organelles, called type 1 fimbriae.[94] FimH lectin mediates binding to glycoproteins that have N-linked oligosaccharides presenting terminal mannose residues.[95] This specific FimH based adhesin–carbohydrate adhesion of bacteria to mannosylated surfaces has been used for many applications in the field of medicine. For example, carbohydrate microarrays have been used to detect pathogens and screen anti-adhesion therapeutics based on the carbohydrate binding specificities of bacteria.[96-99]

1.2.1.1.2 Controlling bacterial adhesion by engineering bacteria surface with adhesion molecules

An alternative powerful approach to control bacterial adhesion is to engineer the bacterial surface with new adhesion molecules. The ability to modify the surfaces of bacteria cells with non-native molecules is vital to engineer bacterial communication, biofilm formation and cell behavior in synthetic biology.

One effective strategy to add molecules to the bacterial cell membrane is called bacterial display, which uses genetic methods to fuse a protein or a peptide with a transmembrane protein. Sankaran *et al.* reported a novel method to control the specific, dynamic and reversible bacterial adhesion based on a supramolecular interaction between a peptide displayed on the bacterial surface and cucurbit[8]uril (CB[8]) They genetically modified *E. coli* such that a transmembrane protein displayed a CB[8]-binding motif at the bacterial surface. The binding of this motif to CB[8] and formation of intercellular complexes induce the bacterial aggregation within the solution in the presence of CB[8] and specific adhesion to CB[8] modified surfaces. Furthermore, these adhesions can be chemically reversed using an excess of CB[8] as a competitor.[100]

Another strategy is to introduce molecules to the bacterial cell surface through chemical ligation to membrane proteins or carbohydrates. For example, Elahipanah *et al.* introduced bio-orthogonal groups to engineer the surface of gram-negative bacteria cells by using a liposome fusion based method. These groups can subsequently be conjugated to a range of molecules for further studies on bacterial adhesion and controlling bacterial behavior.[101]

1.2.1.2 Controlling bacterial adhesion with light

Many stimuli-responsive methods have been proposed for the control of bacterial adhesion and for bacteria patterning. Among them, the light-responsive methods provide the highest spatial and temporal resolution, which is required to construct stable/viable biofilms with a high level of precision. This is particularly significant as the arrangement of bacteria with respect to each other at the micro scale defines the extent of their interaction in a biofilm as

described above. Additionally, light is a noninvasive trigger as it can be applied remotely without disturbing of other processes. In contrast, invasive triggers, such as chemicals, can have unpredictable side effects in the system by interacting with not only the targets but other biomolecules and do not provide the desired high spatiotemporal control. Moreover, it is easy to adjust the light intensity, illumination time and wavelengths to tune interactions and address different functionalities which respond to different colors of light independently. Therefore, the unique advantages of light make it particularly attractive as an external stimulus to regulate diverse biological processes.

1.2.1.2.1 Controlling bacterial adhesion by modifying surfaces with light responsive molecules

Azobenzene linkers, which undergo reversible *trans* to *cis* isomerization under UV light, have been used to reversible control bacterial adhesion to surfaces. Weber *et al.* showed that bacterial adhesion can be reversibly and photochemically controlled by functionalizing the surfaces with azobenzene linked α-D-mannoside (**Figure 1.5**). In this study, α-D-mannoside groups were attached on a gold surface through azobenzene linkers.[103] The photoisomerization of the azobenzene moiety under UV light allowed altering the presentation of the attached mannose, which was recognized by the receptor FimH on the bacterial surfaces and mediated the adhesion. Upon UV-light illumination (365 nm), the bacterial adhesion was blocked due to the *trans* to *cis* isomerization of azobenzene and could be reestablished upon blue light illumination.[104-106]

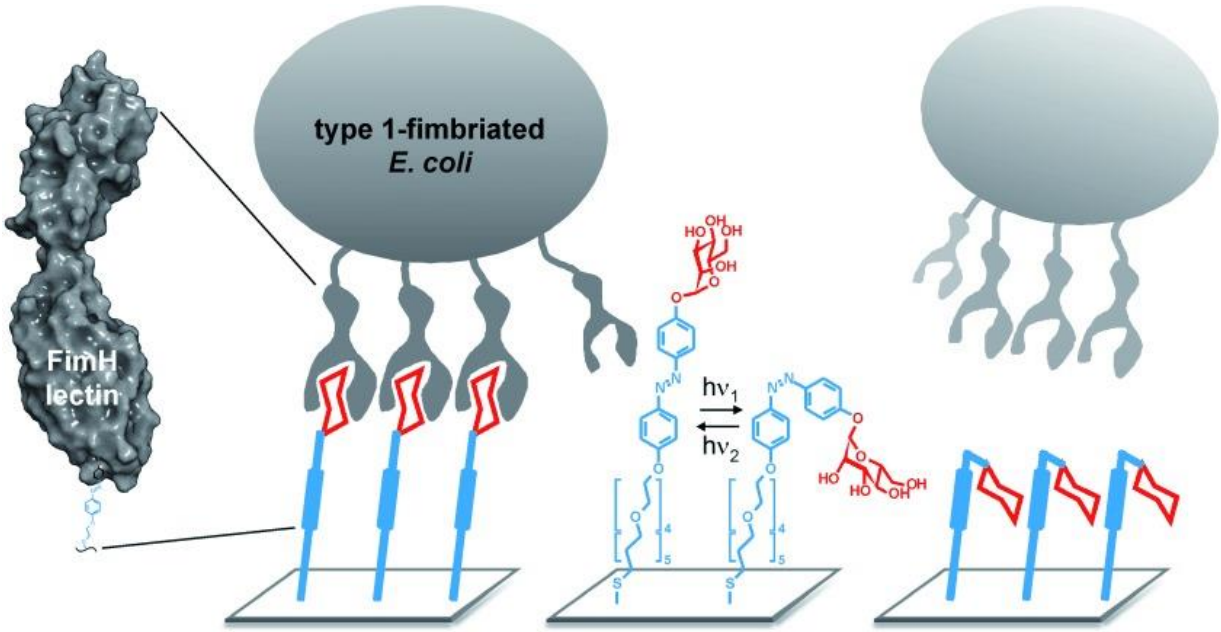

Figure 1.5 Photoswitchable adhesion of type 1 fimbriated *E. coli* cells to the surface immobilized with α-D-mannoside ligands via the azobenzene linkers.[101] Reproduced with permission from Ref. 101. Copyright 2014 WILEY-VCH Verlag GmbH & Co. KGaA.

Nitrobenzyl groups have also been widely used as UV-light cleavable linkers in surface coating. To control cell-surface interactions, the nitrobenzyl group has been used to attach anti-adhesive PEG coatings as a linker to surfaces. Upon UV-light irradiation, the PEG coatings release and the surfaces become adhesive for cell adhesion.[107] For example, mammalian cells have been patterned in confined and complex geometries using photocleavable 2-nitrobenzyl groups via projection exposure to UV light through a photomask.[108] Similarly, these photocleavable groups have been used as a caging group on the backbone of RGD to block mammalian cell adhesion and to turn on cell adhesion upon illumination.[109] Yet, analogous approaches are missing for bacterial cells.

1.2.1.2.2 Optogenetic control of bacterial adhesion

Recently, optogenetic methods have been developed to control bacterial adhesion and patterning using light with unique advantages including high spatiotemporal control,

tunability and non-invasive remote regulation. These optogenetic approaches use light controlled protein activity and genetic engineering of the cells to render them light responsive. For example, Jin and Riedel-Kruse have developed a genetically encoded biofilm patterning tool ("Biofilm Lithography") by engineering bacteria such that the expression of membrane adhesion proteins antigen 43 (Ag43) responsible for surface attachment is optically regulated.[110] (**Figure 1.6**) Accordingly, these *E. coli* only formed biofilm on blue illuminated regions of the surface and could be patterned with 25 μm spatial resolution. Huang *et al.* reported a similar strategy for microprinting living biofilms through optogenetic regulation of the c-di-GMP levels, which regulates biofilm formation in *P. aeruginosa.* In the presence of near-infrared light, the synthesis of c-di-GMP molecules was activated through the cyclization of the guanosine triphosphate (GTP) molecules, regulated by the genes *bphO* and *bphS*. While illuminated with blue light, c-di-GMP molecules were hydrolyzed due to the activation of gene *blrP1*. Therefore, combining these optogenetic modules enabled the precise manipulation of the c-di-GMP levels in *P. aeruginosa* through dual-color illumination.[111]

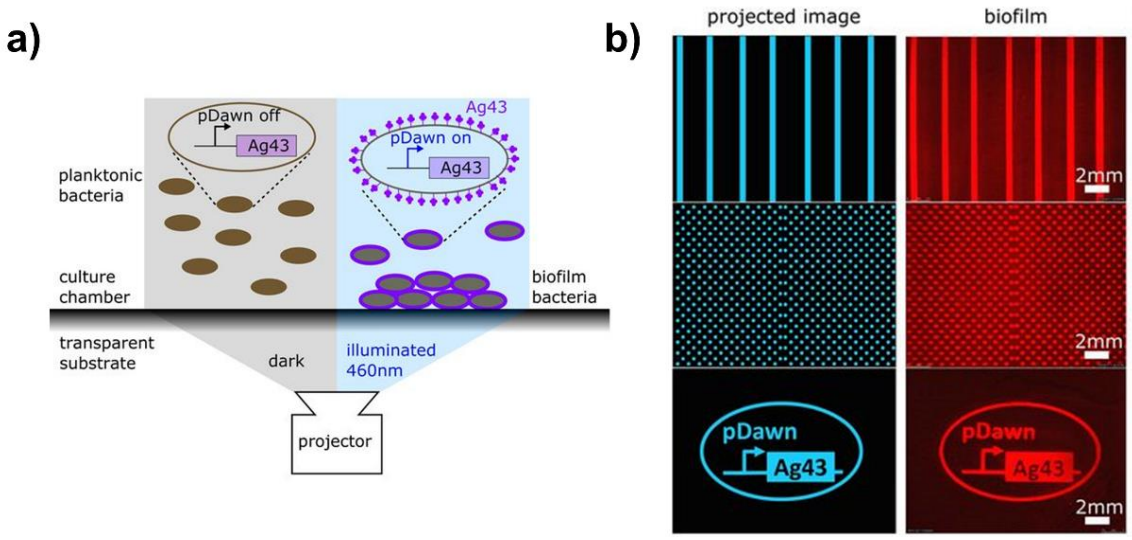

Figure 1.6 a) Schematic illustration of biofilm photolithography. b) Biofilm patterns created by biofilm lithography.[110] Reproduced with permission from Ref. 110. Copyright 2018 National Academy of Sciences.

1.2.2 Bacteria-bacteria adhesion

Adhesions between bacterial cells to form multicellular clusters are crucial for the development of biofilm structures. Bacterial aggregation plays an important role in a variety of ecological processes such as competition, adaptation, epidemics, and succession.[112] Bacteria-bacteria adhesions are also a key factor for regulating spatial organization and heterogeneity within biofilms. Manipulation of bacteria-bacteria adhesion has potential applications in many areas including antimicrobial therapy, modulation of bacterial signaling such as quorum sensing and engineering multicellular communities and microbial consortia. Therefore, multiple strategies have been proposed to control bacteria-bacteria adhesion and associated cell behavior and communication.

1.2.2.1 Controlling bacterial aggregation with native adhesion molecules

Antigen 43 (Ag43) is a surface-located autotransporter protein and one major determinant of autoaggregation in *E. coli*. The interactions between Ag43 α-subunits of adjacent cells in a head-to-tail fashion lead to dimer formation and cell aggregation.[113] Therefore, bacterial aggregation can be controlled by regulating the Ag43 expression through the gene *OxyR* or *Dam*.[114]

Laganenka *et al.* showed that autoinducer 2 (AI-2) produced by the bacteria itself is an attractant and leads to chemotaxis towards leading to autoaggregation of *E. coli*. Furthermore, AI-2-dependent autoaggregation enhanced bacterial stress resistance and promoted biofilm formation.[115] It was also reported that cells of chemotactic bacterial strains aggregated in response to gradients of attractant and this interaction led to collective phenomena such as the formation of dense multicellular clusters, moving bands and geometric patterns.[116-118]

1.2.2.2 Triggering bacterial aggregation with external molecules

Synthetic materials with multivalent interactions have been used to induce bacterial aggregation in order to prevent infections at an early stage and blocking the interaction between microbial adhesins and host epithelial cell receptors. Examples of these are polysaccharide, polymers, dendrimers or chemically modified nanoparticles.[119-124]

Cationic polymers are an obvious starting point in the development of antimicrobial agents that cluster bacteria. Because of their positive charge, these polymers can efficiently bind the negatively charged bacterial surfaces and result in the aggregation of these bacteria. In addition, adhesion of cationic materials to bacterial membranes can result in membrane damage and have bactericidal activity.[121, 125] Lui *et al.* reported a cationic polymer poly(*N*-[3-(dimethylamino)propyl]methacrylamide) induced bacterial aggregation through electrostatic interactions.[126] Furthermore, *Vibrio harveyi* showed enhanced bioluminescence in response to polymer-mediated clustering, indicating the quorum sensing was activated upon clustering. Bacteria-polymer aggregates undergo rapid autoinduction and achieve quorum sensing at bacterial densities far below those required for autoinduction in the absence of polymers. [126-128]

Glycopolymers carrying carbohydrate functional groups have also been widely reported for the controllable bacterial aggregation.[129] They can interact with the lectins on the surface of bacteria and induce the bacterial aggregation. Pasparakis *et al.* described a reversible control of bacterial aggregation by thermoresponsive glycopolymers.[130] They synthesized the polymer with multiple glucose moieties, which were hidden above 40 °C and revealed below this temperature. This thermal switchable process enabled the controllable bacterial aggregation based on the interaction of glucose and lectin.

1.2.2.3 Controlling bacterial aggregation through genetic engineering

Recently, Glass *et al.* developed a synthetic cell-cell adhesion toolbox for *E. coli* that enables controlled multicellular self-assembly with high specificity and tunability.[15] For this purpose, nanobodies (Nb) and their corresponding antigens (Ag) were displayed on the bacterial surface by fusing them adhesin to the N-terminus of intimin, an autotransporter and surface display system. Expression of the fusion protein was regulated by the addition of inducers anhydrotetracycline (ATc) or arabinose (Ara). Two *E. coli* strains displaying a nanobody and a corresponding antigen would specifically adhere to each other via the Nb-Ag interaction, which mediated self-

assembly of multicellular aggregates with defined patterns and morphologies (**Figure 1.7**). Furthermore, this toolbox enabled the rationally design of diverse and complex multicellular patterns.

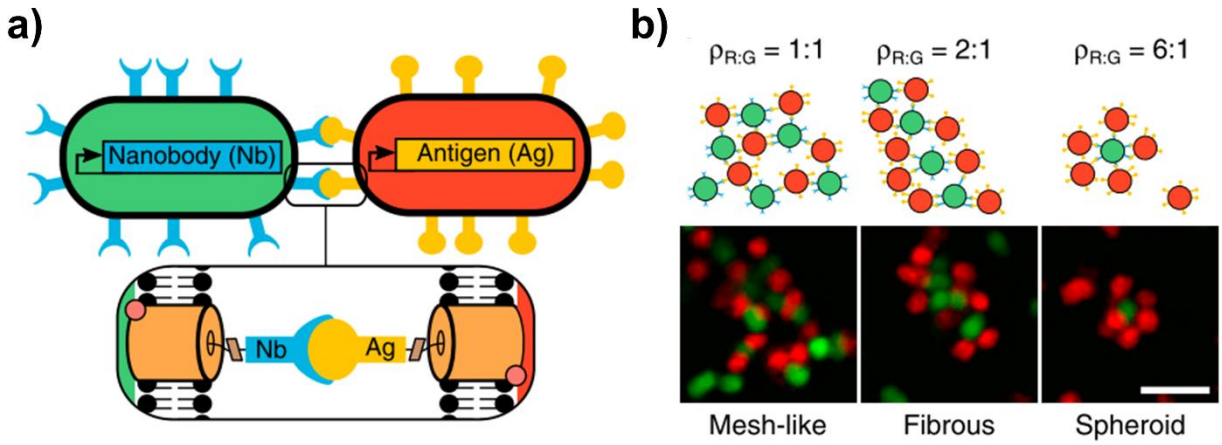

Figure 1.7 a) Bacteria-bacteria aggregation based on the interactions of nanobody and antigen. b) The morphology and patterning of bacterial clusters altered by the ratio of green and red cells.[131] Reproduced with permission from Ref. 131. Copyright 2018 Elsevier.

For natural multicellular organisms, cell-cell adhesion is the key tool for directing the spatial organization. To produce biofilms with a deliberate arrangement, methods for dynamically controlling bacteria-bacteria adhesions with high spatial and temporal precision are required.[11-13] However, none of the existing approaches provide the required crucial dynamic and spatiotemporal control over the bacteria-bacteria adhesions.

1.3 Photoswitchable proteins for optogenetic control

Optogenetic tools are genetically encored photoswitchable proteins used for regulating cellular processes with light as an external stimulus.[132, 133] Optogenetics has been used to regulate diverse cellular functions with visible light, including receptor activation, gene expression, enzyme activity, protein clustering and protein localization both in mammalian and bacterial cells.[134-137] As part of this thesis the photoswitchable proteins nMag and pMag have been used and will be detailed below.

1.3.1 The photoswitchable protein pair nMag and pMag

A widely studied and used blue light responsive class of protein domains is the light, oxygen, and voltage (LOV) domain found in bacteria, fungi, algae or plants.[140-142] The Vivid (VVD) protein is the LOV-domain from the filamentous fungus *Neurospora crassa*. Similar to other LOV domains, VVD forms a covalent bond between a key cysteine residue (Cys108) and its cofactor flavin adenine dinucleotide (FAD) upon blue light illumination. This reaction induces a conformational change in the N-terminal helix α of VVD, which rearranges on the protein surface so as to release the N-terminus from the protein core. This conformational change results in the homodimerization of VVDs (**Figure 1.8**).[139, 143] Moreover, this process is reversible in the dark.

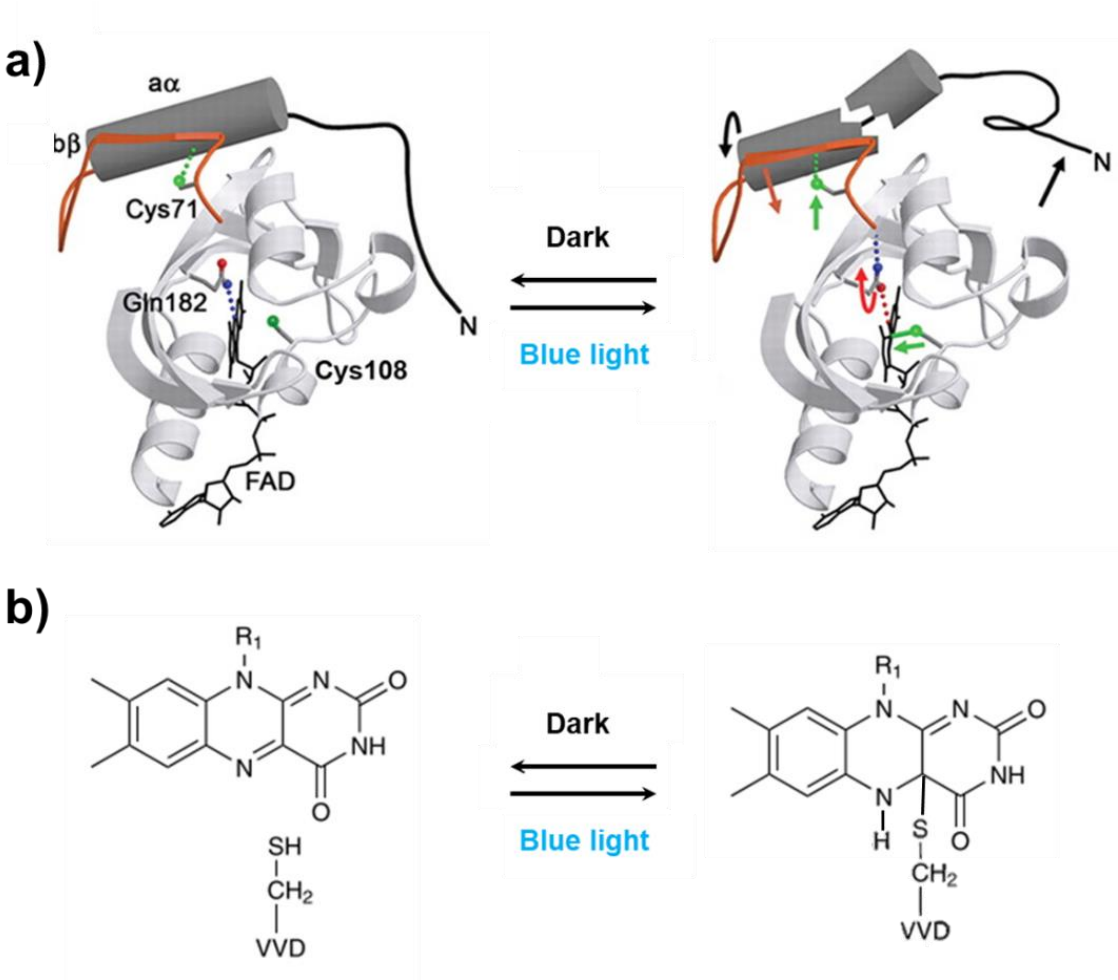

Figure 1.8 Conformational switching in the VVD photosensor. a) Conformation of VVD under blue light and in the dark.[138] Adapted with permission from Ref. 138. Copyright 2017 the American Association for the Advancement of Science. b) The activation of FAD by blue

light illumination leads to the formation of a photoadduct between the flavin ring and VVD.[139] Adapted with permission from Ref. 139. Copyright 2019 Springer Nature.

To convert the light dependent homodimerizer VVD into a heterodimerizer the protein pair nMag and pMag were developed by engineering the homodimerization interface Ncap (from Ile47 to Asn56) of VVD through incorporating either positive or negative charged amino acids into the VVD N-terminal helix. The engineered proteins were called Magnets based on their electrostatic interactions (attraction and repulsion), which favored heterodimerization and prevented homodimerization (**Figure 1.9a**). Proteins with negatively charged amino acids were called nMag (I52R/M55R) and positively charged amino acids were called pMag (I52D/M55G). To optimize the dissociation kinetics and dimerization efficiency of nMag and pMag ($t_{1/2}$ = 1.8 h, K_d = 1.1 × 10^{-4}), mutations were added to Ile74, Ile85, Met135 and Met165 within the Per-Arnt-Sim (PAS) core of nMag or pMag (**Figure 1.9b**). The mutation I85V (pMagFast1 or nMagFast1) exhibited an accelerated dissociation in the dark and lower affinity under blue light ($t_{1/2}$ = 4.2 min, K_d = 2.7 × 10^{-3}). On the other hand, the mutations of M135I and M165I (pMagHigh or nMagHigh) slowed down the dark reversion and increased the extent of heterodimerization under blue light ($t_{1/2}$ = 4.7 h, K_d = 4.1 × 10^{-5}).

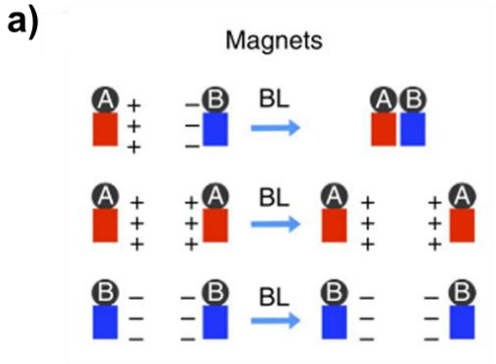

	Ncap		PAS core			
	52	55	74	85	135	165
nMagHigh	D	G	I	I	I	I
pMagHigh	R	R	I	I	I	I
pMag	R	R	I	I	M	M
pMagFast1	R	R	I	V	M	M

Figure 1.9 a) Magnets proteins (A and B) selectively heterodimerize under blue light but not homodimerize due to the electrostatic. b) The mutations of nMagHigh and pMag variants.[148] Adapted with permission from Ref. 148. Copyright @ 2015 Springer Nature.

The nMag and pMag proteins have been successfully used for optogenetically controlling of genome editing,[144, 145] cellular signaling and transcription,[146-148] colloids assembly and social

sorting[149]. The tunable binding affinities and kinetics make Magnets a very versatile class of photoswitchable proteins and allow for precise subcellular control of protein association with high spatial and temporal resolution.

Chapter 2. Bacterial Photolithography: Patterning *Escherichia coli* biofilms with high spatiotemporal control using photocleavable adhesion molecules

Copyright

Aim

Bacteria in nature usually do not only exist as free-floating cells but predominantly live in a biofilm, where collective functions arise from the social interactions and spatial organization of bacteria. Controlling bacterial adhesion as key steps in biofilm formation with high spatial and temporal precision is essential for controlling the formation, organization and microstructure of biofilms. To study how the spatial arrangement of bacteria influences their social interactions, such as quorum sensing, this work focuses on developing a method of patterning bacteria into complex geometries with high resolution. Photocleavable adhesion molecules can be synthesized to functionalize the surface and thereby bacterial attachment can be controlled by UV light. Using this method, patterning biofilms with high resolution can be obtained and provides a tool to study the spatial organization of bacterial cells on the quorum sensing.

2.1 Abstract

Biofilms are not only a leading cause of chronic infections and biofouling, but they also have a tremendous positive potential in biotechnology for biocatalysis and waste treatment. Biofilms are spatially structured communities of microbes, which exchange chemicals and communicate with each other. By spatially controlling bacterial adhesion to surfaces and therefore the microstructure of biofilms, we have developed a promising method of understanding social interactions between bacteria and designed biofilms. The bacterial photolithography approach described here allows us to photopattern specific bacteria adhesion molecules, to control surface adhesion, and to guide the formation of biofilms. To do this, α-D-mannoside, which is recognized by *Escherichia coli* FimH receptor, is linked to a non-adhesive poly(ethylene glycol) (PEG) surface through a photocleavable 2-nitrobenzyl linker. When a pattern of UV light in a specific shape is projected onto these surfaces, the light-exposed areas become non-adhesive and bacteria only adhere to the dark, unexposed areas in the photopattern. Bacterial photolithography enables bacterial patterning with high spatial resolution down to 10 μm without mechanical interference. Additionally, patterning biofilms with complicated geometries allows us to study the importance of microscale spatial organization on the collective behavior of bacteria such as quorum sensing.

2.2 Introduction

Biofilms are an emergent form of bacterial life as they allow bacteria to survive in hostile environments and to resist antimicrobial agents.[150, 151] In order to form a biofilm, bacteria first need to adhere to surfaces before they begin to excrete substances that can anchor them to all kinds of material.[10] The formation of biofilms is a major cause of chronic infections[152] and persistent biofouling.[153] Recent research has highlighted the potential of engineered biofilms in biotechnology for antibiofouling,[154] biocatalysis,[155] biosensing,[156] bioremediation[157] and water treatment.[158] The spatial structure of the biofilms on the micrometer scale allows bacteria to work together and perform biochemical transformations, which planktonic bacteria cannot catalyze by

themselves.[159, 160] To control the spatial structure of biofilms more efficiently and to investigate its specific effect on the biofilm's function as well as collective phenomena such as quorum sensing, we need to establish a reliable way to obtain patterned biofilms with high resolution.

The formation of a biofilm begins with the adhesion of free-floating bacteria to a surface, which determines the later spatial organization in biofilms.[153, 161] This is particularly significant as the arrangement of bacteria with respect to each other defines the extent of their interaction and exchange of chemicals present in a biofilm. Different strategies have been proposed to control bacterial adhesion and to pattern bacteria on surfaces, such as microfluidic devices,[59] microcontact printing,[162] inkjet printing,[163] hydrogels patterning,[164] substrates modified with stimuli-responsive chemicals,[103] and optogenetic methods.[165-167] Among these approaches, the light-responsive methods provide the highest spatial and temporal resolution, are the least invasive and provide remote controlled. All these factors are required to construct stable/viable biofilms with a high level of precision. For instance, azobenzene linkers, which undergo reversible *trans* to *cis* isomerization when exposed to UV light, have been used to control bacterial adhesion to surfaces by exposure to light. This is achieved by altering the orientation or the presence of mannoside groups, which are recognized by the bacterial surface adhesion receptor FimH.[103, 104, 168] Likewise, in optogenetic approaches, bacterial adhesion has been dynamically controlled in genetically modified bacteria in response to low intensities of blue or red light by either controlling protein expression with light or displaying light responsive protein pairs on the bacteria surface.[165-167] Yet, these optogenetic methods require the genetic manipulation of bacteria and expression light responsive proteins by the bacterial. While the reversible control provided by the azobenzene-based approaches and the optogenetic approaches is an advantage to switch adhesions dynamically, it also requires constant illumination with light. This limits the practical use for long term studies and increases the risk of light toxicity, which is especially problematic in the

case of UV-light. Therefore, we developed a new tool termed bacterial photolithography where we photopatterned specific bacterial adhesion molecules on a non-adhesive surface for spatiotemporally controlled and specific bacterial adhesion. In previous reports, mammalian cells have been patterned like this using photocleavable 2-nitrobenzyl groups, which can be cleaved with UV-light (365 nm). Nitrobenzyl groups have been used as linkers connected to PEG (polyethylene glycol), or as photocaging groups on adhesion peptides to release them on demand and obtain the cell adhesive domains.[19] Bacterial photolithography is an easy to handle and highly reproducible way for the stable patterning of bacteria and allows for straightforward long term studies without interference. In addition, unlike the optogenetic approaches, this approach does not require genetic manipulation of *E.coli.*

For bacterial photolithography, we connected α-D-mannoside to a non-fouling PEG-coated glass surface through a photocleavable 2-nitrobenzyl linker. Synthetic glycosylated surfaces are valuable tools when studying specific bacterial adhesion,[103, 169] as bacteria adhere to the surface of host cells through the FimH receptor, which specifically recognizes oligomannoside residues of the glycoprotein.[170] In our experiment, the bacteria adhered specifically to the α-D-mannoside monolayer on top of the PEG coating, where the FimH receptor on the bacteria was able to bind to mannoside groups **(Scheme 2.1)**.

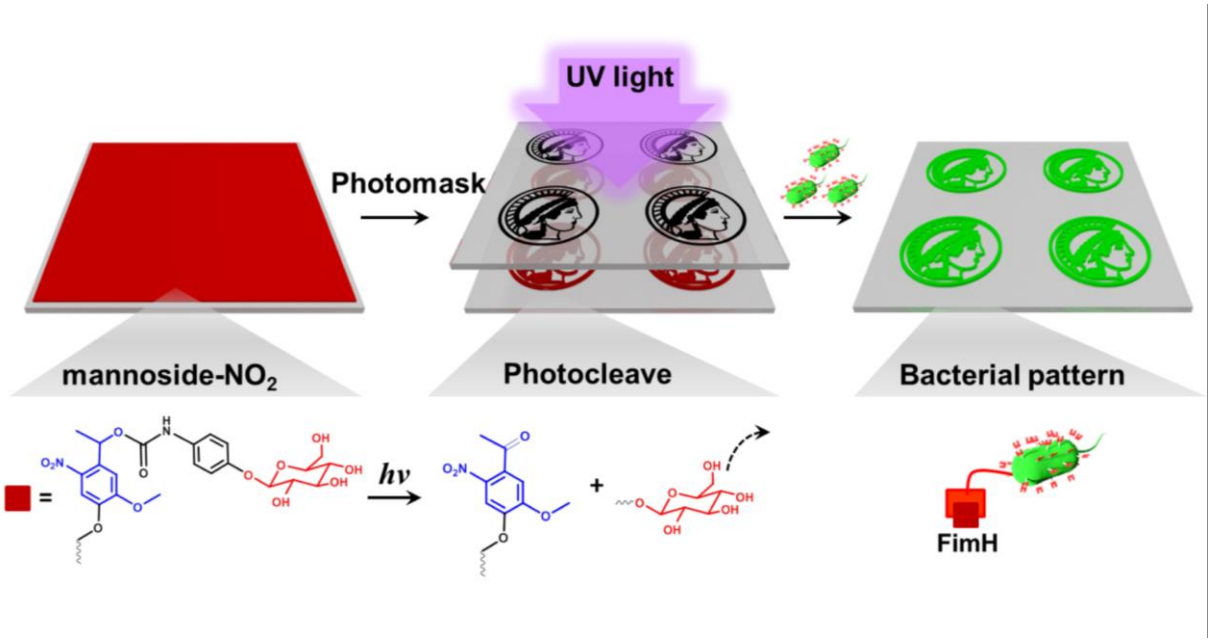

Scheme 2.1 Schematic illustration of bacterial photolithography. The bacterial adhesion molecule α-D-mannoside is conjugated to a glass surface with a non-adhesive PEG coating through a photocleavable 2-nitrobenzyl linker (mannoside-NO_2). Projecting UV light through a photomask using a Minerva pattern onto this surface leads to the local cleavage of mannoside groups in the light-exposed areas and formation of non-adhesive patterns. Therefore, bacteria only adhere to areas which were not exposed to UV-light due to the specific binding of FimH receptors on *E.coli* to mannoside groups on the surface.

Upon UV-light (365 nm) exposure, the α-D-mannoside groups were released from the surface and the underlying non-fouling PEG coating was exposed so that bacteria could not adhere. When a pattern of light is projected through a photomask onto a surface, the mannoside groups only release from areas where light passes through. Therefore, bacteria will only adhere to those areas that were not illuminated, and will not adhere to the illuminated regions. This method allows us not only to pattern bacteria with light, but also to spatially structure stable biofilms in complicated patterns with a resolution as high as 10 µm.

Inside biofilms, bacteria can interact more efficiently and are able to sense the local density of each other through quorum sensing molecules, also named autoinducers.[171] Bacterial photolithography is a useful tool and can be used to engineer microbial

communities by patterning biofilms of desired bacterial clusters, sizes, and spatial distribution. This provides us with an ideal platform for understanding the relationships between bacteria and allows us to study quorum sensing in biofilms with well-controlled spatial organization in complicated geometries.

2.3 Results and Discussion

In the first stage of bacterial photolithography, we covered PEG-coated glass surfaces with photocleavable mannoside groups, which specifically bind to the bacterial surface adhesion receptor FimH. We used a nitrobenzyl linker, which can be photocleaved with UV-light (365 nm), possesses an NHS-ester (N-Hydroxysuccinimide ester) functional group, which reacts with mannoside amine, and this linker processes an alkyne group for convenient attachment to any material with an azide functional group by the CuAAC (copper catalyzed azide alkyne cycloaddition, also known as click reaction).[172, 173] First, we coupled the nitrobenzyl linker to α-D-mannosyl-amine to obtain mannoside-NO_2 (**Figure 2.1a**).

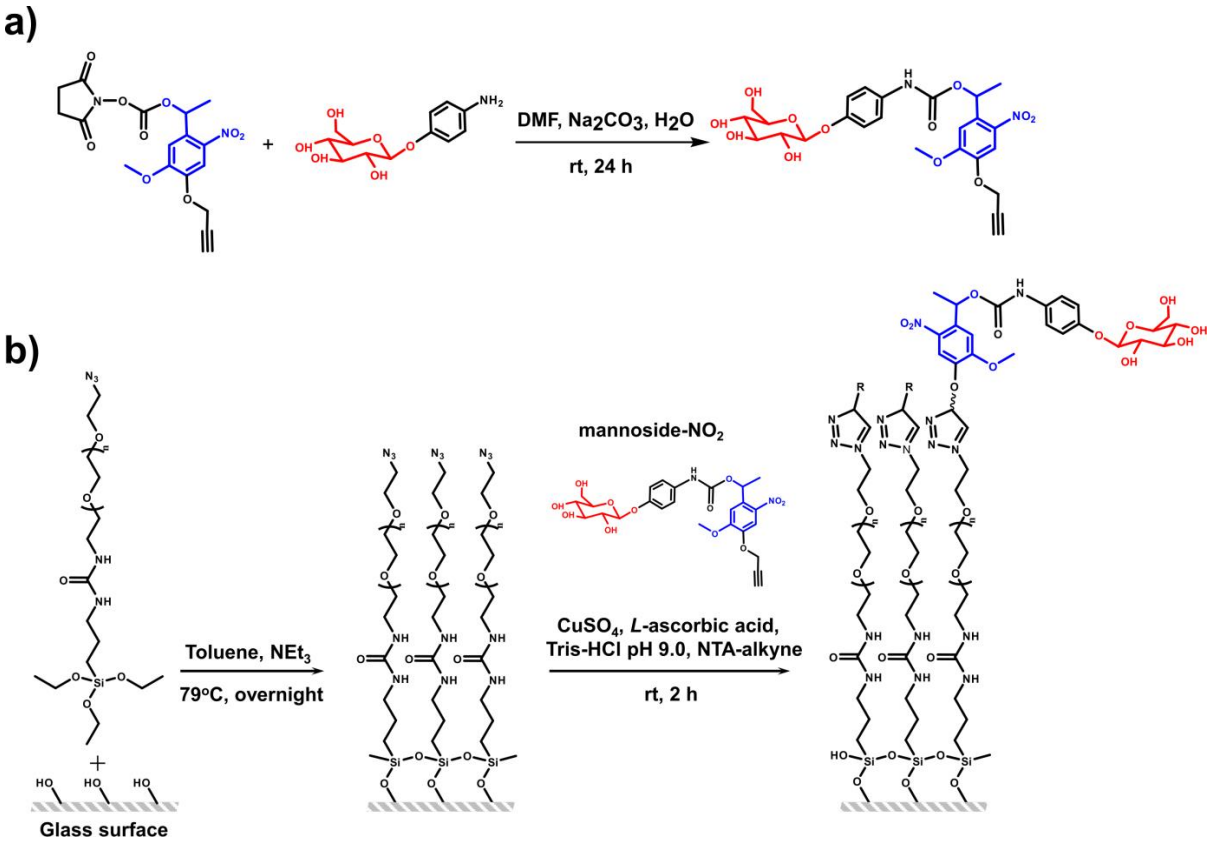

Figure 2.1. a) Synthesis of mannoside-NO_2 and b) its immobilization on PEG coated glass surface. The glass surface was modified by passivation with PEG-azide.

In solution the characteristic peak of mannoside-NO_2 decreased during 30 min of UV-light illumination (**Figure 2.2**), indicating the cleavage of the nitrobenzyl linker. Subsequently, mannoside-NO_2 was immobilized onto glass surfaces coated with a bacteria repellent PEG-azide (a PEG3000 with a terminal azide and triethoxysilane groups) at a density of ca 38 pmol/cm^2 using the CuAAC to form a photo-removable glycol monolayer (**Figure 1b**).[172, 173]

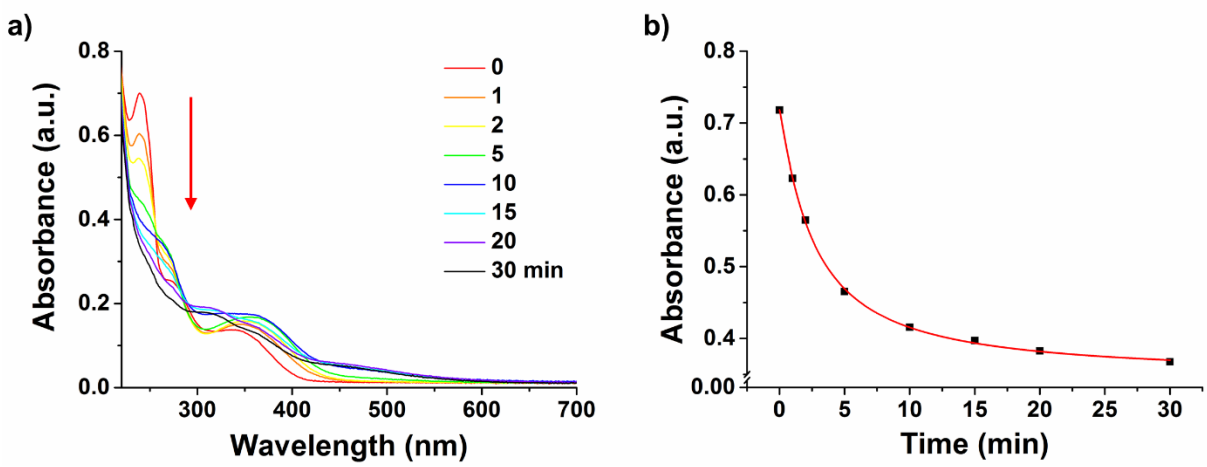

Figure 2.2 a) UV-Vis absorbance spectrum of a 100 µM solution of mannoside-NO_2 in H_2O after exposure to UV light for increasing time. b) Absorbance of mannoside-NO_2 at 239 nm versus time. $t_{1/2}$ = 2.65 min.

We studied bacterial adhesion on these surfaces to determine whether bacteria can adhere to the mannoside-NO_2 functionalized PEG-coated glass surfaces and to see if the mannoside can be released with UV-light to expose the bacteria repellent PEG.

To detect the bacteria, we expressed GFP (green fluorescent protein) in the *E.coli* K12 MG1655 strain, which expresses the FimH receptor. These bacteria were seeded at a density of OD_{600}=1.0 onto mannoside-NO_2 functionalized glass surfaces and incubated for 3.5 h, whereby one mannoside-NO_2 surface was not exposed to UV light (UV-) and one mannoside-NO_2 surface was pre-exposed to UV-light for 1 h beforehand (UV+). As a negative control we used glass surfaces coated with PEG, which prevents unspecific bacterial adhesion. Bacteria could adhere efficiently to the mannoside-NO_2 surfaces, which were not exposed to UV-light (**Figure 2.3a**). In contrast, only a very few bacteria attached to mannoside-NO_2 surfaces, which were pre-exposed to UV-light. Obviously, *E.coli* can adhere to the mannoside groups through the FimH receptor, but when the surfaces are pre-exposed to UV-light the number of bacteria that can adhere decreased dramatically due to the cleavage of nitrobenzene-linked

mannoside. In fact, the number of bacteria that adhered to these surfaces is comparable with the number of bacteria that adhered to the control PEG surfaces (**Figure 2.3b**). This shows that the UV-light used in the experiment was sufficient to photocleave the mannoside groups, but did not damage the underlying non-adhesive PEG coating.

Figure 2.3 a) Fluorescent images of GFP labeled *E.coli* on mannoside-NO_2 functionalized the glass surfaces which were kept in the dark (UV-) or pre-exposed to UV-light for 1 h (UV+) before incubating bacteria on them for 3.5 h. Scale bar is 100 µm. b) The number of bacteria on the surfaces in (a). A PEG-coated surface was used as a negative control.

The number of bacteria that can adhere to such surfaces can be adjusted in several ways. First, the number of bacteria that attached to the mannoside-NO_2 surfaces increased linearly with the time that bacteria were incubated on these surfaces from 10 min to 3.5 h (**Figure 2.4a, Figure 2.5a**).

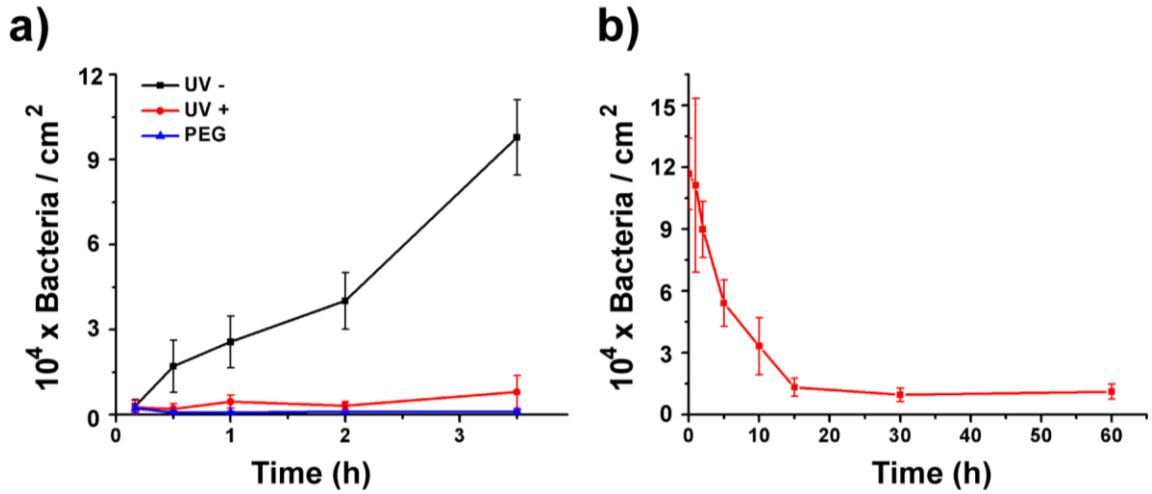

Figure 2.4 a) The number of bacteria on UV-, UV+ and PEG surfaces with increasing incubation time. b) The number of bacteria adhering to mannoside-NO_2 surfaces, which were pre-exposed to UV-light for up to 60 min before incubating with bacteria for 3.5 h. The error bars are the standard deviation error from nine images.

This can either be due to more bacterial adhesions forming, or the result of bacterial growth on the surfaces. Conversely, if the mannoside-NO_2 surfaces are pre-irradiated for 1 h with UV-light (365 nm), bacteria could not adhere efficiently to these surfaces. The number of adherent bacteria on the surface did not change with increasing incubation time. Secondly, the number of bacteria that attached to these surfaces could be controlled by changing the pre-exposure time to UV-light, which controls the density of mannoside groups on the surface. For this purpose, we irradiated the mannoside-NO_2 surfaces for up to 60 min and subsequently seeded bacteria at a concentration of OD_{600} = 1.0 for 3.5 h (**Figure 2.4b, Figure 2.5b**). Depending on the initial exposure time to UV-light, which determines the remaining density of mannoside-NO_2 on the surface, the number of bacteria that adhered to the surfaces decreased gradually from ca 98 000 to ca 1 100 per cm^2. In the first 15 min the number of bacteria that adhered to the substrates decreased dramatically due to the cleavage of nitrobenzene mannoside. After 15 min the number of bacteria that adhered to the substrate was much reduced, which indicates that most of the mannoside groups were cleaved and released from the surfaces. For instance, if bacteria were seeded after 5 min of irradiation about half as many bacteria adhered to the substrate as before illumination. After 30 min of irradiation the number of bacteria that attached was comparable to the negative control on a PEG surface.

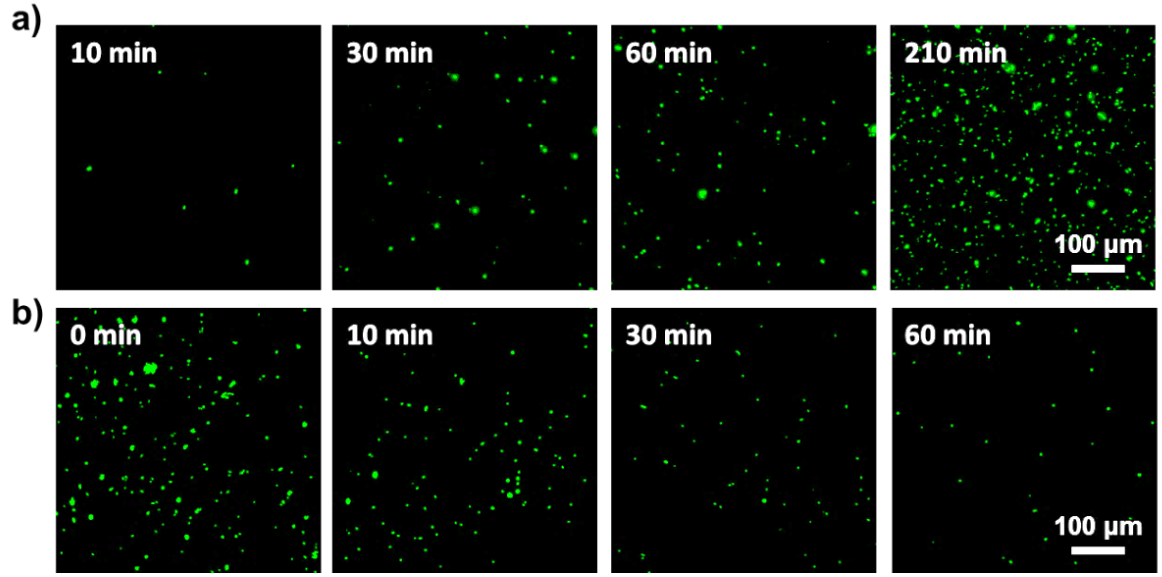

Figure 2.5 a) Fluorescence images of bacterial attaching to mannoside-NO_2 functionalized surfaces which were not exposed to UV light after 10, 30, 60, 210 min incubation with bacteria. b) Fluorescence images of bacterial attaching to mannoside-NO_2 functionalized surfaces which were pre-exposed to UV-light for 0, 10, 30, 60 min after 2 h incubation with bacteria.

The photopatterning of mannoside groups provides high spatial resolution determining where bacteria adhere and enables us to pattern biofilms in any desired geometry.[59, 162] To control the local attachment of bacteria, we irradiated the mannoside-NO_2 surfaces using a photomask with 358 nm UV-light (DAPI channel) for 2 min on an inverted fluorescence microscope (DMi8, Leica) through a 5x objective. We used a number of different photomasks, including the logo of the Max Planck Society, the head of Minerva, with a diameter of 800 µm, a reversed Minerva with a diameter of 400 µm and a hexagonal honeycomb structure with 250 µm edges. Then, we incubated bacteria on top of these pre-irradiated surfaces for 4 h and washed off any unbound bacteria with buffer. We observe that bacteria only adhered to the areas that were not

exposed to light and that they did not adhere to the illuminated regions following the projected patterns. (**Figure 2.6, Figure 2.7**).

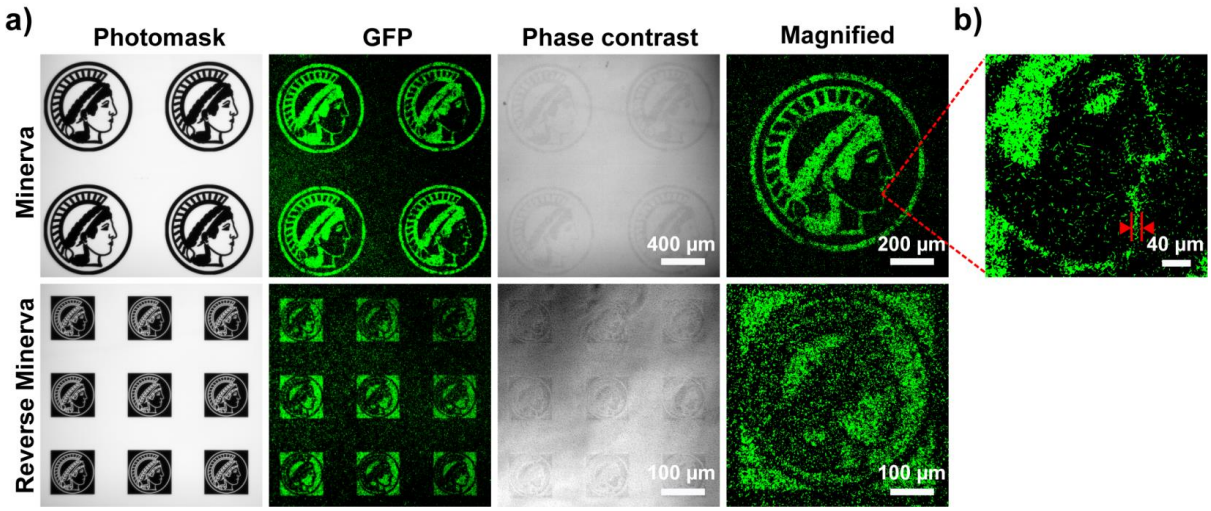

Figure 2.6 a) Microscopy images of the photomasks and photopatterned bacteria. UV-light was projected onto mannoside-NO_2 functionalized glass surfaces through photomasks of the Minerva and reverse Minerva patterns. After incubation with GFP labeled E.coli, they only adhered to areas which were not exposed to light. b) Magnification of the bacterial pattern. The distance between the arrows in red is 10 µm.

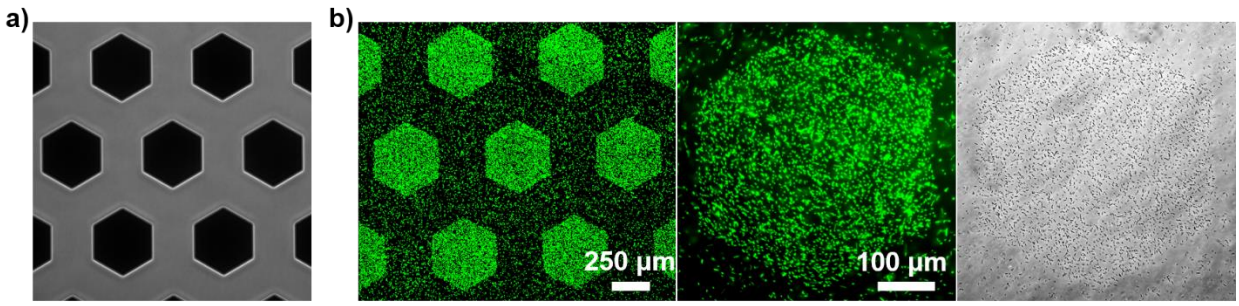

Figure 2.7 a) Bright field image of the photomask and b) fluorescent image of bacteria attached to mannoside-NO_2 functionalized surface only in areas that are not illuminated with

UV light through the photomask. The bacteria are labelled with GFP for detection. Fluorescent image (middle) and bright field image (right) of a single hexagon is magnified.

The process of bacterial photolithography described here allows us to achieve extremely fine structure in complex patterns. For example, in the Minerva pattern we observed lines of bacteria with 10 µm spatial resolution (**Figure 2.6**). More examples of biofilm patterns are shown demonstrating that our method is highly reliable. (**Figure 2.8**)

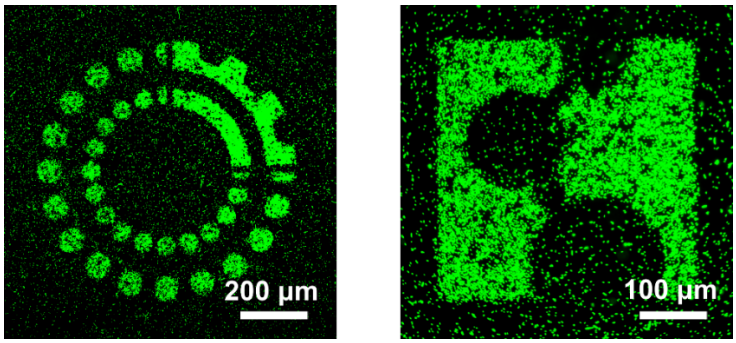

Figure 2.8 Fluorescent images of other biofilm patterns generated with Bacterial Lithography.

This strategy is not only useful to obtain patterns of bacteria, but also a way of studying the importance their spatial distribution for the collective behavior in biofilms such as quorum sensing and material exchange between bacteria. Quorum sensing strongly depends on the spatialtemproal distribution and local density of bacteria and is also affected by bacterial clustering. Photoswitchable versions of autoinducers allow turning quorum sensing on and off in response to light[167, 174] but since these autoinducer diffuse rapidly in liquid cultures it is not possible to pattern bacteria into biofilms and study the influence of the spatial distribution on quorum sensing. Our method provided the possibility to study the dynamics of quorum sensing in a spatially well-defined biofilm. We transformed *E.coli* using the quorum sensing reporter plasmid P_{lsr}-*egfp*, which induces GFP expression when quorum sensing is activated.[175] In addition, the bacteria also expressed mCherry to detect bacterial

patterns. We placed these bacteria on a Minerva pattern and monitored the activation of quorum sensing under the microscope (**Figure 2.9a**).

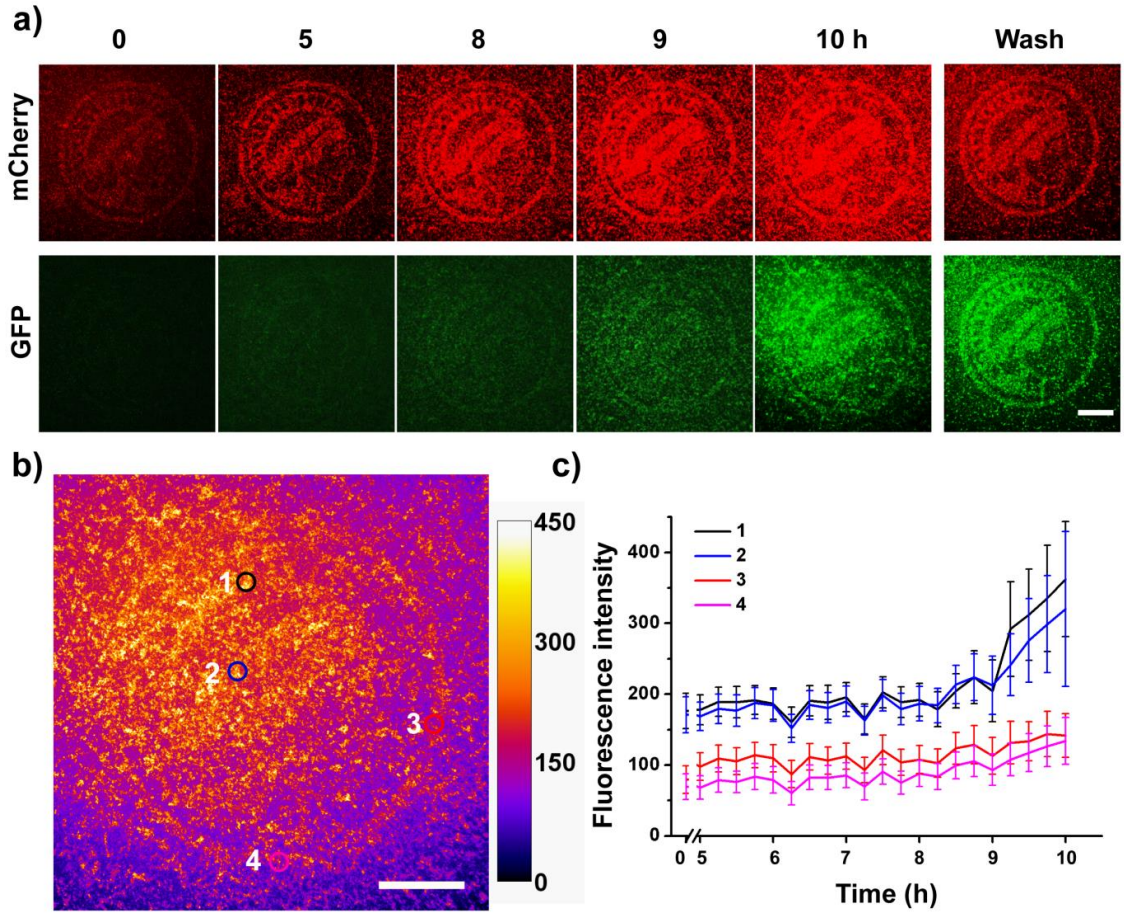

Figure 2.9 a) Activation of quorum sensing in bacteria on a Minerva micropattern recorded over time. *E. coli* constantly express mCherry (red fluorescence) for detection and start to express GFP (green fluorescence, Plsr-egfp reporter) when quorum sensing is activated. Scale bar is 200 µm. b) GFP intensity map of *E.coli* on the Minerva pattern after 10 h. Areas 1 & 2 are in regions of higher local bacterial density compared to Areas 3 & 4, which are at the periphery of the Minerva pattern. Scale bar is 200 µm. c) GFP fluorescence intensity in the selected areas over time.

During the first few h a biofilm formed following the Minerva pattern, as can be observed in the red fluorescence channel. After about 8 h the bacteria initiated quorum sensing, which was observed as an increased GFP expression. The activation in

quorum sensing was not uniform over the entire pattern; areas which have a higher local density of bacteria in the middle of the pattern (areas 1 & 2) produced a higher fluorescence then bacteria which were at the periphery of the Minerva pattern (areas 3 & 4) (**Figure 2.9b-c**). This showed the potential of bacterial photolithography as a tool to study the importance of the spatial distribution of bacteria in activating quorum sensing and how patterned biofilms of bacteria can be used to alter local densities of bacteria to regulate activation of quorum sensing.

2.4 Conclusions

To conclude, we present here a new strategy named bacterial photolithography to photopattern bacteria. This tool uses photocleavable mannoside groups on non-fouling PEG coatings to spatially control bacterial adhesion and biofilm formation. Bacterial photolithography provides high flexibility in creating complex patterns with a resolution down to 10 µm. This fine level of resolution represents an important step towards the engineering of precise biofilm communities, as the microstructure of natural biofilms has a major impact on their function. Bacterial photolithography is not only a useful tool in the field of biofilm photopatterning, but it can also be used to study the effect of spatial distribution of bacterial on collective behaviour in biofilms and interactions as shown above for quorum sensing. This patterning method has significant potential for future applications in guiding the formation and spatial organization of bacteria on a biofilm, as well as improving our understanding of naturally existing biofilms and the design of bacterial consortia.

Chapter 3. Blue light switchable bacterial adhesion as a key step towards the design of biofilms

Copyright

Aim

The method of bacterial photolithography developed in chapter 2 enables the patterning of biofilms with high resolution. However, it required UV light illumination which is toxic for cells and is not reversible for the controlling of bacterial adhesion. Optogenetic switches are emerging molecular tools for studying cellular processes as they offer higher spatiotemporal precision than classical, chemical-based switches. New tools from optogenetics can be introduced to control the bacterial adhesion and biofilm formation. Here, by expressing the optogenetic protein pair pMag on the bacterial surface and immobilizing nMag on the substrates, bacterial attachment can be controlled in a reversible and spatiotemporal controlled manner with blue light.

3.1 Abstract

The control of where and when bacterial adhere to a substrate is a key step towards controlling the formation and organization in biofilms. This study shows how we engineer bacteria to adhere specifically to substrates with high spatial and temporal control under blue light, but not in the dark, by using photoswitchable interaction between nMag and pMag proteins. For this, we express pMag proteins on the surface of *E.coli* so that the bacteria can adhere to substrates with immobilized nMag protein under blue light. These adhesions are reversible in the dark and can be repeatedly turned on and off. Further, the number of bacteria that can adhere to the substrate as well as the attachment and detachment dynamics are adjustable by using different point mutants of pMag and altering light intensity. Overall, the blue light switchable bacteria adhesions offer reversible, tunable and bioorthogonal control with exceptional spatial and temporal resolution. This enables us to pattern bacteria on substrates with great flexibility.

3.2 Introduction

In biofilms different bacteria work as a community, share metabolites and are more resistant towards environmental stress, providing them with a clear survival advantage.[153, 176] Controlling the formation of biofilms is not only a crucial step towards understanding how different bacteria interact with each other in naturally occurring biofilms,[150] but is also essential when designing biofilms for biotechnological applications in biocatalysis, biosensing and waste treatment.[177, 178] Until recently the focus has been on preventing bacterial adhesion and biofilm formation,[179] but lately the better understanding of biofilms has led integrating genetic circuits into bacteria in order to engineer multispecies bacterial consortia with diverse functions.[180, 181]

The first step during biofilm formation is the adhesion of bacteria to a substrate, a key determinant of the spatial organization in biofilms.[153, 176] Controlling bacterial adhesion has involved modifying the surface of the bacteria using bio-orthogonal reactive groups through

liposome fusion,[182] displaying surface tags on bacteria[99, 183, 184] and substrate modification with adhesion molecules.[126, 185, 186] Among these approaches the light responsive methods provide the highest spatial and temporal control. This is particularly significant as the arrangement of bacteria with respect to each other defines the extent of their interaction in a biofilm.[153, 176] Photoswitchable azobenzene linkers have been used to alter the presentation of mannose, which is recognized by the bacterial adhesion receptor FimH, to reversibly turn off bacterial adhesion upon UV-light illumination (365 nm).[103-105] Likewise, some azobenzene-based molecules allow to modify bacterial attachment to mammalian cells,[187] biofilm formation,[188] antibiotic activity[189] and quorum sensing in bacteria with UV-light.[190] However, these photoswitches require UV-light illumination, which is toxic to bacteria. Consequently, the challenge of controlling bacterial attachment to substrates in space and time in a non-invasive, reversible and tuneable manner to guide biofilm formation remains an ongoing goal.

In this paper, we present a new approach of how to control bacterial adhesion to substrates non-invasively and reversibly with light based on photoswitchable proteins. Photoswitchable proteins have recently been used in the field of optogenetics to regulate cellular functions with visible light, including receptor activation, gene expression and protein localization both in mammalian and bacterial cells.[134, 135] These systems are bioorthogonal and noninvasive because they rely on specific protein-protein interactions and respond to low intensity visible light. Additionally, these proteins are genetically encoded, providing sustainable expression in the cell. To photoswitch bacterial adhesion, we used the blue light responsive proteins, nMag and pMag, which heterodimerize under blue light (480 nm) and dissociate from each other in the dark.[143] The nMag and pMag interaction can be tuned in terms of strength and back conversion kinetics in the dark, thus providing an extensive dynamic range. The point mutant pMagHigh (and nMagHigh) has a stronger interaction with its binding partners and slower back conversion (k_{dark}=5.6 x 10^{-6} s^{-1}), while the opposite is true for the mutant pMagFast1 (and nMagFast1) (k_{dark}= 1.3 x 10^{-3} s^{-1}).[139]

3.3 Results and Discussion

In our design, we expressed one of the proteins, pMag, on the surface of *E.coli* and immobilized the complementary interaction partner, nMagHigh, on a glass substrate with a poly(ethylene glycol) (PEG) coating. We hypothesized that the surface engineered bacteria would adhere to the substrate under blue light due to the nMag-pMag interaction, but would not adhere in the dark (**Figure 3.1a**). Additionally, the bacteria that adhered under blue light should detach from the substrate in the dark. To express pMag variants (pMagHigh, pMag and pMagFast1, **Scheme 3.1**) on the surface of *E.coli*, we fused these proteins to the circularly permutated outer membrane proteins OmpX (CPX), a surface protein commonly used for bacterial display.[191]

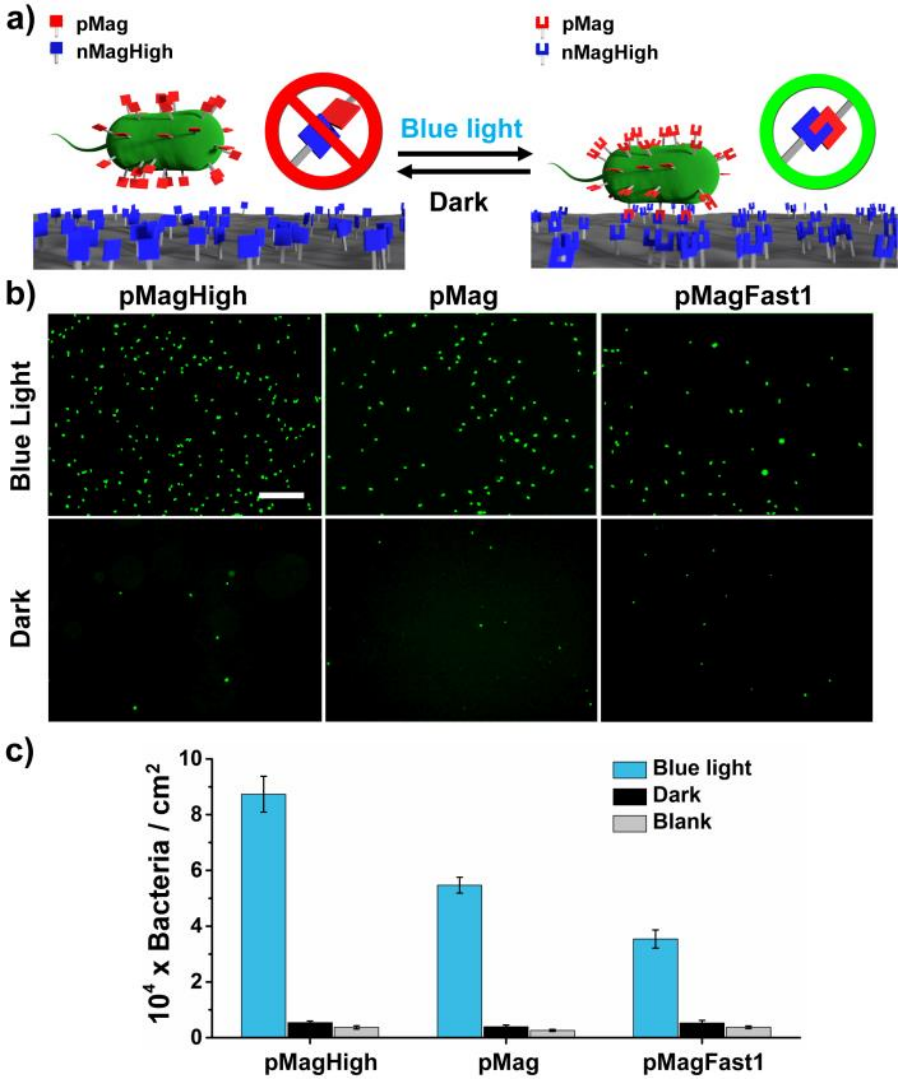

Figure 3.1 a) The surface engineered *E.coli* that express pMag proteins on their surface adhere to nMagHigh modified substrates under blue light. In the dark the pMag-nMag interaction is reversed, which leads to the detachment of the bacteria from the substrate. b) Fluorescence images of *E.coli* displaying pMag variants which adhere on nMagHigh functionalized substrates under blue light but not in the dark. The bacteria are labelled with GFP for detection. Scale bar is 25 µm. c) Quantification of the number of adherent bacteria under blue light, in the dark and on substrates without nMagHigh. The error bars are the standard error from nine images.

	52 55	74 85 135 165
nMagHigh	D--G-	I----I----I----I
pMagHigh	R--R-	I----I----I----I
pMag	R--R-	I----I----M---M
pMagFast1	R--R-	I----V----M---M

Scheme 3.1 Point mutations to transform nMagHigh into the different pMag variants.

In fact, we observed the expression of a new protein with the molecular weight of pMag-CPX in lysates of these bacteria on a SDS-PAGE gel and the expression levels of the three pMag variants are similar (Supporting Information, **Figure 3.2**).

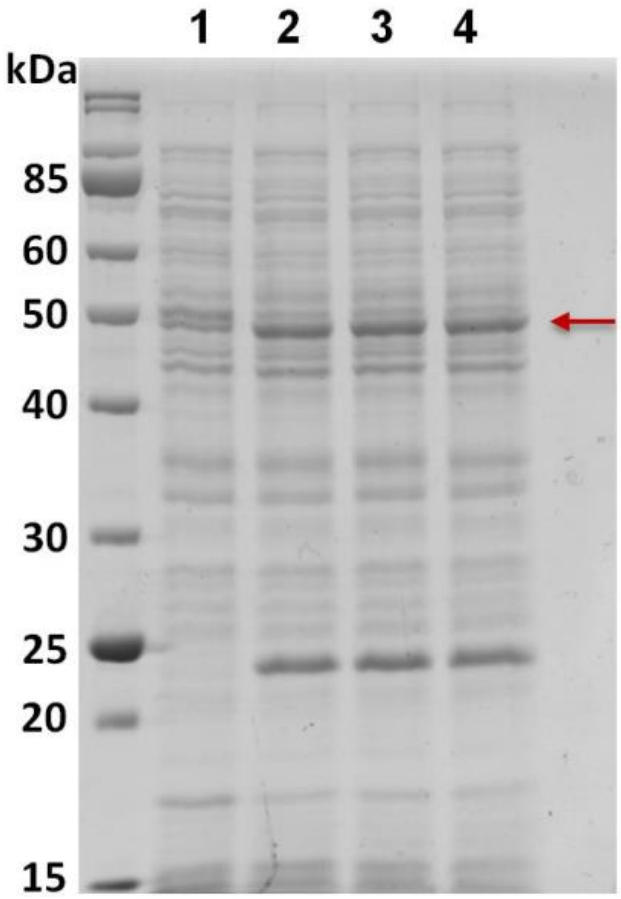

Figure 3.2 a) 10% SDS-PAGE of MG1655 bacteria, which displayed 1. no pMag protein 2. pMagHigh, 3. pMag, 4. pMagFast1 on the outer membrane surface. NEB 10-200 unstained protein marker was used. Molecular weights of pMag, eCPX and pMag-eCPX fusion protein are 17.3, 21.7, 40.8 kDa, respectively.

In parallel, we coated glass surfaces with a PEG layer, which prevents unspecific bacterial attachment and bares Ni^{2+}-nitrilotriacetic acid (NTA) end groups. This allowed us to immobilize purified nMagHigh with a His6-tag on these substrates as measured by quartz crystal microbalance (QCM) (Supporting Information, **Scheme 3.2**, **Figure 3.3**). We seeded bacteria, which expressed different pMag variants on their surfaces, onto these glass substrates with immobilized nMagHigh, both under blue light and in the dark (**Figure 3.1b**). To detect the bacteria, we co-expressed green fluorescent protein (GFP) inside the bacteria. In all cases more bacteria adhered to the substrates under blue light than in the dark due to the blue light dependent interaction between nMag and pMag proteins.

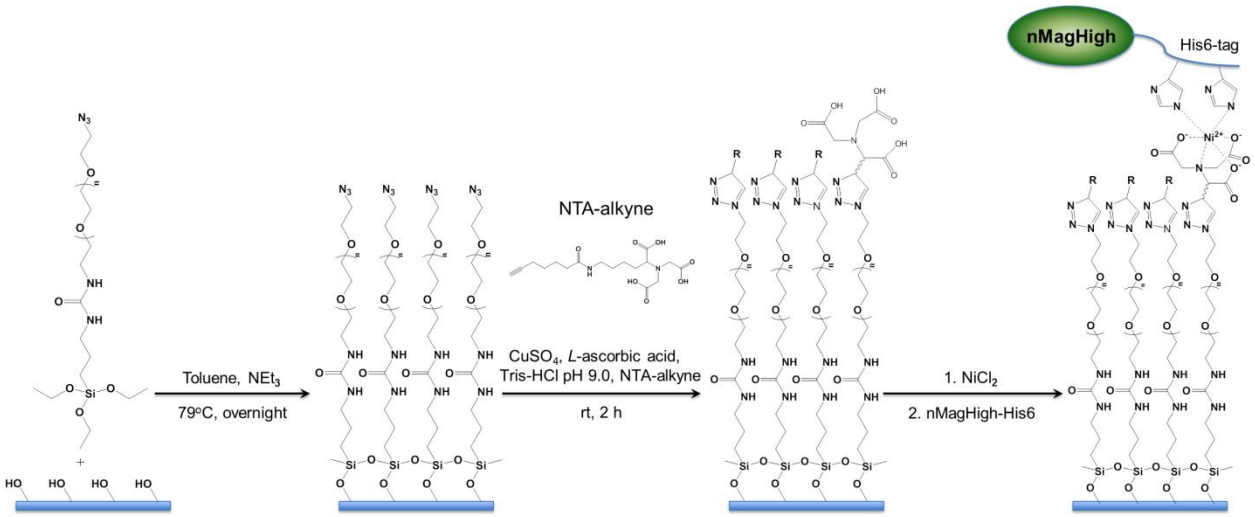

Scheme 3.2 Functionalization scheme of nMagHigh immobilized substrates.

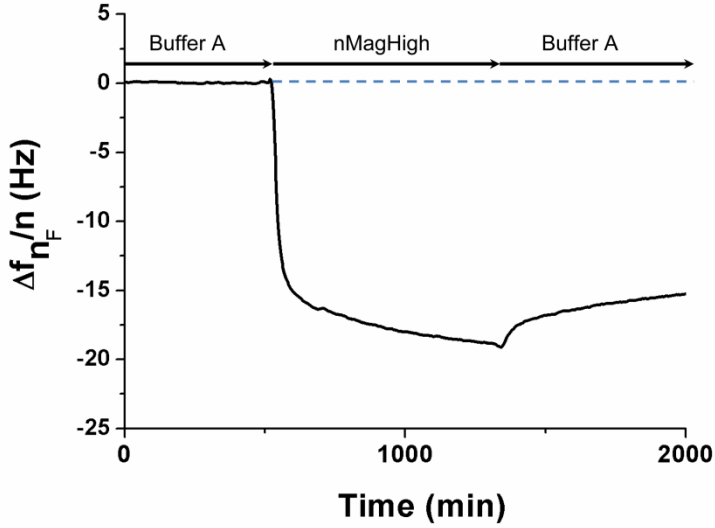

Figure 3.3 QCM measurement showing that the nMagHigh-His6-tag binding to Ni^{2+}-NTA-PEG functionalized surfaces.

We also confirmed these findings in a biofilm formation assay. pMagHigh bacteria cultured on nMagHigh functionalized glass substrates formed biofilms more efficiently under blue light than in the dark (Supporting Information, **Figure 3.4**).

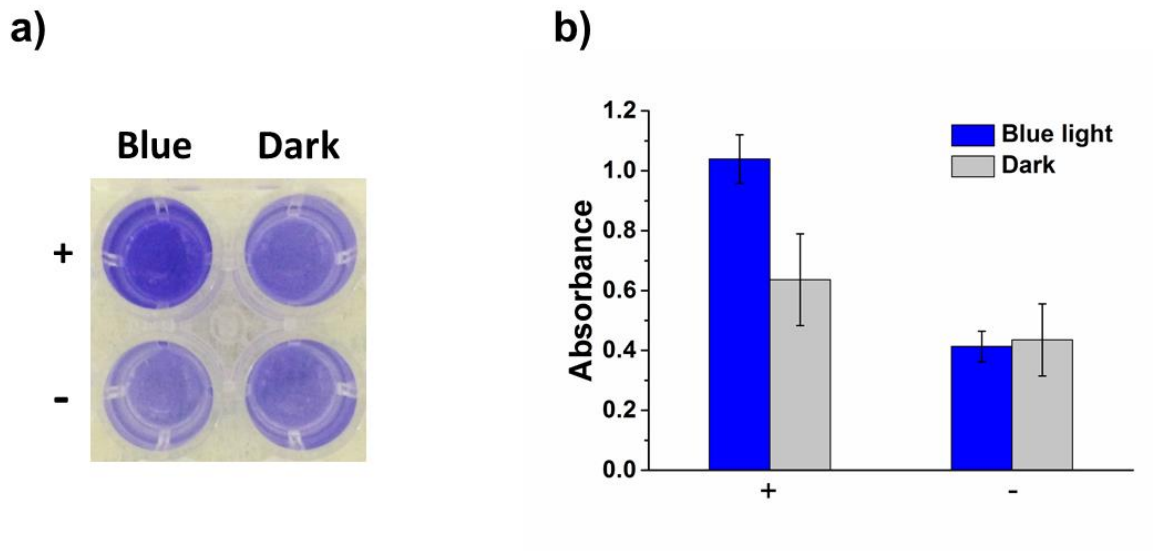

Figure 3.4 Biofilm assay formation of pMagHigh displaying bacteria on glass substrates with or without nMagHigh protein functionalization under blue light or in the dark. +: Substrates with immobilized nMagHigh protein, –: Substrates without immobilized nMagHigh protein. a) A top-down view of solubilized biofilm stain (crystal violet). b) Absorbance at 550 nm. The error bars are the standard deviation from 3 independent measurements.

The nMag-pMag based interaction between the bacteria and the substrate can be tuned in several ways. First of all, different mutants of pMag have different interaction strengths with nMagHigh under blue light and switching off kinetics in the dark. Most bacteria adhere to the nMagHigh functionalized substrate under blue light when the bacteria display the strongest binder pMagHigh, followed by pMag and lastly the weakest binder pMagFast1 (**Figure 3.1c**). These results also show that sufficient pMag proteins are displayed on the *E.coli* surface to mediate bacterial adhesion. As we observe similar protein expression levels for the three pMag variants, the differences in the number of bacteria that adhere to the substrate are due to the differences in interaction strength. In the dark, very few bacteria attach to the substrate no matter which pMag variant is displayed on the bacteria. In fact, the number of bacteria that adhere to the substrate in the dark is comparable to those which adhere to the PEG coating without the immobilized nMagHigh protein. This shows that residual bacterial adhesion in the dark is very weak.

The second way to adjust the number of bacteria that adhere under blue light is to control the time of attachment to the substrate (**Figure 3.5a**). In the first 10 min the number of bacteria that adhered to nMagHigh functionalized substrates was similar for all nMag variants and was probably limited by the sedimentation speed of the planktonic bacteria in solution. After 30 min differences in the number of bacteria that adhered to the substrate became apparent depending on the pMag variant they expressed on their surface. At this point the number of bacteria on the surface correlated with the interaction strength with nMagHigh, being pMagHigh>pMag>pMagFast1. Further, after 1 h the number of bacteria on the surface reached a plateau.

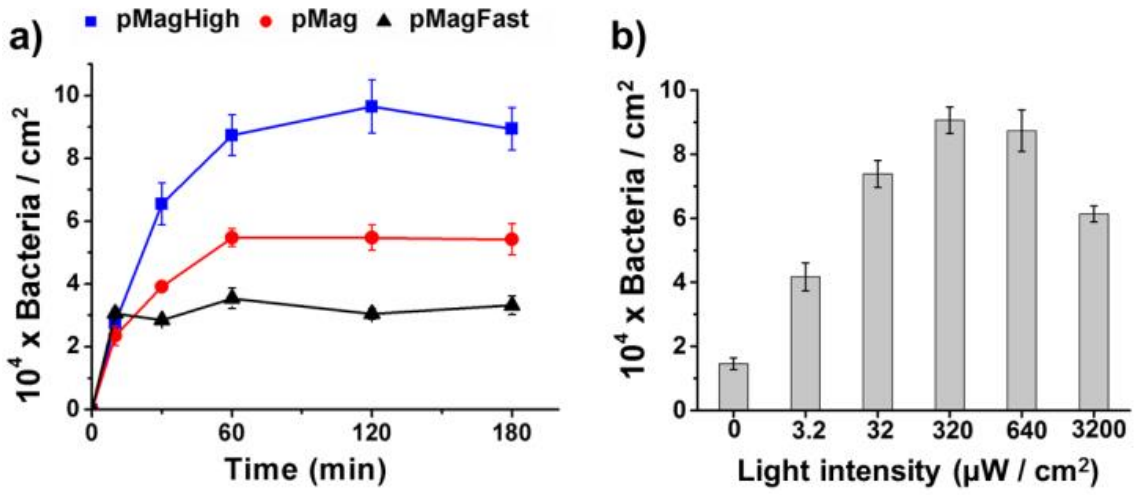

Figure 3.5 a) Attachment kinetics of bacteria displaying different pMag variants on nMagHigh functionalized substrates under blue light. b) Influence of blue light intensity on bacterial adhesion. pMagHigh displaying bacteria were incubated on nMag functionalized substrates for 1 h. The error bars are the standard error from nine images.

Controlling the illumination intensity is another way of altering the blue light switchable bacterial adhesion. We examined the number of pMagHigh expressing bacteria that adhere to nMagHigh functionalized substrates under varying blue light intensities (**Figure 3.5b**). We found that even a light intensity of 3.2 µW/cm^2 can partially activate, and an intensity of 320 µW/cm^2 can completely activate the blue light dependent adhesion. These blue light

intensities are extremely low and even exposure after many hours proved to be non-toxic to the bacteria. Only after exposure of 10 times higher light intensity did 25% of the bacteria on the substrate die after 1 h. This confirms that the blue light responsive interactions are a noninvasive way of controlling bacterial adhesion and can be tuned by altering the light intensity.

Bacteria rearrange themselves within the biofilm over time and subsequently leave the biofilm when it has matured to colonize new substrates. The blue light switchable bacterial adhesions presented here also capture this aspect of biofilms as they are reversed in the dark. To study the detachment kinetics in the dark, we let bacteria displaying different pMag variants adhere to nMagHigh functionalized substrates for 1 h under blue light and subsequently moved these substrates into the dark. All the surface engineered bacteria detach from the nMagHigh substrates in the dark, but the detachment kinetics are highly dependent on the pMag variant expressed on the bacteria (**Figure 3.6a**). The bacteria detach slower beginning with bacteria displaying pMagFast1 to pMag to pMagHigh and the detachment half-lives are 12, 43 and 66 min, respectively. This order reflects the trend reported for dark reversion kinetics of pMag variants, pMagFast1 being the fastest and pMagHigh the slowest.[143] Additionally, the detachment experiments show that most bacteria can reversibly detach in the dark. Only in the case of pMagHigh displaying bacteria some bacteria are already irreversibly attached to the substrate, which could be due to secondary interactions.

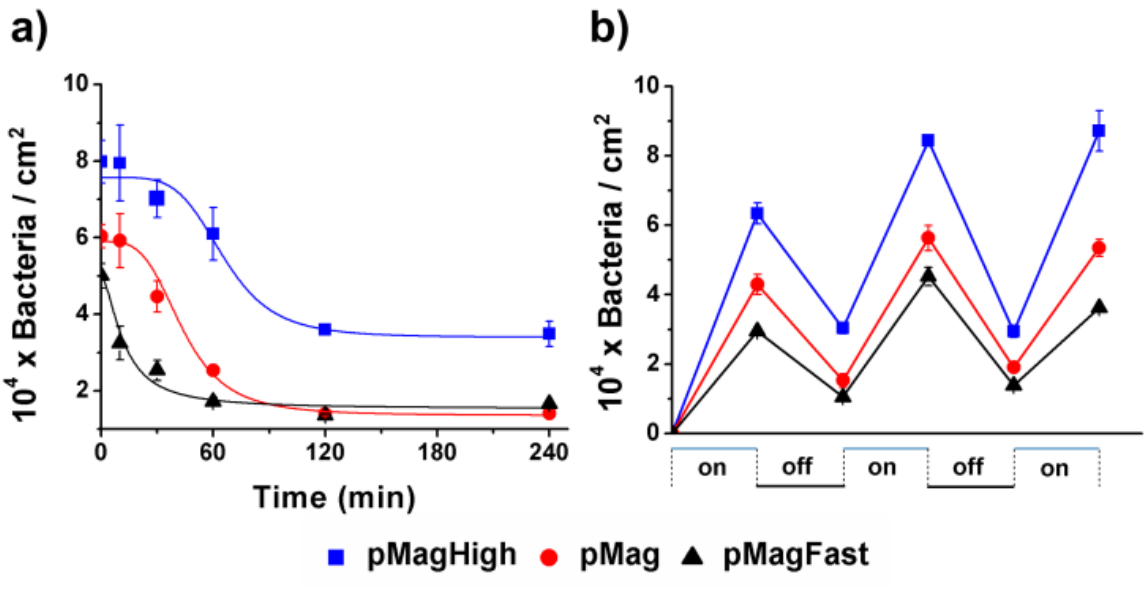

Figure 3.6 a) Bacterial detachment kinetics of bacteria displaying different pMag variants from nMagHigh functionalized substrates in the dark. Bacteria were allowed to attach for 1 h under blue light prior to placing the samples in the dark. b) Multiple attachment and detachment cycles for bacteria displaying pMag variants on nMagHigh functionalized surfaces. The samples are incubated for 1 h under blue light and for 2 h in the dark for each attachment and detachment step, respectively. The error bars are the standard error from nine images.

Reversible light controlled bacterial adhesion allows us to switch this interaction dynamically on and off repeatedly. To demonstrate this, we kept bacteria displaying different pMag variants on nMagHigh functionalized substrates, alternating between 1 h under blue light and 2 h in the dark. At the end of each step we quantified the number of adherent bacteria. We observed for all pMag variants a high number of bacteria after each blue light illumination step, and the number decreased substantially after keeping the substrate in the dark (**Figure 3.6b**). Switching between blue light and dark several times produced similar results after each cycle.

The high spatial resolution that the blue light dependent bacteria adhesions provide enabled us to photopattern these bacteria in a desired geometry. To control the local attachment of pMagHigh expressing bacteria, we illuminated a nMagHigh functionalized substrate through

a photomask with blue light for 1 h. We detected obvious bacterial patterns on the substrate that correspond to the projected photomask (**Figure 3.7**).

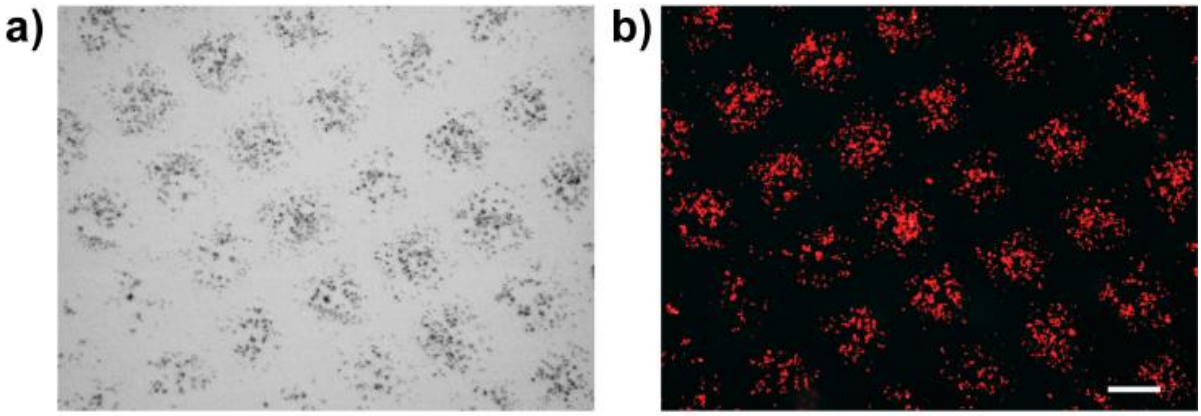

Figure 3.7 a) Bright field and b) fluorescent image of pMagHigh displaying bacteria attached to nMagHigh functionalized substrates only in areas that are illuminated with blue light through a photomask. The bacteria are labelled with mCherry for detection. Scale bar is 100 µm.

3.4 Conclusions

In summary, we present here a new platform for controlling bacteria surface adhesions based on the blue light dependent interaction between nMag and pMag proteins. This optogenetic approach is the first method that provides non-invasive, bioorthogonal and reversible control over bacterial attachment with unprecedented spatial and temporal control. The photoswitchable bacteria adhesions allow us to control and tune bacterial attachment and detachment to a high degree. These unique properties can be used to guide the formation and spatial organization of bacteria in a biofilm, which is vital in engineering bacterial consortia.

Chapter 4. Photoswitchable bacteria-bacteria adhesions for blue light controlled bacterial communities

Copyright

Aim

In chapter 3, we introduced the controlling of bacterial adhesion to surfaces in a reversible and high spatiotemporal resolution expressing the optogenetic protein pair pMag on the bacterial surface and immobilizing nMag on the substrates. Optogenetic protein pair nMag-pMag can be furtherly used to engineer the bacteria with photoswichable properties by display techniques. Therefore, blue light can induced the bacterial multi-cellular assembly and this process is reversible in the dark. Through this light controllable bacterial adhesion, multiple bacterial social interactions can be regulated, such as aggregation, quorum sensing, biofilm formation and metabolic cross-feeding between auxotrophic strains.

4.1 Abstract

Although the fundamental importance and biotechnological potential of multi-bacterial communities, also called biofilms, are well known, our ability to control them is limited. We present a new way of dynamically controlling bacteria-bacteria adhesions by using blue light and how these photoswitchable adhesions can be used to regulate multicellularity and associated bacterial behavior. To achieve this, the photoswitchable proteins nMagHigh and pMagHigh were expressed on bacterial surfaces as adhesins to allow multicellular clusters to assemble under blue light and reversibly disassemble in the dark. Regulation with visible light provides unique advantages including high spatiotemporal control, tunability and non-invasive remote regulation. These photoswitchable adhesions make it possible to regulate collective bacterial functions including aggregation, quorum sensing, biofilm formation and metabolic cross-feeding between auxotrophic bacteria with light. Overall, the photoregulation of bacteria-bacteria adhesions provides a new way of studying bacterial cell biology and will enable the design of biofilms for biotechnological applications.

4.2 Introduction

Bacteria have the outstanding ability to live in biofilm as social communities. Biofilms allow them to perform complex functions as a group that cannot be accomplished by a single bacterium.[24] Multi-bacterial communities are different from their planktonic counterparts as they share metabolites and are shielded from environmental stresses and antibiotics, allowing them to colonize diverse and even hostile environments.[150, 192] Bacterial consortia have great potential for applications in synthetic biology due to their ability to split complex biosynthetic pathways and share tasks among different specialized members, thus increasing their productivity and decreasing the metabolic burden on each member of the consortium.[45, 153] Specifically designed bacterial consortia could therefore be used in future industrial, medical and environmental applications including the synthesis of complex molecules in bacterial factories, biocatalysis,[193] waste treatment and drug delivery.[194, 195]

The fundamental importance and biotechnological potential of bacterial communities are already recognized, whereas our current understanding and ability to engineer multi-bacterial communities to perform desired tasks are both still in their infancy. Part of the complexity arises from assembling unicellular planktonic bacteria into multicellular assemblies. During this process the organization of bacteria at the micrometer length scale into multicellular structures strongly affects the fate of the co-culture because it determines diffusion rates of shared metabolites and toxins. Moreover, the interaction between bacteria is dynamic and changes over time as fluctuations in the environment and within the cells occur.[45, 196, 197] To produce biofilms with a deliberate spatiotemporal arrangement, methods for dynamically controlling bacteria-bacteria adhesions with high spatial and temporal precision are required.[49, 198, 199] Yet, methods for controlling bacteria-bacteria adhesions are very limited.[49, 152] A prime example of engineering bacteria-bacteria adhesions by Glass *et al.* uses outer membrane-displayed nanobodies and antigens as adhesins to control multicellularity, aggregation pattern and morphology.[131] In other examples, native and surface engineered bacteria were clustered together using external small molecules, polyvalent nanoparticles and polymers.[99, 104, 123, 126, 200] Yet, none of these approaches provides the required crucial dynamic and spatiotemporal control over the bacteria-bacteria adhesions.

High spatiotemporal control has been achieved using light as a trigger in the case of bacterial adhesions onto substrates, which is the first step in biofilm formation. Different approaches include the optogenetic regulated expression of adhesion molecules on bacterial surfaces[110, 111, 165, 201-203] and the modification of substrates and/or bacteria with light responsive molecules that alter bacterial adhesion.[102, 104, 168, 204] Using light as a trigger provides unique advantages. Most importantly, being able to illuminate an area of interest at a chosen time provides incomparable spatial and temporal control over the interactions. Secondly, visible light is biocompatible and offers non-invasive remote control. This is particularly advantageous for biotechnological applications when compared to small molecule inducers, as it does not require later removal and is cost efficient. Additionally, by using different intensities and light frequencies it is possible to modulate interactions in light-responsive

systems. Some light-responsive interactions are also reversible in the dark offering dynamic on/off switching. This is also why photo-regulation has been introduced to regulate other important bacterial processes including gene expression, growth, biofilm formation,[188] quorum sensing,[190, 205] bacterial attachment to mammalian cells and antibiotic activity.[126]

In this paper, we present an optogenetic approach to control reversible bacteria-bacteria adhesions with high spatiotemporal control using visible light. Photoswitchable bacteria-bacteria adhesions allow for the assembly of *E.coli* into multicellular aggregates with high spatiotemporal control and specificity in a noninvasive, reversible, sustainable and tunable manner. The fundamental properties of bacteria-bacteria adhesions have also allowed us to control associated bacterial processes including quorum sensing, biofilm formation and metabolic cross-feeding between different auxotrophic bacteria. These examples reveal that the photoswitchable bacteria-bacteria adhesions offer new design possibilities for dynamically modulating bacterial consortia, which in turn opens up new possibilities for studying both bacterial cell biology and biotechnological applications.

4.3 Results and Discussion

Engineered bacteria displaying photoswitchable proteins. As bacterial adhesins, we chose to use those photoswitchable protein interactions recently used in the field of optogenetics to regulate diverse cellular functions with visible light, including receptor activation, gene expression, protein localization and activity as well as cell adhesions.[143, 165, 206] Important benefits of optogenetic protein-protein interactions are their response to low intensity visible light, the high specificity of the protein-protein interactions and their sustained production in the cells. In this study, we used the protein pair nMag and pMag as adhesins, which heterodimerize under blue light (480 nm) and dissociate from each other in the dark.[143] Different point mutants of nMag and pMag enable us to alter the strength and back conversion in the dark; the variants nMagHigh and pMagHigh have stronger interactions with binding partners and a slower rate of reverse conversion in the dark. In contrast, nMagFast1

and pMagFast1 have weaker binding abilities and a faster rate of reverse conversion in the dark (**Scheme 4.1**).

	52 55	74 85 135 165
nMagHigh	--D--G--	I---- I---- I ---- I
pMagHigh	--R--R--	I---- I---- I ---- I
pMag	--R--R--	I---- I----M----M
pMagFast1	--R--R--	I----V----M----M

Scheme 4.1. Schematic representation of the variants with point mutations from nMagHigh to pMagFast1.

In our design, we expressed different photoswitchable proteins, nMagHigh or different variants of pMag (pMagHigh, pMag or pMagFast1) on the surface of *E.coli*. We hypothesized that co-cultures of bacteria expressing complementary interaction partners on their surfaces would reversibly aggregate under blue light and disaggregate in the dark due to the light-switchable nMag-pMag binding (**Figure 4.1a**).

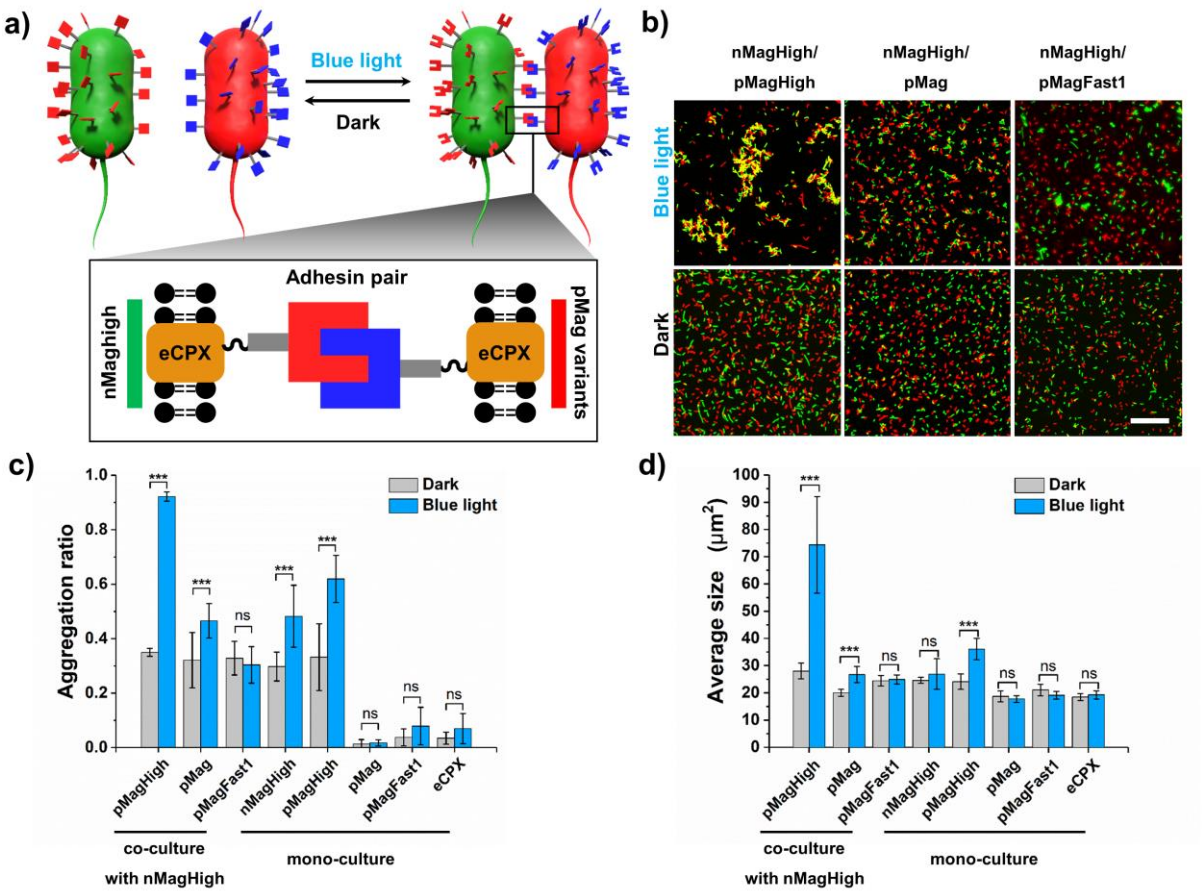

Figure 4.1. a) Photoswitchable bacteria-bacteria adhesions. *E.coli* expressing complementary blue light photoswitchable proteins on their surfaces adhere to each other under blue light and reversibly dissociate in the dark. The photoswitchable proteins nMagHigh or pMag variants were displayed on the cell surface and act as photoswitchable adhesins by fusing them to the outer membrane protein eCPX. b) Blue light-dependent aggregation of bacteria expressing nMagHigh and pMag variants. *E. coli* displaying nMagHigh (labeled with GFP) or pMag variants (labeled with mCherry) were mixed in a 1:1 ratio (OD_{600}= 0.15) and incubated for 2 h under blue light or in the dark. Scale bar is 30 μm. c) Aggregation ratio, and d) the average cluster size in co-cultures and mono-cultures of bacteria displaying photoswitchable adhesins under blue light and in the dark. The aggregation ratio is the area of bacteria clusters (objects with an area > 15 μm^2) divided by the area occupied by all bacteria. The error bars are the standard error from 25 images. ***$p < 0.001$.

To express the photoswitchable proteins on the surface of *E.coli*, we fused the C-terminal of each protein to the N-terminal of the circularly permutated outer membrane proteins OmpX

(CPX), a surface protein commonly used for bacterial display.[191, 205] Using one construct at a time (nMagHigh-eCPX or pMag-eCPX variants), each one was transformed into *E.coli* MG1655 wild-type K-12 and the expression of the new protein with the molecular weight corresponding to the surface displayed protein was observed in lysates of these bacteria on an SDS-PAGE gel (**Figure 4.2**).

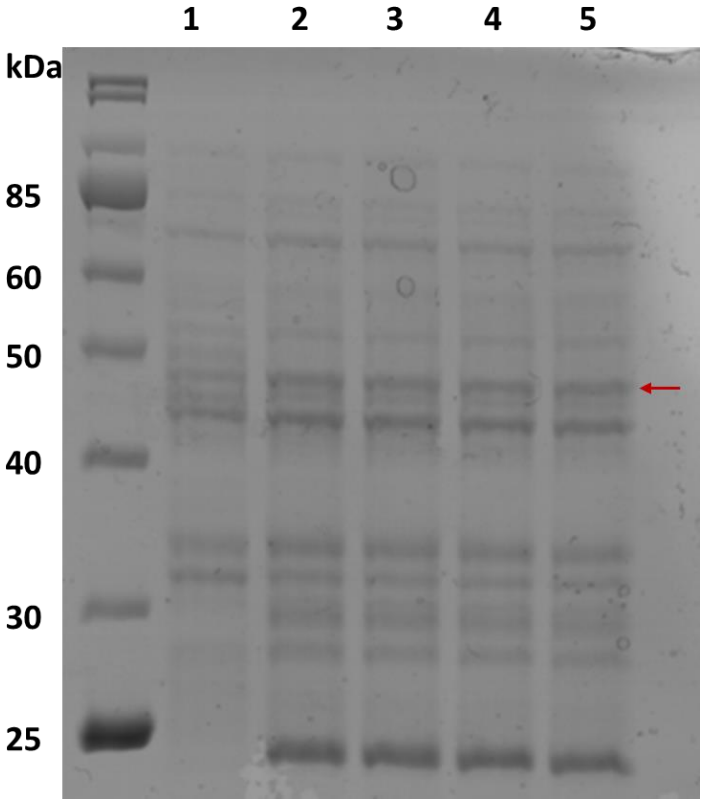

Figure 4.2. 10% SDS-PAGE of *E. coli* MG1655 bacteria, which displayed 1. no pMag protein 2. nMagHigh, 3. pMagHigh, 4. pMag, 5. pMagFast1 on the outer membrane surface. NEB 10-200 unstained protein marker was used. Molecular weights of nMagHigh-eCPX or pMag-eCPX fusion protein are 40.8 kDa.

Blue light-switchable nMag-pMag protein interactions enable bacteria cell-cell adhesion. Given that the proteins were sufficiently accessible on the cell surface, we expected that co-cultures of bacteria displaying nMagHigh and pMag proteins would form cell-cell adhesion interactions under blue light and be visible as large bacterial aggregates. To test if the photoswitchable proteins were able to mediate light dependent bacteria-bacteria adhesions, we mixed bacteria displaying nMagHigh with bacteria displaying one of the pMag

variants on their surface in a 1:1 ratio (OD_{600} is 0.15), either under blue light or in the dark. For detection we co-expressed green fluorescent protein (GFP) and a red fluorescent protein (mCherry) inside the bacteria displaying nMagHigh and pMag variants, respectively. After 2 h incubation under blue light bacteria aggregates were, in fact, visible under the fluorescent microscope, but not in samples kept in the dark (**Figure 1b**). The most prominent bacterial aggregates were formed under blue light in co-cultures of bacteria displaying nMagHigh and pMagHigh, followed by co-cultures of nMagHigh and pMag. However, almost no aggregation was observed in co-cultures of pMagHigh with the weakest binder being pMagFast1. The blue light-triggered aggregation was clearly due to the photoswitchable proteins displayed on the bacteria since bacteria just displaying eCPX (negative control) did not aggregate and were homogeneously distributed over the sample.

Next, we quantified the extent of aggregation and the aggregate sizes under blue light and in the dark. This was done for both mixed cultures of nMagHigh with different pMag-displaying bacteria and mono-cultures in order to gain not only an insight into the specificity of the photoswitchable interactions, but also to assess the contribution of heterophilic and homophilic interactions between bacteria. As a parameter, the aggregation ratio was defined as the area occupied by clusters of bacteria (objects with an area > 15 μm^2, the average area of a single *E.coli* is 2.5 μm^2, only objects bigger than 6 bacterial cells were considered to be clusters) divided by the total area occupied by all bacteria (**Figure 4.1c**). This quantification showed that in co-cultures of nMagHigh and pMagHigh-displaying *E.coli,* 90% of the bacteria were integrated into clusters under blue light, whereas only 30% of bacteria were clustered in the dark. Moreover, the average cluster size (only objects with an area > 15 μm^2 were counted as clusters) was 75 μm^2 under blue light, which was significantly larger than the clusters observed in the dark (average size of 30 μm^2) (**Figure 4.1d**). The aggregation ratio analysis also confirmed the initial qualitative observation that co-cultures of nMagHigh and pMag partially formed clusters under blue light, whereas co-cultures of nMagHigh and pMagFast1 did not. Mono-cultures of bacteria displaying nMagHigh or pMagHigh aggregated to some extent when exposed to blue light with up to 50% of the bacteria being

integrated into clusters. On the other hand, pMag and pMagFast1-displaying bacteria did not self-aggregate and showed comparable aggregation with the control strain, eCPX. The partial self-aggregation of nMagHigh and pMagHigh-displaying bacteria was not surprising as both of these proteins can homodimerize to some degree, whereas the heterophilic interaction between these proteins is much stronger.[35] Hence, some of the aggregation observed in co-cultures of nMagHigh with either pMag or pMagFast1-displaying bacteria could be attributed to the homophilic interaction of nMagHigh-displaying bacteria. In the case of the co-cultures of nMagHigh and pMagHigh-displaying bacteria, the heterophilic interactions were the dominating factor leading to aggregation as observed by the high aggregation under blue light in these cultures and the overall larger clusters. Also, confocal laser scanning microscopy (CLSM) scans showed intermixed 3D aggregates of nMagHigh and pMagHigh bacteria under blue light (**Figure 4.3**).

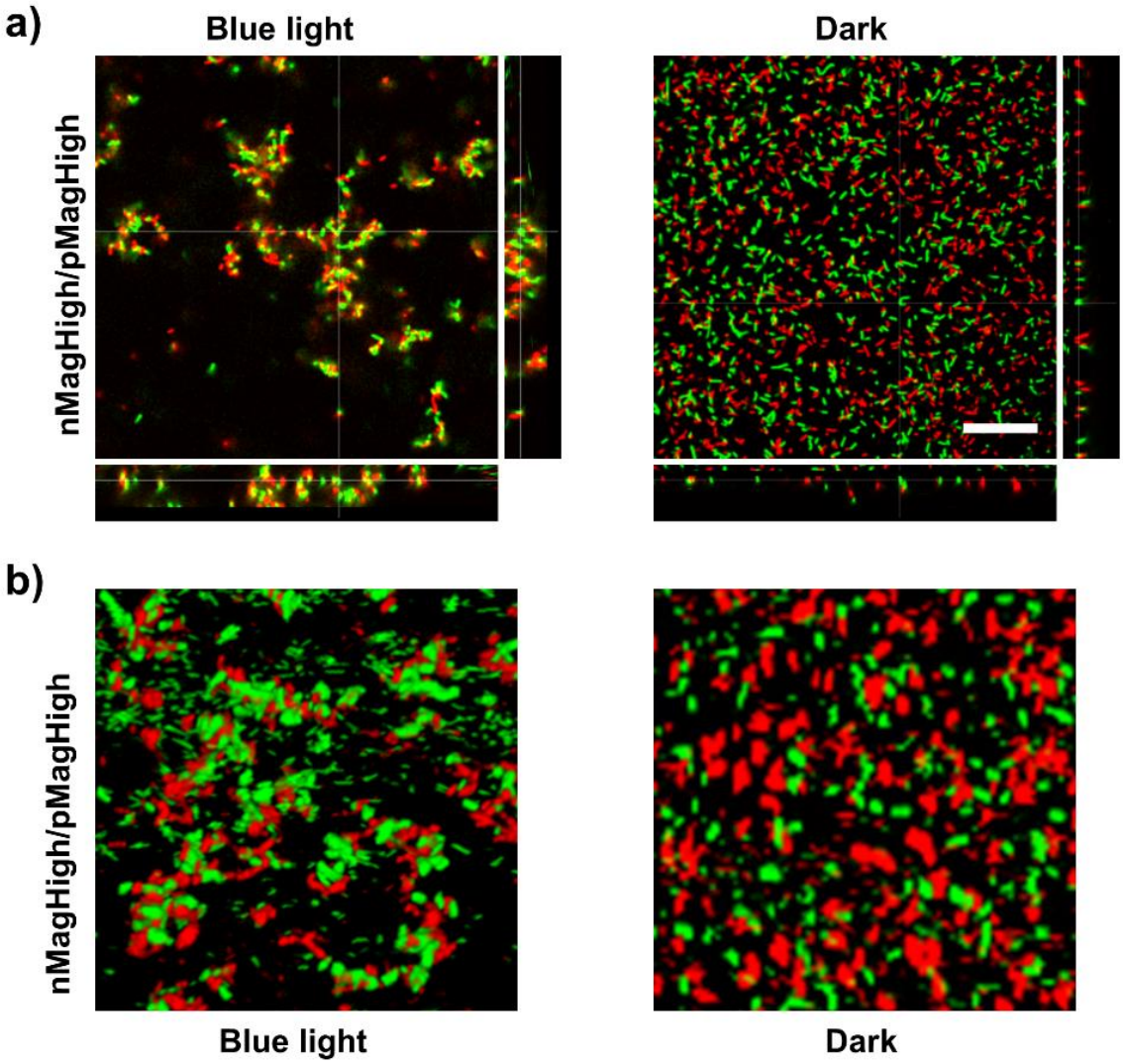

Figure 4.3 a) Stacks scanning images of *E. coli* co-cultures. *E. coli* displaying nMagHigh (labeled with GFP) or pMagHigh (labeled with mCherry) were mixed in a 1:1 ratio (OD_{600}= 0.15) and incubated for 2 h under blue light and in the dark. Scale bar is 30 µm. b) 3D reconstruction images of *E. coli* co-cultures under blue light and in the dark.

Additionally, the aggregation ratios in co-cultures of nMagHigh and pMagHigh displaying bacteria mixed in different ratios (nMagHigh:pMagHigh= 1:1, 2:1, 4:1, and 6:1) showed that aggregation was the most efficient in 1:1 mixed cultures with 87 % of the bacteria being part of a cluster after 2 h under blue light (**Figure 4.4**). Yet, also at higher mixing ratios bacterial aggregation was still significant, as each bacterium displays many copies of the photoswitchable proteins and can interact with multiple bacteria around it.

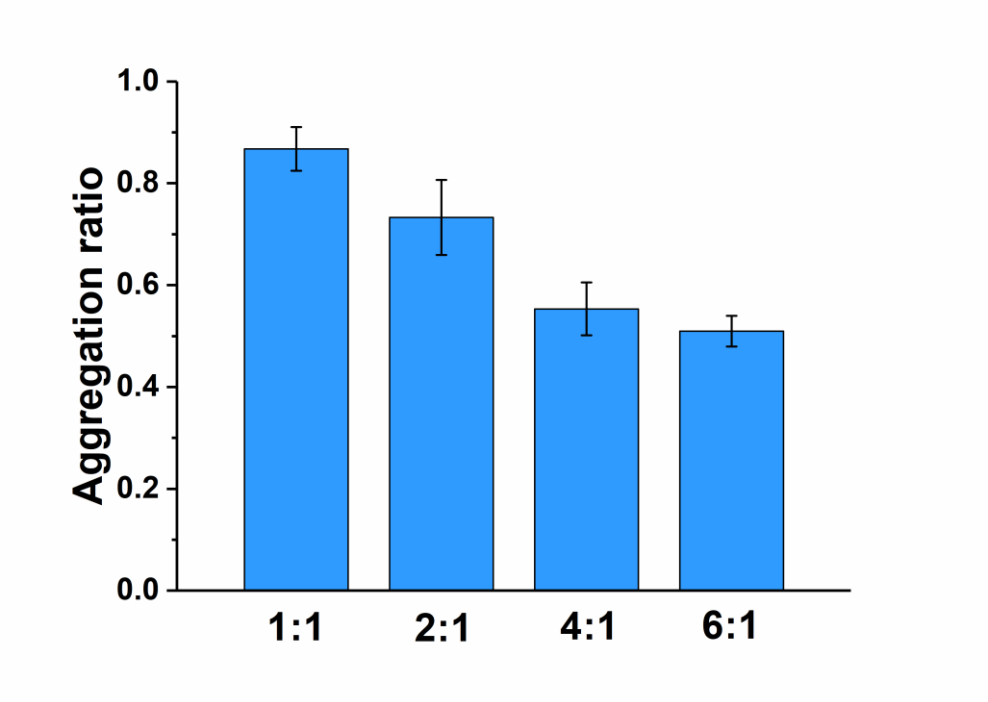

Figure 4.4 *E. coli* displaying nMagHigh (GFP labeled) and pMagHigh (mCherry labeled) were mixed in a ratio of 1:1, 2:1, 4:1, 6:1 (OD600= 0.15) and incubated for 2 h under blue light or in the dark. The error bars are the standard error from 25 images.

Bacterial aggregation leads to faster sedimentation. To confirm the results on the photoswitchable cell-cell adhesions, we allowed mixed cultures of nMagHigh and pMag-expressing strains or mono-cultures (OD_{600}= 1.0) to stand unshaken. We then quantified bacteria sedimentation by measuring optical density (OD_{600}) of the cells remaining in the upper half of the cultures after 1 h. We found that mixed cultures of nMagHigh with pMag variants all settled faster when exposed to blue light than in the dark (**Figure 4.5**).

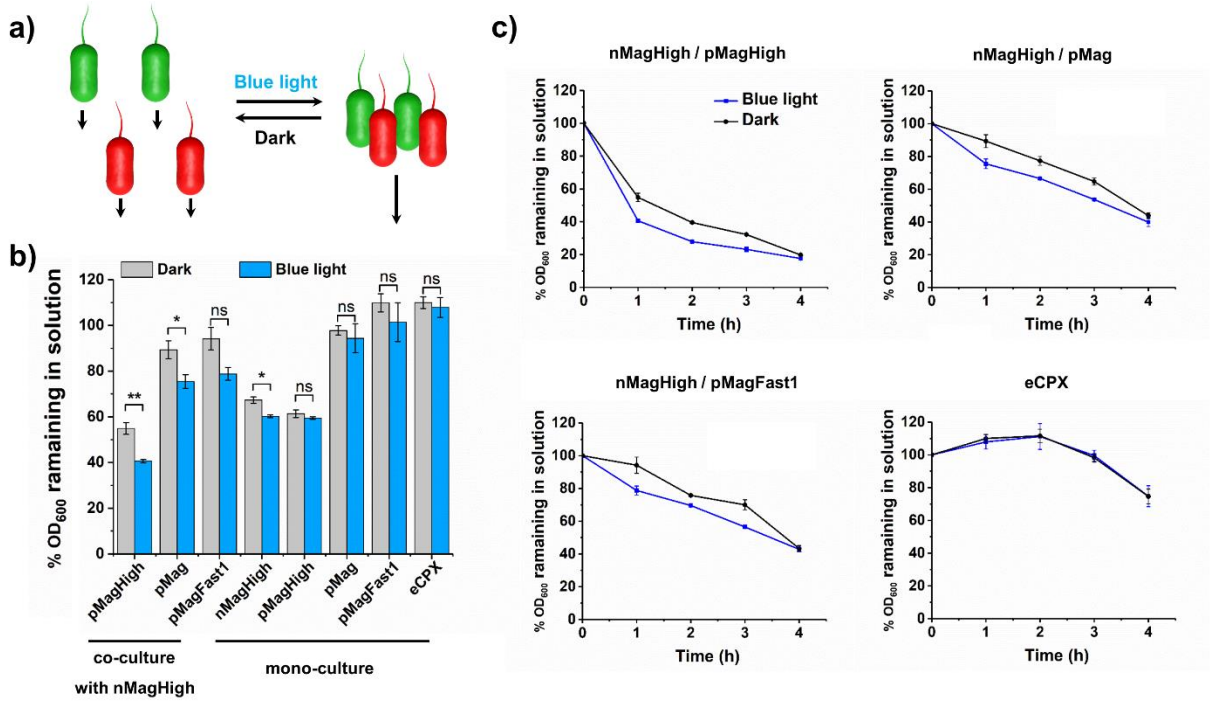

Figure 4.5 a) A schematic illustration of enhanced bacterial sedimentation due to the co-aggregation under blue light. nMagHigh or pMag variants displaying bacteria were labeled in green or red color, respectively. b) Bacterial sedimentation in co-cultures and mono-cultures of *E. coli* displaying nMagHigh or pMag variants in a 1:1 ratio (OD_{600}= 1.0) for 1 h under blue light and in the dark. The difference in sedimentation under blue light and in the dark was most obvious for mixtures of nMagHigh and pMagHigh cultures. eCPX bacteria were used as control. $^{**}p < 0.01$. $^{*}p < 0.05$. c) Sedimentation kinetics of bacterial co-cultures in a 1:1 ratio under blue light illumination and in the dark for 4 h.

The difference in sedimentation under blue light and in the dark was most obvious for mixtures of nMagHigh and pMagHigh cultures. Contrastingly, mono-cultures and the control strain, eCPX, showed no significant differences in sedimentation either after exposure to blue light or in the dark. As co-cultures of nMagHigh and pMagHigh-displaying bacteria showed the most significant co-aggregation under blue light, subsequent experiments were carried out using this adhesin pair.

Bacteria-bacteria adhesions can be tuned by means of multiple strategies. The adhesions between bacteria displaying nMagHigh and pMagHigh can be adjusted by controlling

illumination time, illumination area, light intensity and bacterial density. The first way to adjust the bacteria-bacteria co-aggregation was done by controlling the time of illumination. When the co-aggregation of nMagHigh and pMagHigh-displaying bacteria under blue light was monitored in real time over 12 h, initially bacteria clusters formed quickly within the first 2 h (**Figure 4.5a-b**). After 2 h, the increase of the aggregation ratio slowed down and reached a plateau after 6 h (**Figure 4.5b**). Even though the aggregation ratio did not increase much after this point, the sizes of the clusters increased significantly over time. The reason for this was that existing clusters dynamically fused and rearranged to maximize bacteria-bacteria interactions. On the other hand, when nMagHigh and pMagHigh-displaying bacteria were incubated in the dark for 12 h, no obvious bacterial clusters were observed.

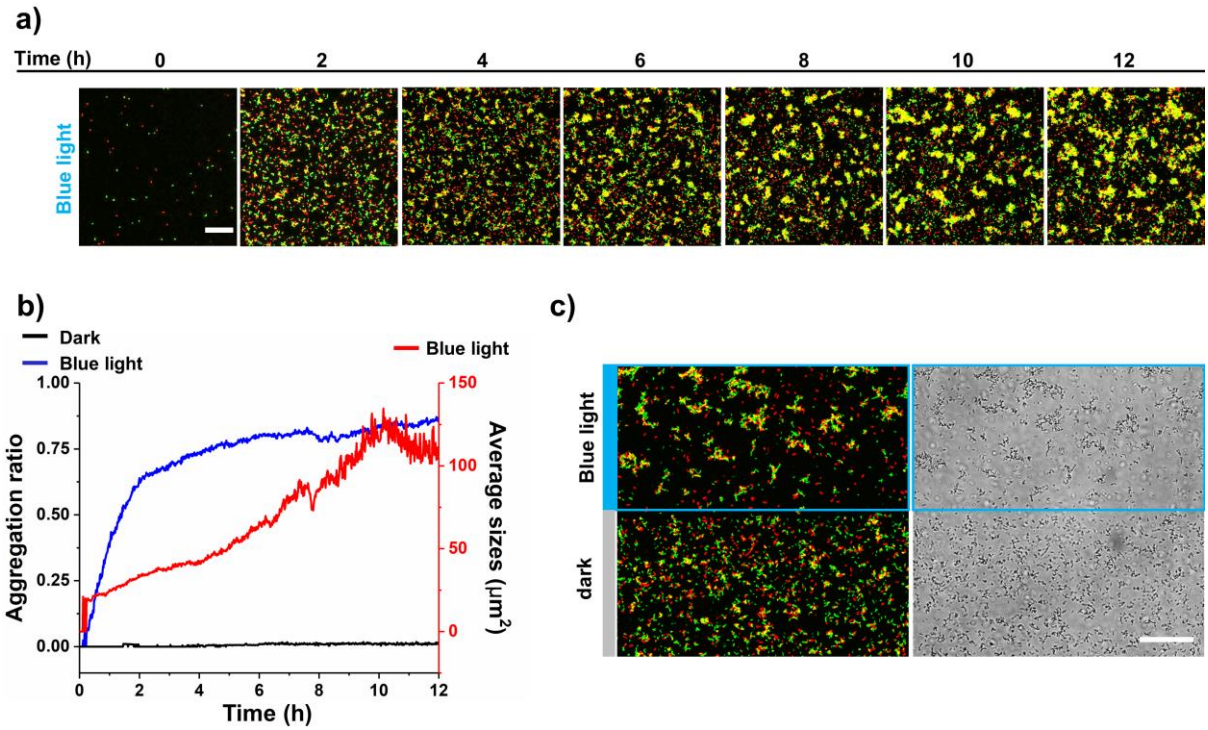

Figure 4.5 Temporal and spatial control of photoswitchable bacteria-bacteria adhesions. a) Co-aggregation of bacteria displaying nMagHigh (GFP labeled) and pMagHigh (mCherry labeled) under blue light over time monitored with fluorescence microscopy. Scale bar is 50 μm. b) The aggregation ratio and average aggregate size over time under blue light and in the

dark. c) The blue light illumination in the upper part of the field of view leads to spatially controlled co-aggregation, which is not observed in the lower part of the image kept in the dark. Scale bar is 50 μm.

It should be noted that bacterial growth under the conditions of the experiment (in PBS at room temperature over 12 h) was negligible (**Figure 4.6a**) and hence had no effect of the aggregation ratio. Overall, bacterial aggregation that occurred under blue light came about in two steps: first bacteria aggregate into clusters and then clusters coalesce into larger clusters.

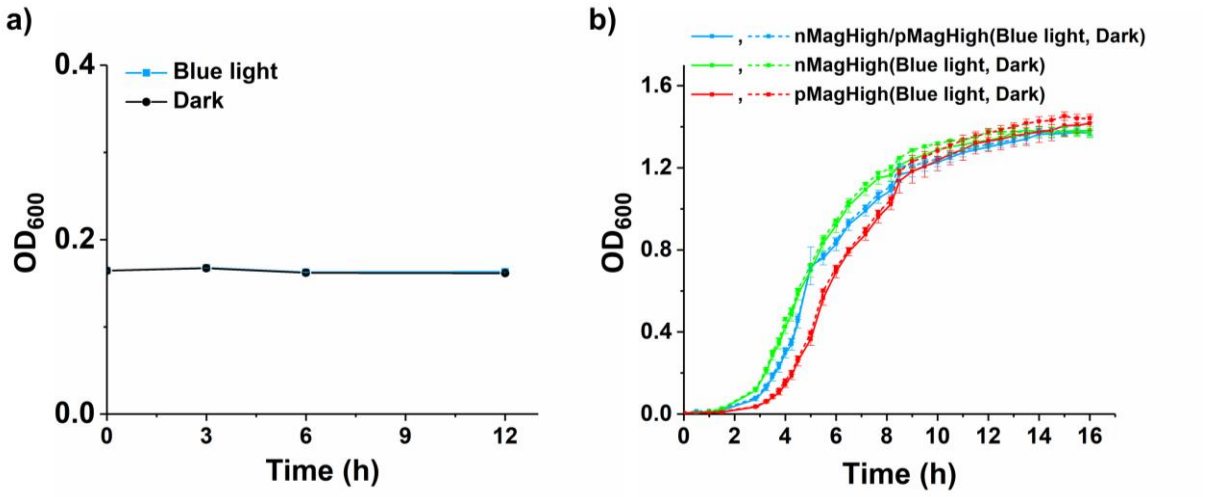

Figure 4.6. Bacterial growth curves in the dark and under blue light. a) Optical density of a 1:1 mixed co-culture of nMagHigh (GFP labeled) and pMagHigh (mCherry labeled) displaying bacteria in PBS at room temperature over 12 h. (initial OD_{600} = 0.15) b) Growth curve of nMagHigh (GFP labeled) and pMagHigh (mCherry labeled) displaying bacteria in mono- and 1:1 co-cultures in LB medium at 37 ^{o}C, 300 rpm over 16 h under blue light and in the dark. The error bars are the standard deviation from 3techinical replicates.

The second important feature that photoregulation provides is spatial control by selecting the area of light illumination. To demonstrate the spatial control over bacteria aggregation, we firstly allowed mixed cultures of nMagHigh and pMagHigh displaying bacteria (OD600= 0.2) to settle down on a surface and then stimulated half of the field of view with blue light

(confocal 488 nm laser) for 2 h. Large bacterial clusters formed only in the blue light illuminated area but not in the dark part (**Figure 4.5c**). The quantification of the aggregation ratio and the average cluster size showed that in the illuminated area 80% of the bacteria were integrated into clusters but were more than twice as big as the clusters in the dark (**Figure 4.7**). Taken together, the photoswitchable bacteria-bacteria adhesion allow controlling when and where bacteria co-aggregate.

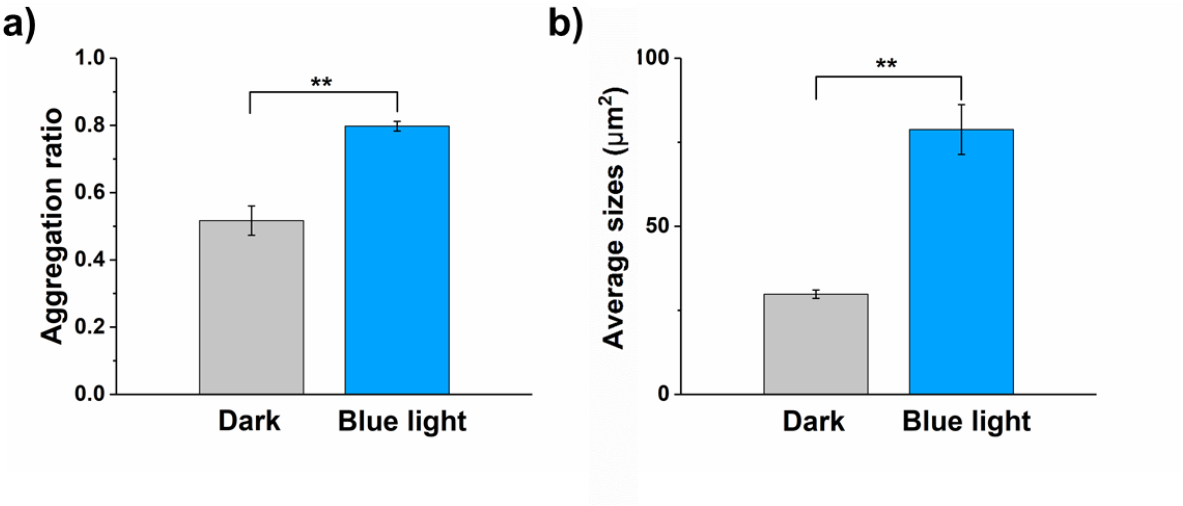

Figure S6. a) Aggregation ratio, and b) the average cluster size of bacteria in the upper (blue light activated) and lower (dark) area of the images in Figure 2c. The error bars are the standard deviation from 3technical replicates. $^{**}p < 0.01$.

An important advantage of light-controlled interactions is that they can be tuned using different intensities of light, which only partially activate the interactions. To tune the strength of bacteria-bacteria interactions, we examined the bacterial co-aggregation of nMagHigh and pMagHigh-displaying bacteria under varying blue light intensities after 2 h (**Figure 4.8a, Figure 4.9**). Even a blue light intensity of just 17 μW/cm^2 partially activated the bacterial aggregation, resulting in 40% of the bacteria integrating into clusters. In comparison, when applying a blue light intensity of 270 μW/cm^2 blue light-dependent aggregation was completely activated, resulting in 90% of the bacteria integrating into clusters.

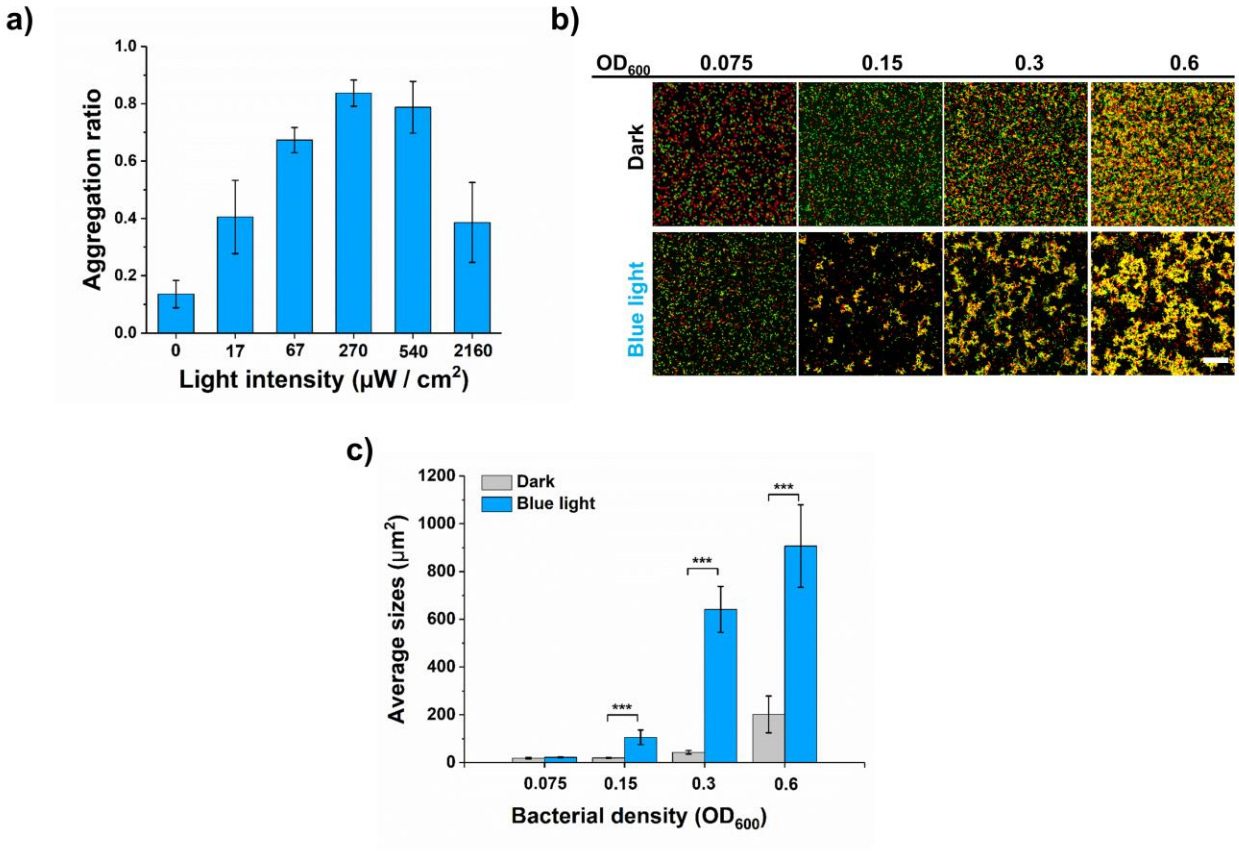

Figure 4.8 Tuning photoswitchable bacteria-bacteria adhesions. a) The influence of blue light intensity on the co-aggregation of nMagHigh and pMagHigh-displaying E.coli. b) Microscopy images and c) average cluster size of 1:1 mixed co-cultures at different cell density under blue light and in the dark. Scale bar is 50 μm. The error bars are the standard error from 25 images. ***$p < 0.001$.

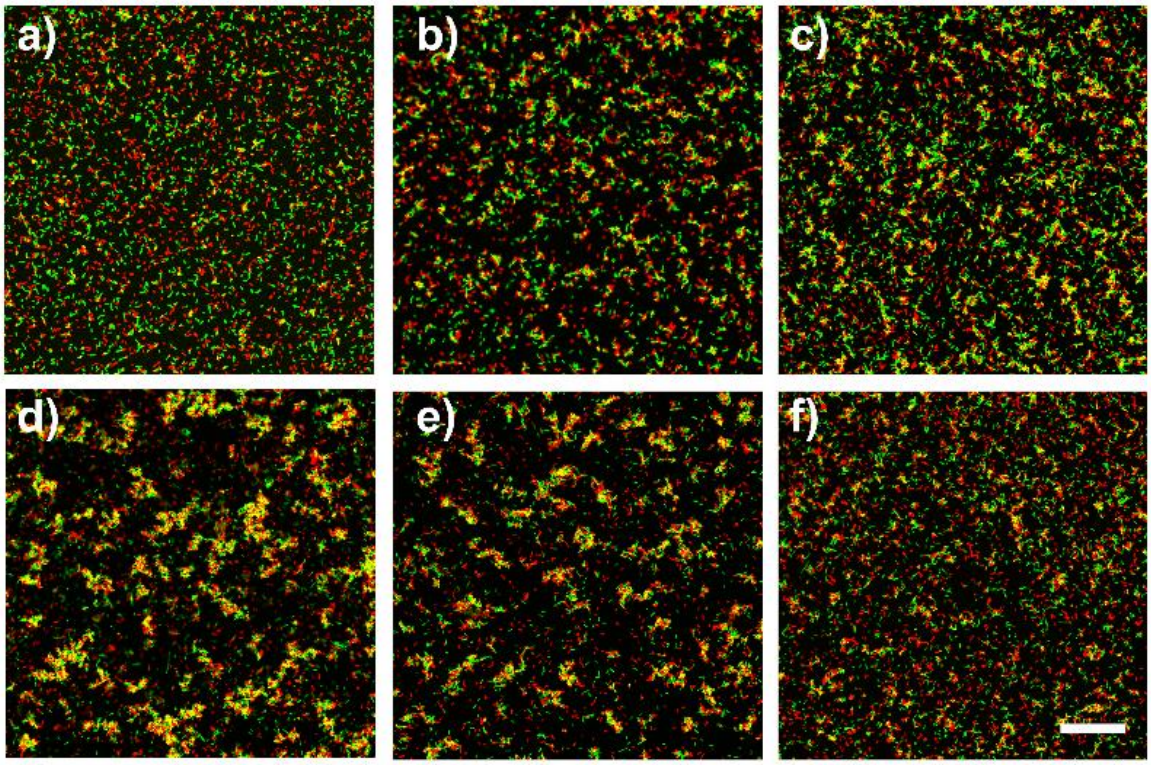

Figure 4.9 Co-aggregation of *E.coli* under blue light with an intensity of a) 0; b) 17; c) 67; d) 270; e) 540; f) 2160 µW / cm^2. *E. coli* displaying nMagHigh (labeled with GFP) or pMagHigh (labeled with mCherry) were mixed in a 1:1 ratio (OD_{600}= 0.15) and incubated for 2 h. Scale bar is 50 µm.

It should be noted that the blue light intensities applied are extremely low and are nontoxic to the bacteria as observed in live/dead staining for bacteria (**Figure 4.10**). Only a blue light intensity of 2160 µW/cm^2, which is 8 times higher than the light intensity used in our experiments, reduced the bacterial aggregation ratio to 40%, potentially due to the light toxicity. These findings demonstrate that photoswitchable bacteria-bacteria interactions are tunable over a wide range simply by altering the intensity of the blue light exposure.

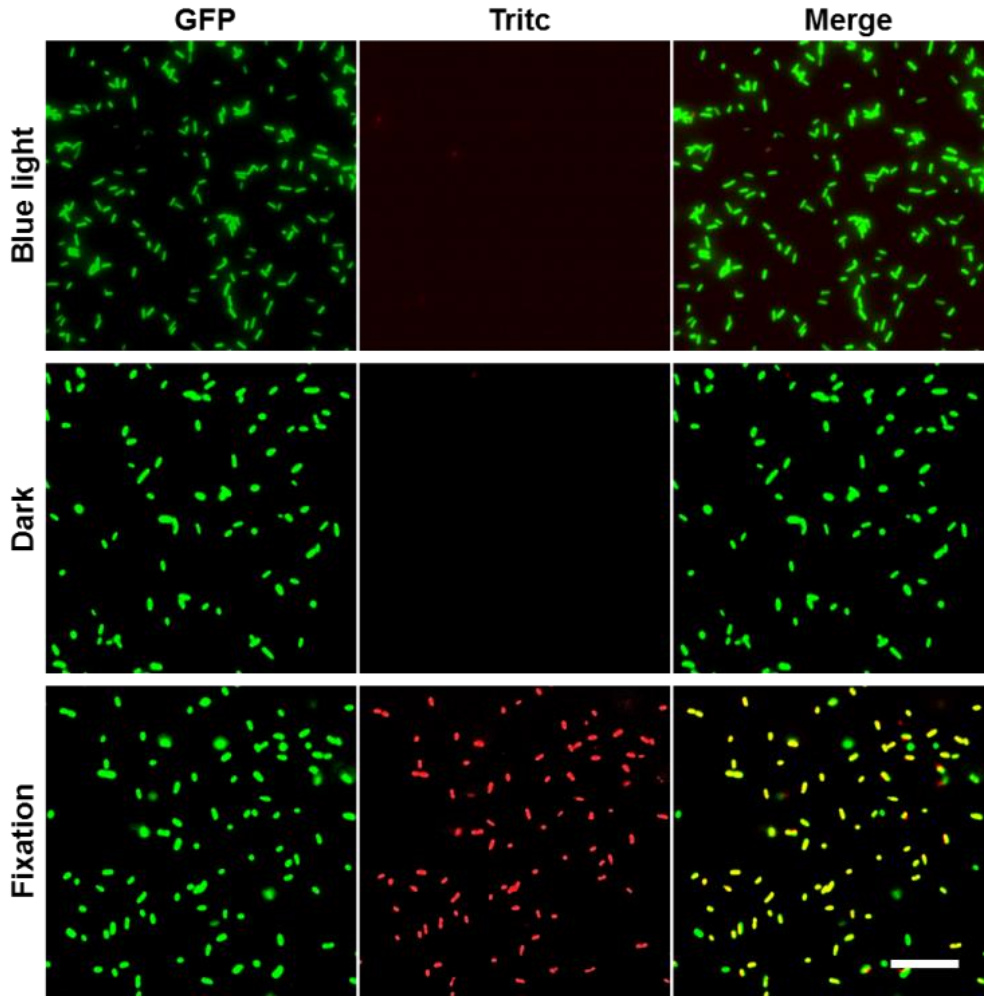

Figure 4.10 Dead cell staining of *E. coli* after incubation under blue light, in the dark or fixation with 4% PFA for 2 h. Bacteria were labelled by GFP for observation. Dead cell staining dye is from the kit of Live and Dead Cell Assay. Dead bacteria were stained with red fluorescence. The blue light (intensitiy is 540 μW / cm^2) applied is nontoxic to the bacteria as observed and comparable to the dark control. Scale bar is 20 μm.

Bacterial density is also an important parameter in controlling bacterial aggregation. To determine what minimal bacterial density is needed in order to assemble bacterial clusters under blue light and how clustering depends on bacterial density, we measured the aggregation of nMagHigh and pMagHigh-displaying bacteria at different bacterial densities. Bacteria aggregated more significantly and formed larger clusters with increasing bacterial density (**Figure 4.8b-c**).

At very low densities (OD_{600} = 0.075), aggregation was negligible after 2 h, presumably due to the low probability of bacteria encountering one another. When the density was above 0.15, bacteria co-aggregated under blue light, but not in the dark. The blue light-dependent aggregation was also observed at higher densities (OD_{600} = 0.6), whereas in the dark only little bacterial aggregation was observed despite high crowding. In previous reports, *E. coli* MG1655 was shown to auto-aggregate at an even higher density (OD_{600} = 2.0), which depends on the adhesin antigen 43 (Ag43).[115] Therefore, the blue light-triggered bacterial aggregation reported here is significant for bacterial cultures at low bacterial density, where also the cultures are translucent enough to permit light delivery as an external stimulus (**Figure 4.11**).

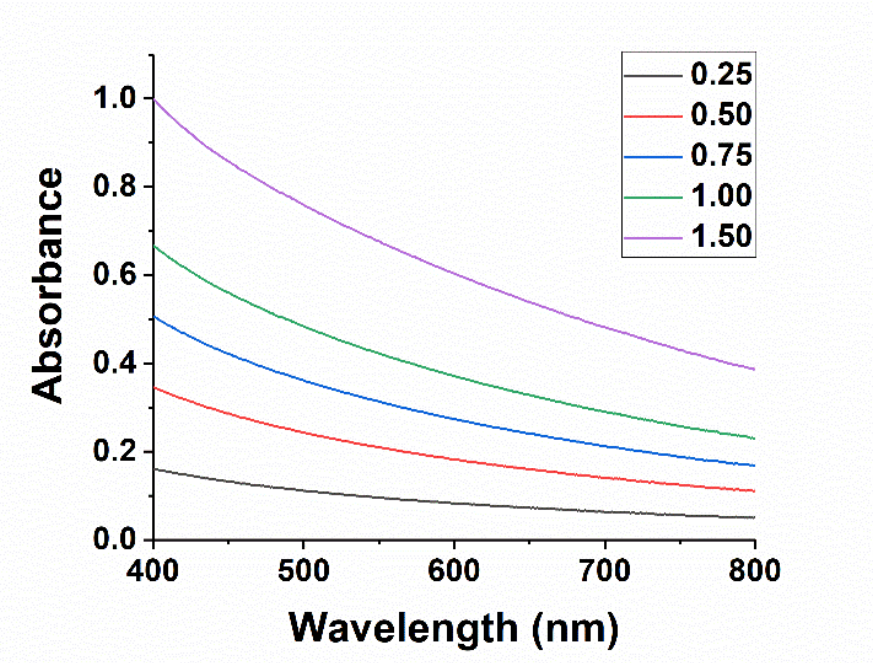

Figure 4.11 UV-vis spectrum of *E. coli* in series of optical density (OD_{600} is 0.25, 0.50, 0.75, 1.00, 1.50). The absorbance at 480 nm is below 1. indicating the possibility for efficient blue light delivery.

Reversibility of bacterial co-aggregation. A key feature of the nMagHigh and pMagHigh adhesin pair is their ability to reverse in the dark. Reversibility is an important feature, as in bacterial communities the relationship and interactions between different bacteria change

over time depending on the phase in their lifecycle and in environmental conditions. For example, the detachment of bacteria from mature biofilms and the reversion to a planktonic state enable bacteria to form new biofilms in other places. To date, engineered bacterial-bacterial adhesions are not reversible; once the interactions are established they keep bacteria in place permanently. The reversibility of the nMagHigh-pMagHigh protein interaction in the dark allowed us repeatedly to switch bacterial cell-cell adhesions dynamically on and off. To demonstrate this, we kept a mixture of nMagHigh and pMagHigh-displaying bacteria, alternating between 1 h under blue light and 1 h in the dark and at the end of each step quantified the bacterial aggregation. The bacterial aggregation ratio increased after each exposure to blue light illumination and decreased after each incubation phase in the dark (**Figure 4.12**).

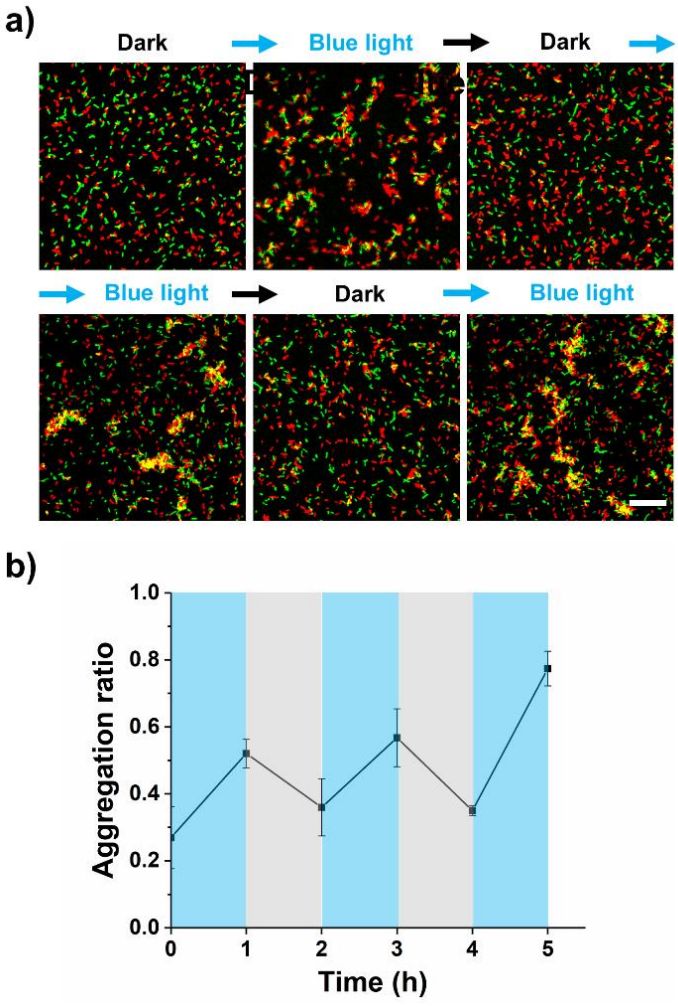

Figure 4.12 Reversibility of the photoswitchable bacteria-bacteria adhesions during multiple blue light and dark cycles. a) Fluorescent images of nMagHigh (GFP labeled) and pMagHigh (mCherry labeled) bacteria incubated in turn for 1 h under blue light and 1 h in the dark. After each blue light step multicellular clusters assembled and after each dark step the clusters disassembled. Scale bar is 25 μm. b) Changes in the aggregation ratio over multiple blue light/dark cycles. The error bars are the standard error from 25 images. Blue and grey shaded backgrounds indicate 1 h periods where the blue light illumination was turned on and off, respectively.

The duration of the blue light induced bacterial clustering is an important parameter for their reversibility as longer contacts can lead to the production of extracellular polymeric substances and abolish the reversibility. While after up to 2 h of blue light illumination the aggregates still mostly disassembled upon stopping the blue light illumination, aggregates assembled under longer blue light illumination (4 hours) were no longer reversible (**Figure 4.13**). The reversibility and the repeated switchability of the nMagHigh-pMagHigh-mediated bacterial adhesions provide us with not only with unprecedented dynamic control over bacteria interactions, but can also be used to switch related bacterial functions on and off.

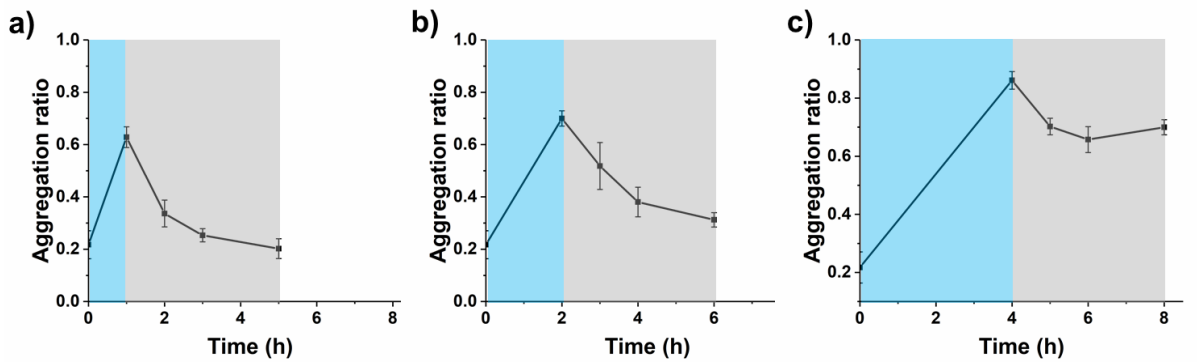

Figure 4.13 Reversibility of the photoswitchable bacteria-bacteria. Co-cultures of nMagHigh and pMagHigh bacteria incubated for a) 1 h b) 2 h c) 4 h under blue light before placing the cultures in the dark. The error bars are the standard error from 25 images. Blue and grey

shaded backgrounds indicate the periods where the blue light illumination was turned on and off, respectively.

Blue light-switchable bacterial aggregation-induced quorum sensing activation. The aggregation of bacteria is not just a physical phenomenon, but also profoundly impacts bacterial cell biology. The light-triggered bacteria-bacteria adhesions, therefore, provide a unique tool to photoregulate bacterial behavior. Given this, we tested whether we can control bacterial quorum sensing, biofilm formation and cross-feeding in bacterial communities by using light.

Bacteria use quorum sensing to sense their own local density and thereby regulate diverse cellular functions and population behavior including biofilm formation, virulence gene expression, bioluminescence, and antibiotic resistance.[126, 190, 207, 208] In the case of quorum sensing, bacteria release small molecules, called autoinducers, into their environment in order to detect their local concentration in such a way that bacteria then activate quorum sensing once a critical level is reached. The starting hypothesis was that blue light-triggered bacterial clustering would lead to a higher local concentration of autoinducers within the clusters and activate quorum sensing at lower bacterial densities compared to non-clustered bacteria. For this purpose, we transformed nMagHigh and pMagHigh-displaying bacteria with the quorum sensing reporter plasmid, *Plsr*-egfp, which expresses a green fluorescent protein upon quorum sensing activation.[115] In co-cultures of nMagHigh and pMagHigh-expressing bacteria the green fluorescence signal was significantly higher after 2 h in cultures incubated under blue light than in the dark as detected by fluorescence microscopy and flow cytometry (**Figure 4.14, Figure 4.15**). In a control experiment with eCPX bacteria that do not display photoswitchable proteins, quorum sensing was not enhanced under blue light. Therefore, the stronger activation of quorum sensing was clearly due to the light-triggered clustering of bacteria. These results demonstrate the feedback between bacteria clustering and quorum sensing and that the blue light-switchable bacteria-bacteria interaction can be used to change quorum sensing behavior.

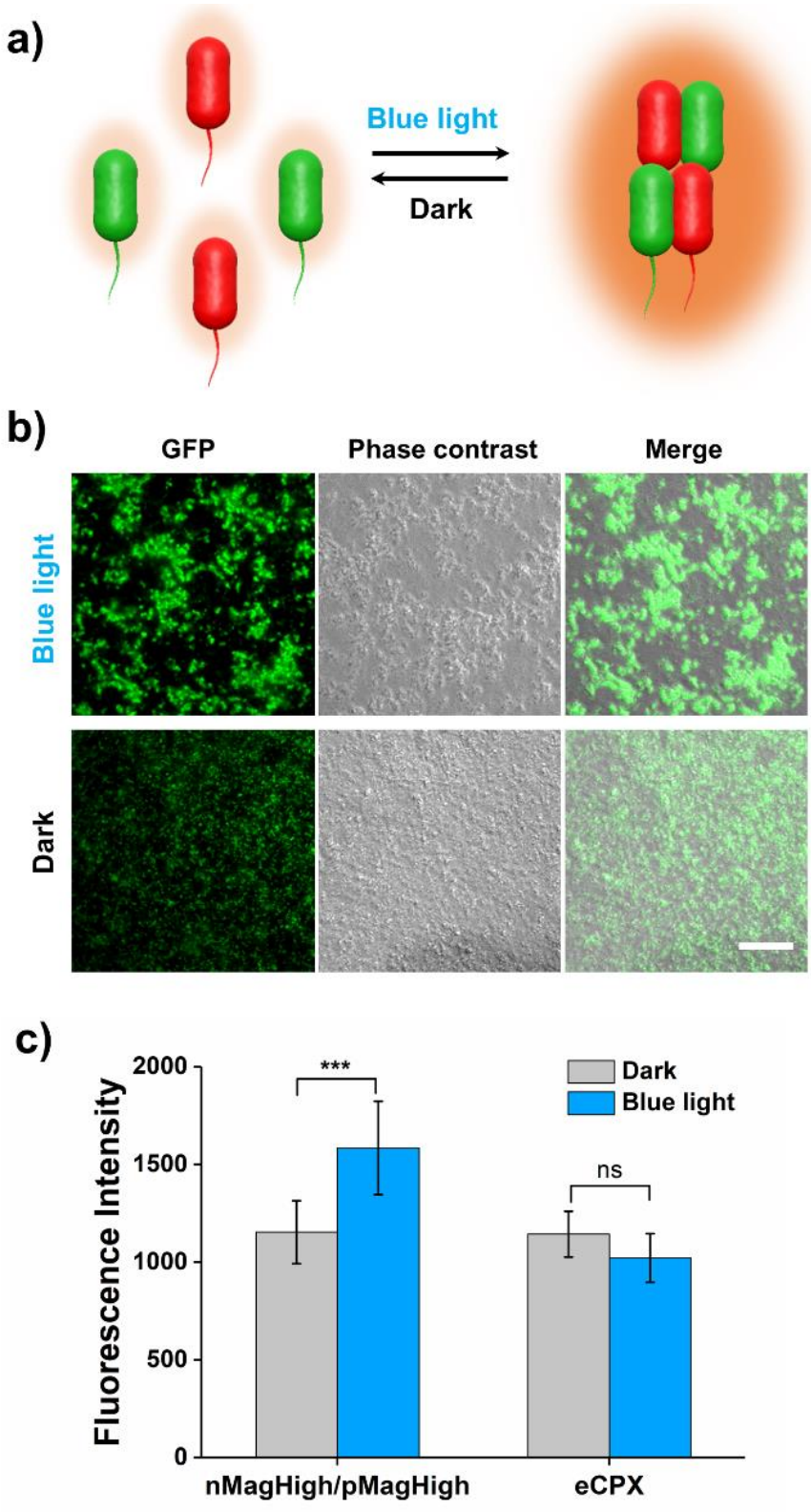

Figure 4.14 Photoswitchable adhesions trigger quorum sensing under blue light. a) A schematic illustration of bacterial quorum sensing triggered by photoswitchable adhesions under blue light. nMagHigh or pMagHigh displaying bacteria were labeled in green or red

color, respectively. b) Fluorescence and bright field microscopy images of co-cultures of nMagHigh and pMagHigh-displaying bacteria transformed with a green fluorescence quorum sensing reporter under blue light or in the dark after 2 h. Under blue light, bacteria aggregated and became fluorescent due to the activation of quorum sensing, but not in the dark. Scale bar is 50 μm. c) Quantification of the green fluorescence b) and control bacteria just displaying eCPX. The error bars are the standard error from 9 images. ***$p < 0.001$.

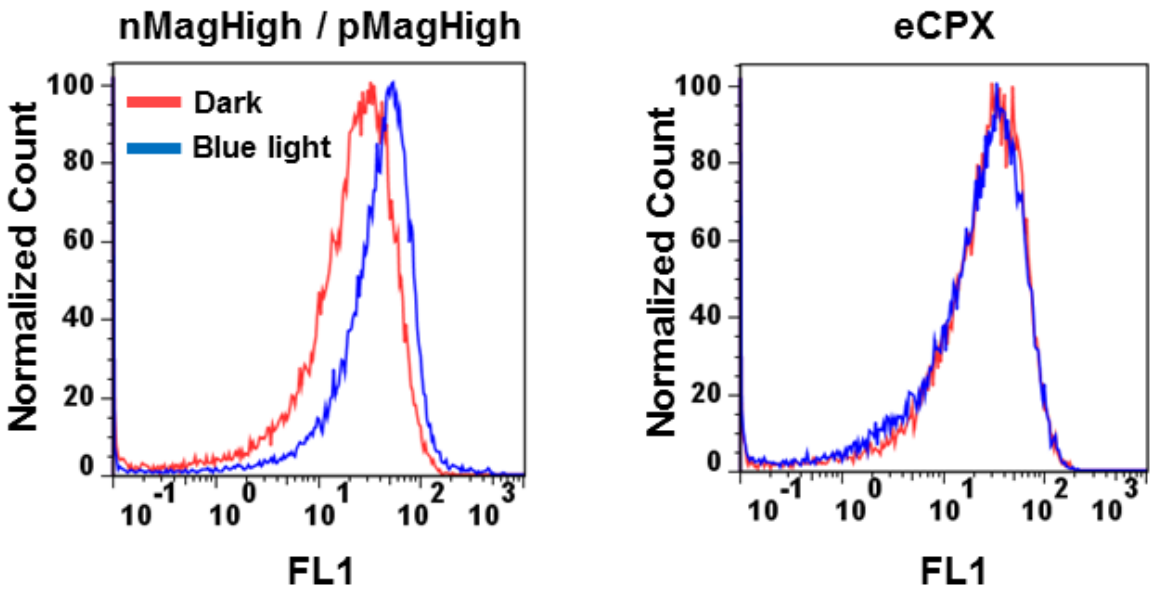

Figure 4.15 Flow cytometry analysis of bacterial quorum sensing activation by the measurement of GFP fluorescence. Co-cultures of nMagHigh and pMagHigh-displaying bacteria transformed with a green fluorescence quorum sensing reporter were incubated under blue light or in the dark for 2 h. Under blue light, bacteria aggregated and became fluorescent due to the activation of quorum sensing, but not in the dark.

Blue light-switchable bacterial aggregation enhanced bacterial biofilm formation. Biofilm formation is closely coupled to bacterial aggregation mediated by *E.coli* adhesin Ag43 and curli fibers.[115] To test if the engineered nMagHigh and pMagHigh adhesin pair can enhance biofilm formation under blue light, we seeded a mixture of bacteria displaying nMagHigh and pMagHigh into glass chambers, either under blue light or in the dark, for 48 h at 37 °C. The bacteria were labelled with GFP for observation and bacteria just displaying

eCPX were used as a negative control. A denser biofilm formed under blue light than that in the dark for a mixture of bacteria displaying nMagHigh and pMagHigh, as observed with confocal microscopy (**Figure 4.16a-b**). Moreover, for bacteria displaying nMagHigh and pMagHigh the biofilm was thicker under blue light than in the dark and in the dark the biofilm was comparable to the control eCPX bacteria (**Figure 4.16c**).

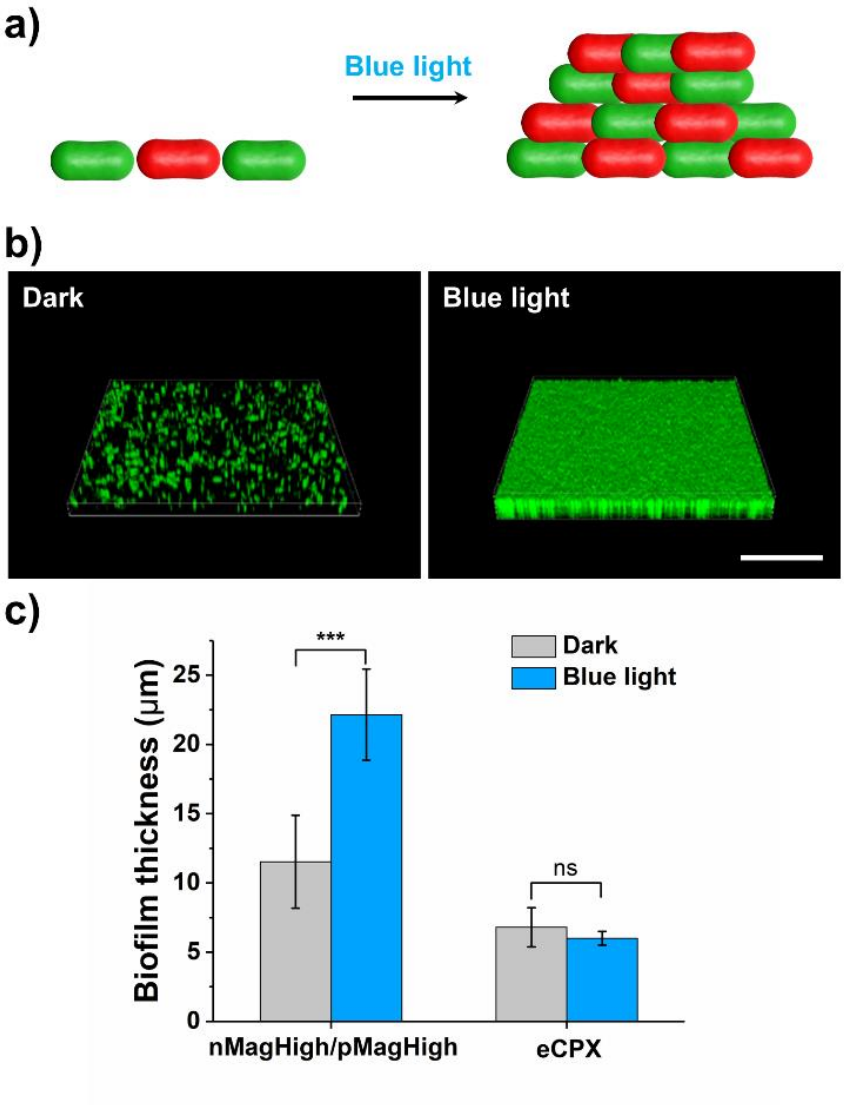

Figure 4.16 Photoswitchable adhesions enhance biofilm formation under blue light. a) A schematic illustration of biofilm formation enhanced by photoswitchable adhesions under blue light. nMagHigh or pMagHigh displaying bacteria were labeled in green or red color, respectively. b) Confocal laser scanning microscopy images of biofilms formed with co-

cultures of nMagHigh and pMagHigh-displaying bacteria (both labeled with GFP) after 48 h in the dark and under blue light. Scale bars, 100 μm. c) Biofilm thickness in the dark and under blue light for bacteria with and without photoswitchable adhesins. The error bars are the standard error from 3 replicates. ***$p < 0.001$.

Also, crystal violet staining of surface-attached biofilms grown for 48 h at 37 ºC in microplates confirmed the augmented biofilm formation under blue light for bacteria with photoswitchable adhesins (**Figure 4.17**). Overall, it is interesting to note that not only native adhesion molecules such as Ag43 and curli fibers, but also engineered adhesins like nMagHigh and pMagHigh can result in to biofilm formation. These photoswitchable bacteria-bacteria adhesions hence provide remote control over biofilms by using light.

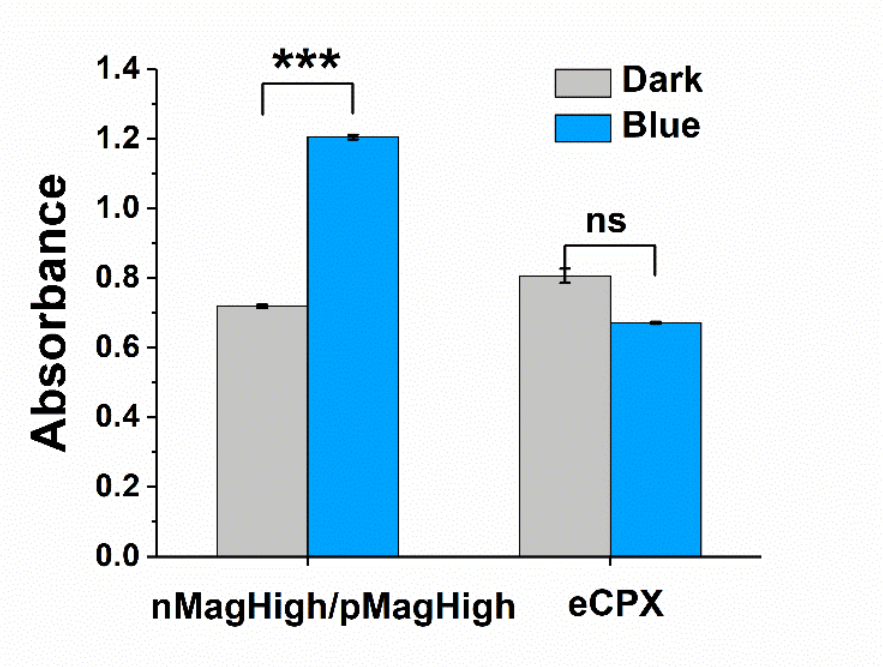

Figure 4.17 Biofilm formation assay using crystal violet staining for quantification. nMagHigh and pMagHigh-displaying bacteria were mixed in a 1:1 ratio (OD_{600}= 0.01) and incubated for 48 h in the dark or under blue light. Biofilm formation was quantified using crystal violet (CV) staining. The absorbance at 550 nm was measured. In both experiments, cells with eCPX expression were used as negative control. ***$p < 0.001$.

Blue light-controllable bacterial aggregation alters metabolic cross-feeding. In nature, bacteria do not exist in isolation, but live as complex multispecies' communities. Within these communities, different members can perform distinct tasks, exchange essential metabolites and form microbial ecosystems, which also have important biotechnological implications.[56, 209] However, designing bacterial communities is far from straightforward as the spatial structure of a microbial community, nutrient availability, diffusion constraints and metabolic burden on different members alters the biochemical phenotypes and abundance of the participating strains. For instance, Mee *et al.* devised a series of synthetic syntrophic communities in co-cultures of different *E. coli* amino acid auxotrophs. While the exchange of essential amino acids in certain mixtures of auxotrophs leads to cooperative growth, the metabolic cross-feeding revealed both positive and negative interactions in communities of a higher complexity.[56] Furthermore, emergence and maintenance of metabolic exchanges depend on particular circumstances and changes over time. Here we asked the question how the aggregation changes cross-feeding between different auxotrophs, as aggregation increases the efficiency of nutrient transfer and potentially can stimulate otherwise unfavorable metabolic processes.[210]

To test how the aggregation alters bacterial cross-feeding and co-culture composition, we expressed either nMagHigh or pMagHigh on the surfaces of *E. coli* BL21 strains that are auxotrophic for one essential amino acid (*P*, *K*, *W*, *M* and *T*). We named each bacterial strain after the amino acid it is auxotrophic for and the protein displayed on its surface (n: nMagHigh, p: pMagHigh), e.g. *K*n: lysine auxotroph displaying nMagHigh.(**Figure 4.18a**) In order to observe if the spatial proximity alters the cross-feeding process, we co-cultured different nMagHigh and pMagHigh-displaying auxotrophs under blue light or in the dark and quantified their growth by measuring the OD_{600} (**Figure 4.18b**). As reported before, each auxotroph was unable to grow on its own in a M9 minimal medium, but a subset of these 1:1 co-cultures showed synergistic growth after 48 h. More importantly, the cooperative growth of some co-cultures was different under blue light and in the dark; *P*n/*K*p co-cultures grew 6-

fold better under blue light than in the dark and *W*n/*M*p, *T*n/*W*p and *W*n/*T*p co-cultures grew better in the dark than under blue light (4, 2 and 3 fold, respectively).

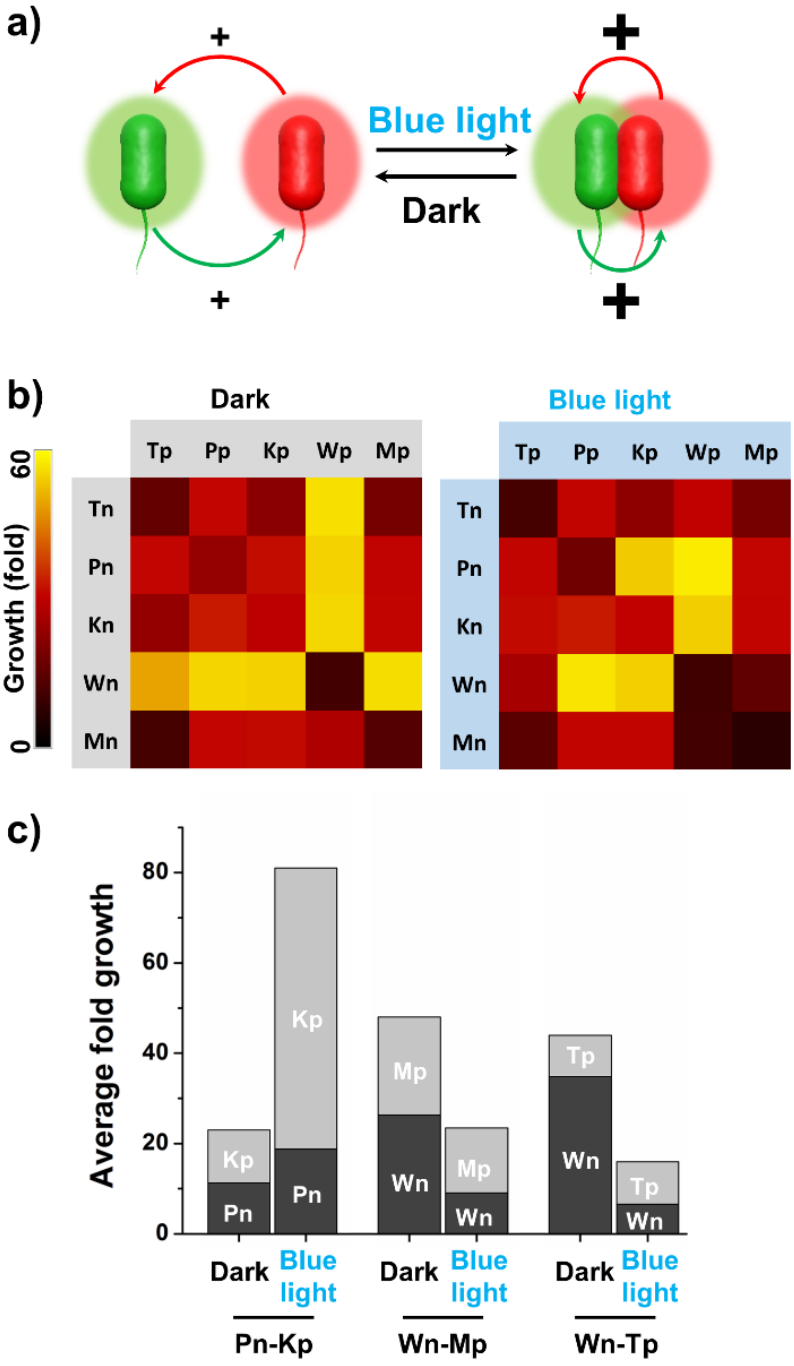

Figure 4.18 Photoswitchable adhesions alter metabolic interactions and cross-feeding. a) A schematic illustration of bacterial metabolic cross-feeding altered by photoswitchable adhesions. nMagHigh or pMagHigh displaying bacteria were labeled in green or red color, respectively. b) Syntrophic growth of different auxotrophic strains displaying nMagHigh or

pMagHigh after 48 h in the dark (left) and under blue light (right). Color intensity indicated in the color bar denotes fold growth after 48 h over the initial population. c) Population distribution of 2-member co-cultures after 48 h incubation in the dark and under blue light as determined by qPCR. Each co-culture was quantified in 3 biological replicates.

The increased growth of *P*n/*K*p co-cultures under blue light is presumably due to the more efficient metabolic exchange between the two strains upon co-aggregation as observed under the microscope. (**Figure 4.19**) The negative effect of blue light-triggered aggregation on the growth *W*n/*M*p, *T*n/*W*p and *W*n/*T*p shows that proximity can also overwhelm the partnership as the biosynthetic burdens on one member becomes too high. On the other hand, some co-cultures grew equally well under blue light and in the dark, showing that spatial proximity does not always determine the cross-feeding, meaning that the effect of clustering has to be evaluated case by case. For this the blue light-switchable adhesins can be a used as a tool to assess and optimize the cross-feeding in co-cultures by controlling aggregation.

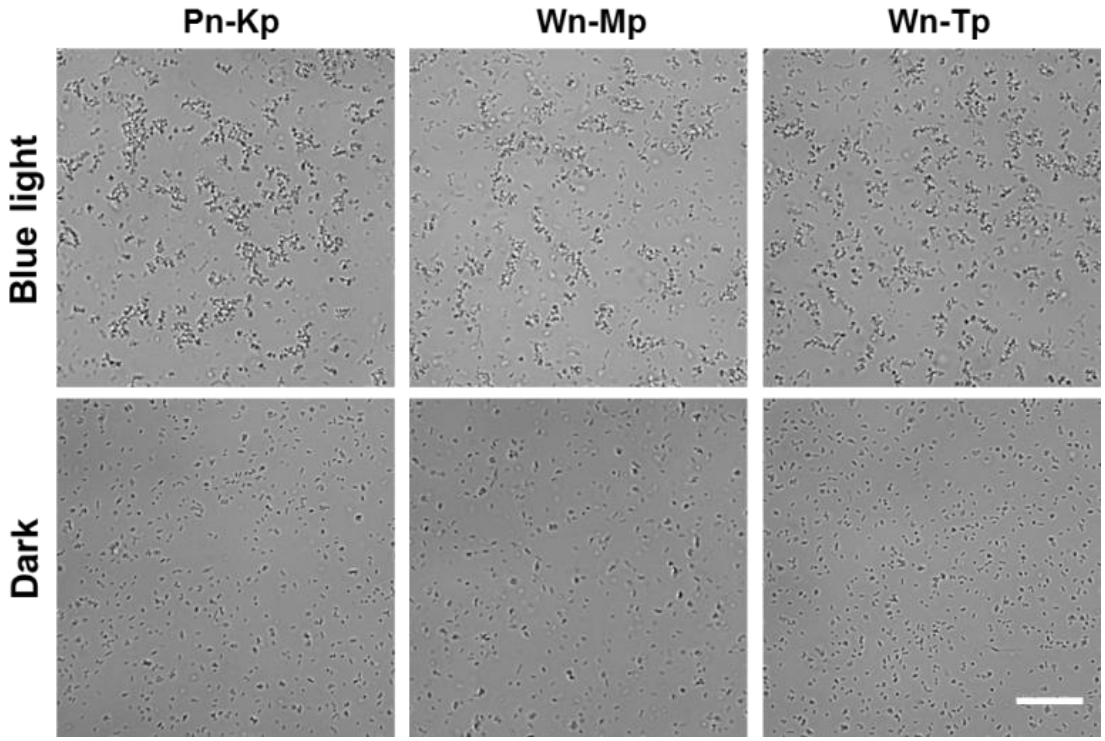

Figure 4.19 Aggregation of the auxotrophic BL21 (DE3) *E. coli* strains. *E. coli* displaying nMagHigh or pMagHigh were mixed in a 1:1 ratio (OD_{600}= 0.15) and incubated for 2 h under blue light or in the dark. The scale bar is 50 μm.

Metabolic cross-feeding promotes the growth of different members to different extents and leads to a change in composition over time. By using quantitative PCR (qPCR), we determined the relative abundance of each member for cultures that showed altered growth under blue light and in the dark (**Figure 4.18c**). For the *P*n/*K*p co-culture, which grew better under blue light, the ratio of the *P*n and *K*p was similar to the initial starter culture ratio of 50:50 in the dark, but under blue light the *K*p strain grew much better resulting in a 20:80 *P*n:*K*p ratio. For the *W*n/*M*p co-culture the relative abundance of the two bacteria types didn't change much with blue light illumination. However, for the *W*n/*T*p co-culture, which grew better in the dark, the *W*n:*T*p ratio was 78:22 in the dark and 40:60 under blue light. Overall, these results show that regardless of whether the effect aggregation under blue light is positive or negative it can still have an impact on the co-culture composition. The nonlinear effect of aggregation on cross-feeding of different auxotrophic strains could be explained by the fact that different amino acids have different metabolic costs and are required in different amounts. Upon aggregation, the excessive consumption of metabolically expensive and rarer amino acids (*W*, *M*)[56] by the auxotroph resulted in the reduced growth of the producing strain and an overall reduction in growth of the co-culture. On the other hand, more efficiently exchange of metabolically cheap and more abundant amino acids within the aggregates (*P*, *K*)[56] led to an overall increase in growth, where one of the strains benefits more from this collaboration. Therefore, the photoswitchable bacteria-bacteria interactions are a significant tool to control both metabolic cross-feeding and culture composition.

4.4 Conclusions

The photoswitchable bacteria-bacteria adhesions presented here provide a new way of assembling multicellular bacterial communities with high spatiotemporal control and unique advantages. The response to low intensity blue light provides non-invasive regulation and is

bioorthogonal to other cellular processes. Photoregulation is especially attractive for biotechnological applications as the application of light is a cheap and easy way of removing stimuli compared to applying chemicals that are used to control bacterial cultures. Interestingly, various microorganisms photoregulates their adhesions in response to light in order to adapt to changing environmental conditions.[211, 212] Implementing a light regulated adhesion module into *E. coli* can similarly be used to photoregulate bacterial behaviour in changing enviroments. The optogenetic proteins used, nMagHigh and pMagHigh, assure specific binding between bacteria expressing interaction partners under blue light and allow for them to arrange themselves into specific patterns. While the photoswitchable protein interactions are strong enough to mediate aggregation, they still allow for dynamic rearrangement and coalescence of aggregates to maximize bacteria-bacteria interactions. Importantly, the multi-bacterial assemblies can be disassembled in the dark allowing for dynamic switching between unicellular and multicellular life forms. This is an important feature when it comes to designing bacterial communities as the relationship between different bacteria can change over time as environmental parameters and the internal state of the bacteria vary. Moreover, bacterial aggregation is highly tunable by altering light intensity and exposure time as well as bacterial density. The sustained production of the genetically encoded proteins makes control in long term cultures possible, as demonstrated in cross-feeding and biofilm formation experiments. This is an important advantage over strategies that involve the chemical modification of the surface of the bacteria, as these modifications are difficult to maintain over time. *E. coli* typically divide every 20 min and quickly dilute the functional groups on their surfaces.

The photoswitchable bacteria-bacteria interactions provide an exclusive combination of features and are a significant new tool in the study of bacterial cell biology and the regulation of bacterial consortia. We have demonstrated how we can photocontrol central bacterial behavior including quorum sensing, biofilm formation and metabolic cross-feeding with this new tool. The modular nature of the photoswitchable adhesins allow to integrate them onto the surface of many different cell types and couple them to cell-cell signaling, quorum

sensing-based gene regulators and gene regulatory logic gates. Moreover, the ability to regulate and optimize cross-feeding in co-cultures opens the way to design more efficient bacterial factories that can perform further complex transformations. The evolutionary transition from single to multi-cellular life forms has resulted in an explosion of diversity. By understanding and controlling multi-cellularity in the field of synthetic biology we hope to achieve more than just the sophistication of bacterial communities.

5. Summary and outlook

Controlling bacterial adhesion with high spatial and temporal precision is essential for controlling the formation, organization and microstructure of biofilms. In this thesis, different methods to control bacterial adhesions using light have been developed to control biofilm formation or the assembly of multicellular structures with high spatiotemporal precision and to study how the spatial organization of bacteria influences their collective functions.

In the first part of the thesis, a new method named bacterial photolithography were created to pattern stable biofilms through irreversible light response. This method provides high flexibility in creating complex patterns with a resolution down to 10 µm, which represents an important step towards the engineering of precise biofilm communities as the microstructure of natural biofilms has a major impact on their function. This method enables the investigation of how microscale spatial organization affects collective bacterial interactions such as quorum sensing. It has significant potential for future applications in guiding the formation and spatial organization of bacteria in a biofilm, as well as improving our understanding of naturally existing biofilms and the design of bacterial consortia.

In the second part of the thesis, photoswitchable proteins nMag and pMag were used to control bacterial adhesions in an optogenetic approach. This approach overcomes the problem of using UV light for photoregulation and chemically modifying the bacteria surface. It provides non-invasive, bioorthogonal and reversible control over bacterial attachment with unprecedented spatial and temporal control. The photoswitchable bacteria adhesions allow us to control the formation and spatial organization of bacteria in a biofilm, which is vital in engineering bacterial consortia.

In the last part of the thesis, the photoswitchable bacteria-bacteria adhesions were developed based on the optogenetic proteins nMag and pMag. It provides a new way to spatiotemporally control the reversible assembly of multicellular clusters with blue light. The photoswitchable bacteria-bacteria interactions provide an exclusive combination of features and are a

significant new tool in the study of bacterial cell biology and the regulation of bacterial consortia. These photoswitchable adhesions made it possible to regulate collective bacterial functions using light including aggregation, quorum sensing, biofilm formation and metabolic cross-feeding between auxotrophic bacteria. Multi-bacterial communities are of fundamental importance and have great biotechnological potentials.

All these work open new possibilities for engineering multicellular communities, understand fundamental bacterial behavior in biofilms and design biofilms with new functions for biotechnological applications. The evolutionary transition from single to multi-cellular life forms has resulted in an explosion of diversity. By understanding and controlling multi-cellularity in the field of synthetic biology, we hope to achieve more than just the sophistication of bacterial communities.

6. Materials and Methods

6.1 Materials

6.1.1 Plasmids

The GFP pTrc99A, mCherry pTrc99A (Ampicillin resistant, IPTG inducible), and P_{lsr}-*egfp* plasmids (Kanamycin resistant) for *E.coli* expression were gifts from Prof. Victor Sourjik. The plasmid pB33eCPX, which contains the gene for the enhanced circularly permutated outer membrane protein OmpX (eCPX), was a gift from Prof. Patrick Daugherty (Addgene plasmid # 23336)[191]. The nMagHigh gene in the pET-21b(+) plasmid between the NdeI and XhoI cutting sites was purchased from Genescript.

6.1.2 Bacterial Strains

E.coli K12 MG1655 was purchased from DSMZ. BL21(DE3) *E.coli* were purchased from NEB. The auxotrophic BL21 (DE3) *E. coli* strains RF2 (Addgene plasmid # 62070, *T*), RF6 (Addgene plasmid # 62074, *P*), RF10 (Addgene plasmid # 62076, *K*), RF11 (Addgene plasmid # 61961, *M*) and RF12 (Addgene plasmid # 62077, *T*) were a gift from Robert Gennis & Toshio Iwasaki.[213]

6.1.3 Other Materials.

The 2,5-dioxopyrrolidin-1-yl (1-(5-methoxy-2-nitro-4-(prop-2-yn-1-yloxy)phenyl)ethyl) carbonate was synthesized following the literature.[26] 4-Aminophenyl α-D-mannopyranoside was purchased from Sigma-Aldrich. PBS (pH 7.4) was prepared by PBS tablets from Gibco. LB-Medium (Luria/Miller) was purchased from Carl Roth. 10 g tryptone and 5 g NaCl were dissolved in 1 L H_2O to obtain TB (Tryptone Broth) medium. LB and TB media were autoclaved prior to use. 20 x 20 mm glass coverslips were purchased from Carl Roth. PEG (3000)-azide was synthesized following previous reports from our lab.[172] QuikChange II Site-Directed Mutagenesis Kit was purchased from Agilent. All chemicals were purchased from Sigma-Aldrich. The live and dead cell Assay kit (ab189818) was purchased from Abcam.

KAPA SYBR® FAST Universal Kit was purchased Sigma Aldrich. 8-well slides (µ-Slide, 8-well glass bottom) were purchased form ibidi.

6.2 Methods

6.2.1 Bacterial culture

E.coli K12 MG1655 were co-transformed with one of the eCPX fused photoswitchable protein plasmids (nMagHigh-eCPX, or pMagHigh-eCPX, or pMag-eCPX, or pMagFast1-eCPX, chloramphenicol resistant, *L*-arabinose inducible), and a fluorescent protein expression plasmid (GFP-pTrc99A or mCherry-pTrc99A, ampicillin resistant, IPTG inducible). 5 mL LB medium containing 35 µg/mL chloramphenicol and 50 µg/mL ampicillin were inoculated with a single colony and incubated overnight at 37 °C at 250 rpm. Then, 50 µL of these cultures was added into fresh 5 mL LB medium containing 35 µg/mL chloramphenicol and 50 µg/mL ampicillin and cultured for 2 h at 37 °C, at 50 rpm. Then, the OD_{600} = 0.4, 0.04% m/v *L*-arabinose and 0.5 mM IPTG were added to the cultures to induce the expression of the eCPX fused proteins and the fluorescent proteins, respectively. The bacteria were cultured at 25 °C, at 250 rpm for 4 h and subsequently diluted in PBS (phosphate buffer saline) to the desired density.

6.2.2 Expression and purification of nMagHigh

The nMagHigh with a C-terminal His6-tag in pET-21b(+) expression plasmid was transformed into BL21(DE3) *E.coli* cells. The protein expression was induced at OD_{600} = 0.6 with 1 mM IPTG and the protein was expressed at overnight at 18 °C, 250 rpm. The cell pellet was suspended in 20 mL buffer A (50 mM Tris-HCl pH 7.4, 300 mM NaCl) with 1 mM protease inhibitor PMSF (phenylmethane sulfonyl fluoride). The cells were lysed by sonication and the lysate was cleared by centrifugation at 12000 rpm for 30 min followed by filtration through a 0.45 µm filter twice. The lysate was passed over a 5 mL of Ni^{2+}-NTA agarose column. The column was washed with 50 mL buffer C (Buffer A with 25 mM imidazole) and the protein was eluted with 10 mL buffer B (Buffer A with 250 mM

imidazole). The purified nMagHigh-His6 was dialyzed against 2 L buffer A twice for at least 6 h and the purity was verified by SDS-PAGE.

6.2.3 Cloning of nMagHigh and pMag variants

To express pMag variants (pMagHigh, pMag and pMagFast1) on the surface of *E.coli*, we fused these proteins to the N-terminal of eCPX. To insert the nMagHigh gene into the plasmid pB33eCPX, the nMagHigh gene was firstly amplified by PCR from nMagHigh pET-21b(+) plasmid and inserted between the KpnI and SacI cutting sites of pB33eCPX. The different pMag variants fused to eCPX were generated by point mutagenesis from the nMagHigh-eCPX plasmid using QuikChange II Site-Directed Mutagenesis Kit (Scheme S1).

6.2.4 Synthesis of mannoside-NO2

To a solution of 2,5-dioxopyrrolidin-1-yl (1-(5-methoxy-2-nitro-4-(prop-2-yn-1-yloxy)phenyl)ethyl) carbonate (1 eq., 271.27 mg, 1 mmol) in 1 mL DMF, a solution of 4-aminophenyl α-D-mannopyranoside (1 eq., 392.09 mg, 1 mmol) in 400 µL Na_2CO_3 buffer (1 M, pH = 8.5) and 600 µL H_2O were added. The reaction mixture was kept at room temperature with stirring for 24 h. The reaction mixture was evaporated under vacuum and the remaining solid was purified by HPLC (column: reverse phase C18). A: Acetonitrile, 0.1% TFA, B: H_2O, 0.1% TFA, flow 1mL/min, gradient 20% to 80% B, retention time 14 min). The concentration of the final product is determined to be 1.0 mM by UV-Vis (ε 350 = 5000 M−1 cm−1). HR-MS(ESI+): [M+ Na]+ observed: *m*/*z* = 571.1541, calc.: *m*/*z* = 571.1540. ^{1}H-NMR (600 MHz; D_3OD): δ (in ppm) = 7.79 (s, 1H), 7.30 (d, J = 9 Hz, 2H), 7.28 (s, 1H); 7.04 (d, J = 8.4 Hz, 2H), 6.39 (q, J = 6 Hz, 1H), 5.38 (s, 1H), 4.85 (d, J = 2.4Hz, 2H), 3.96 (s, 3H), 3.90 – 3.59 (m, 6H), 3.04 (t, J = 2.4Hz, 1H), 1.65 (d, J = 6Hz, 3H).

6.2.5 UV-Vis spectroscopy of mannoside-NO_2

UV-Vis spectra were acquired using plate reader (Tecan, Spark^{TM}). The absorbance of 0.1 mM Mannoside-NO_2 in H_2O was measured from 280 to 700 nm after different irradiation times (0, 1, 2, 5, 10, 15, 20, 30 min) with 365 nm light (UV transilluminator from Syngene's GeneFlash).

6.2.6 Functionalization of glass surfaces with PEG-mannoside-NO_2

The glass surfaces were functionalized similarly to previous reports.[172] Shortly, glass slides (20 × 20 mm) were cleaned in freshly prepared Piranha solution (3:1 (v/v) conc. H_2SO_4:H_2O_2 (30%)) for 1 h, rinsed 3 times with Milli-Q water and dried in an N_2 stream. For the PEGylation reaction, surfaces were immersed in a solution of PEG-azide (10 mg PEG-azide, MW = 3000 g/mol) and a drop of dry triethylamine in dry toluene and kept at 79 °C overnight under a N_2 atmosphere. The surfaces were first washed with ethyl acetate for 5 min by sonication, then with methanol for 5 min by sonication and dried in a N_2 stream. The PEG-coated surfaces were incubated in contact with 50 µL of reaction solution containing 100 mM L-ascorbic acid, 100 mM Tris HCl pH 9.0, 50 µM of the mannoside-NO_2 and 1 mM $CuSO_4$ in a moisture chamber for 2 h. Afterwards the surfaces were washed with 50 mM EDTA (pH 7.4) for 5 min and 3 times PBS for 5 min.

6.2.7 Bacterial adhesion to the mannoside-NO_2 functionalized surfaces.

E.coli K12 MG1655 were transformed with the GFP pTrc99A plasmid (ampicillin resistant) and selected on an LB-agar plate with 50 µg/mL apicillin. 2 m LLB medium containing 50 µg/mL ampicillin was inoculated with a single colony and incubated overnight at 37 °C at 250 rpm. Then, 100 µL of these cultures were transferred into 10 mL fresh LB medium containing 50 µg/mL ampicillin and cultured at 37 °C, 250 rpm. When the OD_{600} = 0.4, the production of the fluorescent protein was induced with 0.5 mM IPTG and the culture was incubated at 37 °C, 250 rpm for 4 h. The bacteria were then spun down at 4000 rpm for 10 min and washed by PBS twice. Finally, the bacteria were resuspended in PBS to OD_{600} = 1.0. For bacterial adhesion assays, 3 mL of bacteria were placed on top of mannoside-NO_2 functionalized surfaces. Prior to bacterial seeding, the surfaces were either kept in the dark or pre-illuminated by UV light (UV transilluminator, Syngene's GeneFlash) for 1 h. Surfaces with just the PEG coating but not modified with mannoside-NO_2 were used as negative controls. The bacteria were incubated on these surfaces at room temperature for 10, 30, 60, 120 or 210 min.

To investigate the effect of UV-light illumination, mannoside-NO_2 functionalized surfaces were firstly pre-illuminated with UV light for 0, 2, 5, 10, 15, 30, 60 min and then bacteria were placed onto these surfaces for 210 min incubation in the dark.

For analysis, after the incubation of the bacteria on the surfaces, the surfaces were gently washed 3 times with PBS to remove unbound bacteria and 3 x 3 fluorescent images (field of view of one image =1.04 mm^2) in the GFP channel were acquired on an inverted fluorescence microscope (DMi8, Leica) through a 20x objective. The number of bacteria on the surface was analyzed using the particle analyzer tool in ImageJ.

6.2.8 Bacterial biofilm photopatterning on the mannoside-NO_2 functionalized surfaces.

A mannoside-NO_2 functionalized surface was locally illuminated with 358 nm UV light through the photomask for 2 min on an inverted fluorescence microscope (DMi8, Leica) through a 5x objective. Then, the photomask was removed and a bacteria solution with OD_{600} = 1.0 prepared as described above is placed on top of the surface and incubate for 4 h. The glass surface was gently washed 3 times with PBS to remove non-attached bacteria before imaging the bacterial biofilm pattern.

6.2.9 Live imaging of patterned biofilms and quorum sensing

E.coli K12 MG1655 were co-transformed with mCherry pTrc99A (ampicillin resistant) and P_{lsr}-*egfp* (kanamycin resistant) plasmids and selected on an LB-agar plate with 50 μg/mL ampicillin and 50 μg/mL kanamycin, then cultured as described above. A mannoside-NO_2 functionalized surface was illuminated through a photomask with UV light as described above. Then, the photomask was removed and a bacteria solution with OD_{600} = 1.0 is placed on top of the surface. 4 h later, non-attached bacteria were removed by washing 3 times with PBS and the bacterial pattern was observed under microscope in the mCherry fluorescence channel. Then, PBS containing 10% TB medium was added on top of the surface. Afterwards the bacterial pattern was imaged in the mCherry and GFP channels every 3 min for 10 h on a fluorescence microscope (DMi8, Leica) with 10x objective. The fluorescence intensity of bacterial biofilm pattern was analyzed using the intensity analyzer tool in ImageJ.

6.2.10 Functionalization of glass surfaces with nMagHigh

The glass substrates were functionalized similarly to previous reports.[28] Shortly, glass slides (20 × 20 mm) were cleaned in freshly prepared Piranha solution (3:1 (v/v) conc. H_2SO_4:H_2O_2 (30%)) for 1 h, rinsed 3 times with Milli-Q water and dried in an N_2 stream. For the PEGylation reaction, surfaces were immersed in a solution of PEG-azide (10 mg PEG-azide, MW= 3500 g/mol) and a drop of dry triethylamine in dry toluene and kept at 79 °C overnight under a N_2 atmosphere. The surfaces were first washed with ethyl acetate for 5 min by sonication, then with methanol for 5 min by sonication and dried in a N_2 stream. The PEG-coated surfaces were incubated in contact with 100 µL of reaction solution containing 100 mM L-ascorbic acid, 100 mM Tris HCl pH 9.0, 150 µM of the NTA-alkyne and 1 mM CuSO4 in a moisture chamber for 2 h (Scheme 2). Afterwards the surfaces were incubated with the following solutions to obtain the nMagHigh functionalized substrates through NTA-Ni^{2+} -His tag interaction: 1) 50 mM EDTA (pH 7.4) for 5 min, 2) Buffer A twice for 5 min, 3) 0.1 M $NiCl_2$ in water for 5 min, 4) Buffer A twice for 5 min, 5) 10 µM purified nMagHigh-His6 protein for 30 min, 7) Buffer A twice for 5 min.

6.2.11 Bacterial adhesion to the nMagHigh functionalized substrates and detachment assays

E.coli K12 MG1655 were co-transformed with the appropriate pMag-eCPX plasmid (chloramphenicol resistant) and the GFP plasmid (ampicillin resistant) and selected on an LB-agar plate with 35 µg/mL chloramphenicol and 50 µg/mL ampicillin. 5 ml LB medium containing 35 µg/mL chloramphenicol and 50 µg/mL ampicillin was inoculated with a single colony and incubated overnight at 37ºC at 250 rpm. Then, 500 µL of these cultures were added into fresh 20 ml LB medium containing 35 µg/ml chloramphenicol and 50 µg/mL ampicillin and cultured for 2 h at 37 °C, 250 rpm. When the OD_{600} = 0.5, 0.04% m/v *L*-arabinose to induce the expression of the pMag-eCPX proteins and 0.5 mM IPTG to induce the production of the fluorescent protein were added and the cultures were incubated at 25 °C, 250 rpm for 4 h. The bacteria were then spun down at 4000 rpm for 10 min and washed by PBS twice. Finally, the bacteria were resuspended in PBS to OD_{600} = 1.0.

For bacterial adhesion assays, 3 mL of bacteria co-expressing one of the pMag protein variants on their surface and GFP protein were placed on nMagHigh functionalized substrates. The bacteria were either incubated under blue light illumination (blue LED panel, 640 µW/cm^2) or in the dark for 1 h. Bacteria incubated on substrates that lack the immobilized nMagHigh protein were used as negative controls. Other bacterial adhesion assays were performed similarly changing one parameter at the time: The illumination intensity (0, 3.2, 32, 320, 640 or 3200 µW/cm^2) or the incubation time under blue light (10, 30, 60, 120 or 180 min).

For bacterial detachment assays, bacteria were placed on nMagHigh substrates and were incubated for 1 h under blue light illumination, and then the samples were moved to the dark for 0, 10, 30, 60, 120 or 240 min, respectively.

For the cycling experiments, bacterial were first incubated under blue light illumination for 1 h for attachment and then kept in the dark for 2 h for detachment. This process was repeated in total for 2.5 cycles.

For analysis, after the incubation with the bacteria, the substrates were gently washed 3 times with PBS to remove unbound bacteria and 3 x 3 fluorescent images (area of one image =1.04 mm^2) in the GFP channel were acquired on an inverted fluorescence microscope (DMi8, Leica) through a 20x objective. The number of bacteria on the surface were analyzed using the particle analyzer tool in ImageJ.

6.2.12 Bacterial patterning on the nMagHigh functionalized substrates.

E.coli K12 MG1655 were co-transformed with pMagHigh-eCPX and mCherry plasmid (ampicillin resistant) plasmids and cultured as described above. A bacteria solution with OD_{600} = 1.0 is placed on top of a nMagHigh functionalized glass substrate and kept in the dark. The glass surface was locally illuminated with blue light through photomask for 1 h on an inverted fluorescence microscope (DMi8, Leica) through a 10x objective. Then, the photomask was removed and the glass surfaces were gently washed 3 times with PBS before imaging the bacterial pattern.

6.2.13 Lysates of MG1655 expressing different pMag variants

Lysates of *E.coli* K12 MG1655 expressing different pMag variants were generated by suspending bacteria to OD_{600} = 1.0 in PBS. 30 µl bacterial solutions and 10 µl 4x protein loading dye were mixed and then heated at 95 ºC for 10 min. 10 µl of the lysates solution was loaded for SDS-PAGE.

Table 4.2.1 SDS-PAGE gel preparation

Component	Stacking gel	Resolving gel (12%)	Resolving gel (10%)
40% Acrylamid	1.48 mL	7.5 mL	6.25 mL
0.5 M TRIS pH=6.8	3.78 mL	-	-
1.5 M TRIS pH=8.8	-	6.25 mL	6.25 mL
10% SDS	150 µL	250 µL	250 µL
H_2O	9.5 mL	10.9 mL	12.1 mL
TEMED	15 µL	12.5 µL	12.5 µL
10% (w/v) APS	75 µL	125 µL	125 µL
Total volume	15 mL	25 mL	25 mL

All components for both stacking and resolving gels were mixed together except for the ammonium persulfate (APS). Then APS was added to the resolving gel, rapidly mixed and poured in between glass plates placed in the holders. The gels were allowed to solidify before adding APS to the stacking gel, mixing and pouring on top of the resolving gel. A comb was then placed in the stacking gel to form the wells. Several gels were prepared in parallel and were stored wrapped in soaked with MilliQ water paper at 4 °C.

SDS-Gels were loaded with 15 µL of protein mixed with 5 µL protein loading dye. Protein marker was run in parallel (5 µL) to be able to identify the protein sizes. 120 mA and 200 V were applied for 37 minutes to run the proteins in the gel. SDS-PAGE was stained with coomassie brilliant blue staining solution, while heating it for 30 seconds in the microwave and allowing soaking for 5 minutes at room temperature. After that, the coomassie staining was removed and destaining solution was added. The gel was left on a shaker for 1 hour or until the gel became transparent and the protein bands became clearly visible. The gels were then scanned for documentation and further analysis.

6.2.14 QCM measurement

All QCM measurements are performed on a Q-Sense E1 system (Q-Sense) with SiO_2 crystals (Q-sense). All measurements are performed with a flow rate of 100 µL/min and at room temperature. The SiO_2 coated QCM crystals are cleaned with a 2% SDS solution overnight, rinsed 3 times with Milli-Q water and dried in an N_2 stream. The QCM crystals are then treated with oxygen plasma (TePla 100-E, 0.2 mbar, 150 W, 10 min). Subsequently, the SiO_2 crystals were functionalized as the glass surfaces with PEG-NTA and loaded with $NiCl_2$ (Scheme S2). In the QCM the following solutions were passed over the crystal: 1) Buffer A, 10 min, 2) 10 µM nMagHigh protein in Buffer A, 15 min, 3) Buffer A, 15 min.

6.2.15 Bacterial aggregation assay

E.coli displaying nMagHigh (labeled with GFP) and one of the pMag variants (labeled with mCherry) were either mixed in a 1:1 ratio or analyzed as mono-cultures (OD_{600}= 0.15). 300 µL of each bacterial culture was added into 8-well slides and incubated in the dark or under blue light illumination (270 µW/cm^2) for 2 h. Then, 200 µL 10% PFA (paraformaldehyde) in PBS was added to each sample for fixation for 30 min before acquiring images. To quantify the bacterial aggregation at various densities, *E.coli* displaying nMagHigh (GFP labeled) and pMagHigh (mCherry labeled) were mixed in a 1:1 ratio in PBS to a final OD_{600} = 0.075, 0.15, 0.3, 0.6 and the bacterial aggregation was performed as described above. Likewise, the influence of the illumination intensity on bacterial aggregation was investigated using the protocol above (*E.coli* displaying nMagHigh (GFP labeled) and pMagHigh (mCherry labeled) were mixed in a 1:1 ratio in PBS, OD_{600} = 0.15), but the blue light intensity was adjusted to 0, 17, 67, 270, 540, or 2160 µW/cm^2 using neutral density filters.

Images were acquired on an inverted Confocal Laser Scanning Microscope (CLSM, Leica TCS SP8) equipped with a 488 nm and 552 nm laser for imaging the GFP and mCherry, respectively and a 40x water-immersion objective lens. For each sample 25 images (290 µm x 290 µm)were acquired in the GFP and mCherry channels. All images were processed in FIJI (FIJI, https://fiji.sc/). To analyze the bacterial aggregation, the images in the GFP and

mCherry channels were merged and converted into a binary image. Using the Analyze Particles function in FIJI, clustered bacteria and all bacteria (single and clustered) in each image were detected by taking into account objects with an area > 15 μm^2 and > 2 μm^2, respectively. Aggregation ratio = sum of the area occupied by clustered bacteria / sum of area occupied by all bacteria. Likewise, the average sizes of clusters were obtained using the results for the particle analysis tool.

6.2.16 Real-time imaging of bacterial co-aggregation

E.coli displaying nMagHigh (or pMagHigh) were diluted in PBS to a final density of OD_{600}= 0.15 and mixed in a 1:1 ratio. 300 µL of bacterial solution was added into 8-well slides and time-lapse images (1 image/min) were acquired for 12 h. The time-lapse images of bacteria under blue light illumination were taken by a CLSM Leica TCS SP8 microscope as described above and the 488 nm excitation also used for imaging in the GFP channel was used for photoactivation. The time-lapse images of bacteria in the dark were acquired on an inverted fluorescent microscope (DMi8, Leica) in the bright field channel and placing a 525 - 900 nm bandpass filter in front of the white light source.

6.2.17 Reversibility of bacterial aggregation

E.coli displaying nMagHigh and pMagHigh were mixed in a 1:1 ratio to a final OD_{600} = 0.15. 1 mL aliquots were added into an Eppendorf tube and the samples were placed on a rocker at 10 rpm/min to prevent sedimentation. To switch the bacteria-bacteria interactions on and off, the samples were alternated between exposure to 1 h of blue light illumination and to 1 h in the dark for 2.5 cycles. At the end of each step, 300 µL bacterial solution was taken from one aliquot, transferred into an 8-well chamber and 200 µL 10% PFA solution was carefully added into each well for fixation. The samples were allowed to settle down for 2 h and subsequently images were acquired on the CLSM TCS SP8 and analyzed as described above.

Bacterial sedimentation assay. 1:1 mixed or mono-cultures were prepared at a density of OD_{600} =1.00 as mentioned above. 200 µL aliquots of each bacterial culture were added into 96-well plates at room temperature and either incubated under blue light (270 $\mu W/cm^2$) or in

the dark. At different time points 50 µL solution from the top 25% of the well was transferred to a new 96-well plate, diluted with 50 µL PBS and the absorbance at 600 nm was measured on a plate reader (Tecan Spark).

6.2.18 Quorum sensing activation

E. coli MG1655 bacteria were co-transformed with the nMagHigh-eCPX (or pMagHigh-eCPX) and P*lsr*-egfp plasmid (egfp gene is inserted into the vector pUA66 with *lsr* operon, kanamycin resistant). 10 mL tryptone broth (TB) medium containing 35 µg/mL chloramphenicol and 50 µg/mL kanamycin was inoculated with a single colony of either nMagHigh or pMagHigh-displaying bacteria and incubated overnight at 37 °C, at 250 rpm. The overnight cultures were diluted 1: 1000 into 10 mL TB medium supplemented with the antibiotics and 0.04% *L*-arabinose. The bacteria were cultured at 37 °C, at 200 rpm for 4 - 5 h until OD_{600} = 0.9. Both cultures were diluted with PBS to OD_{600} = 0.15, mixed in a 1:1 ratio and 300 µl bacterial solution was transferred into an 8-well slide. The samples were either kept under blue light (270 µW/cm^2) or in the dark for 2 h at room temperature. The expression of the quorum-sensing reporter egfp was visualized with an inverted fluorescent microscope (DMi8, Leica) and the egfp signal was quantified with FIJI. For analysis with flow cytometry, samples were diluted 1:20 in PBS, cell aggregates were dispersed by vigorous mixing and the GFP fluorescence was measured with CyFlow ML flow cytometry (Partec, Germany).

6.2.19 Biofilm formation assay

Overnight cultures of *E.coli* expressing GFP and nMagHigh or pMagHigh were diluted to OD_{600} = 0.01 into LB containing 35 µg/mL chloramphenicol, 50 µg/mL ampicillin, 0.04% m/v *L*-arabinose and 0.5 mM IPTG and mixed in a 1:1 ratio. The bacterial co-culture was either transferred into a 96-well polystyrene plate (Greiner Bio-one, round bottom) (200 µL/well) or 8-well slides (350 µL/well) and incubated for 48 h at 37 °C without shaking either under blue light (135 µW/cm^2) or in the dark. Samples in the 96-well plate were rinsed with H_2O, incubated with 200 µL 1% crystal violet (CV) solution for 15 min at room

temperature, the wells were rinsed three times with H_2O. The remaining CV violet was solubilized by adding 200 µL of 30% acetic acid in water, 200 µL of the solution was transferred to a new flat-bottomed 96-well microplate and the absorbance at 550 nm was quantified using a plate reader. The samples in the 8-well slides were rinsed three times with H_2O, z-stacks were acquired using the CLSM and the biofilm thicknesses were analyzed with 3D reconstruction software from Leica.

6.2.20 Metabolic cross-feeding assay

Overnight cultures of amino acids auxotrophic strains transformed with nMagHigh-eCPX or pMagHigh-eCPX were grown from a single colony in LB medium supplemented with 20 µg/mL chloramphenicol. The cultures were diluted 1:100 into 5 mL LB medium containing 35 µg/mL chloramphenicol, cultured at 37 °C, at 50 rpm for 2 h and 0.04% m/v *L*-arabinose was added to the cultures when the OD_{600} = 0.4. The bacteria were cultured at 25 °C, at 250 rpm for 4 h, before harvesting and washing twice with M9 salts (6 g/L Na_2HPO_4, 3 g/L KH_2PO_4, 1 g/L NH_4Cl, 0.5 g/L NaCl) by centrifugation at 25 °C,at 4000 rpm for 10 min and subsequently were resuspended in M9 medium to an OD_{600} = 0.1. For each co-culture 70 µL of bacterial solution of each strain was diluted into 560 µL M9 medium (M9 salts supplemented with 1 mM $MgSO_4 \cdot 7H_2O$, 0.083 nM thiamine, 0.25 µg/L *D*-biotin, and 0.2% (wt/vol) glucose) in a 48-well microplate and incubated at 30 °C, at 300 rpm for 48 h, either in the dark or under blue light (135 µW/cm^2). After 48 h, the OD_{600} was measured using a plate reader. For qPCR analysis of different bacterial strains, the cultures were frozen at -20 °C, and diluted 5-fold before the qPCR reaction was performed following the manufacturer's protocol with gene specific primers.

7. References

1. Wood, T. K.; Hong, S. H.; Ma, Q., Engineering biofilm formation and dispersal. *Trends in Biotechnology* **2011,** *29* (2), 87-94.

2. Hoiby, N., A short history of microbial biofilms and biofilm infections. *APMIS* **2017,** *125* (4), 272-275.

3. Lappin-Scott, H.; Burton, S.; Stoodley, P., Revealing a world of biofilms — the pioneering research of Bill Costerton. *Nature Reviews Microbiology* **2014,** *12*, 781.

4. Costerton, J. W.; Geesey, G. G.; Cheng, K. J., How Bacteria Stick. *Sci Am* **1978,** *238* (1), 86-&.

5. Donlan, R. M., Biofilms: microbial life on surfaces. *Emerg Infect Dis* **2002,** *8* (9), 881-90.

6. Vert, M.; Doi, Y.; Hellwich, K. H.; Hess, M.; Hodge, P.; Kubisa, P.; Rinaudo, M.; Schue, F., Terminology for biorelated polymers and applications (IUPAC Recommendations 2012). *Pure Appl Chem* **2012,** *84* (2), 377-408.

7. Sheng, G. P.; Yu, H. Q.; Li, X. Y., Extracellular polymeric substances (EPS) of microbial aggregates in biological wastewater treatment systems: A review. *Biotechnol Adv* **2010,** *28* (6), 882-894.

8. Watnick, P.; Kolter, R., Biofilm, city of microbes. *Journal of Bacteriology* **2000,** *182* (10), 2675-2679.

9. Flemming, H.-C.; Neu, T. R.; Wozniak, D. J., The EPS matrix: the "house of biofilm cells". *J Bacteriol* **2007,** *189* (22), 7945-7947.

10. Flemming, H.-C.; Wingender, J., The biofilm matrix. *Nature Reviews Microbiology* **2010,** *8*, 623.

11. Høiby, N.; Bjarnsholt, T.; Givskov, M.; Molin, S.; Ciofu, O., Antibiotic resistance of bacterial biofilms. *International Journal of Antimicrobial Agents* **2010,** *35* (4), 322-332.

12. Ehrlich, G. D.; Arciola, C. R., From Koch's Postulates to Biofilm Theory. The Lesson of Bill Costerton. *The International Journal of Artificial Organs* **2012,** *35* (10), 695-699.

13. Jamal, M.; Ahmad, W.; Andleeb, S.; Jalil, F.; Imran, M.; Nawaz, M. A.; Hussain, T.; Ali, M.; Rafiq, M.; Kamil, M. A., Bacterial biofilm and associated infections. *Journal of the Chinese Medical Association* **2018,** *81* (1), 7-11.

14. Reed, D.; Kemmerly, S. A., Infection control and prevention: a review of hospital-acquired infections and the economic implications. *The Ochsner journal* **2009,** *9* (1), 27-31.

15. Klevens, R. M.; Edwards, J. R.; Richards, C. L.; Horan, T. C.; Gaynes, R. P.; Pollock, D. A.; Cardo, D. M., Estimating Health Care-Associated Infections and Deaths in U.S. Hospitals, 2002. *Public Health Reports* **2007,** *122* (2), 160-166.

16. Bryers, J. D., Medical biofilms. *Biotechnology and bioengineering* **2008,** *100* (1), 1-18.

17. Galié, S.; García-Gutiérrez, C.; Miguélez, E. M.; Villar, C. J.; Lombó, F., Biofilms in the Food Industry: Health Aspects and Control Methods. *Frontiers in microbiology* **2018,** *9*, 898-898.

18. Murthy, P. S.; Venkatesan, R., Industrial Biofilms and their Control. In *Marine and Industrial Biofouling*, Flemming, H.-C.; Murthy, P. S.; Venkatesan, R.; Cooksey, K., Eds. Springer Berlin Heidelberg: Berlin, Heidelberg, 2009; pp 65-101.

19. Yousra, T.; Mehri, I.; Lajnef, R.; Rejab, A. B.; Khessairi, A.; Cherif, H.; Ouzari, H.; Hassen, A., Biofilms in bioremediation and wastewater treatment: characterization of bacterial community structure and diversity during seasons in municipal wastewater treatment process. *Environmental Science and Pollution Research* **2017,** *24* (4), 3519-3530.

20. McCarty, N. S.; Ledesma-Amaro, R., Synthetic Biology Tools to Engineer Microbial Communities for Biotechnology. *Trends Biotechnol* **2019,** *37* (2), 181-197.

21. Chang, M. C.; Keasling, J. D., Production of isoprenoid pharmaceuticals by engineered microbes. *Nat Chem Biol* **2006,** *2* (12), 674-81.

22. Zhou, K.; Qiao, K.; Edgar, S.; Stephanopoulos, G., Distributing a metabolic pathway among a microbial consortium enhances production of natural products. *Nature biotechnology* **2015,** *33* (4), 377-83.

23. Zhou, K.; Qiao, K.; Edgar, S.; Stephanopoulos, G., Distributing a metabolic pathway

among a microbial consortium enhances production of natural products. *Nature biotechnology* **2015,** *33* (4), 377-383.

24. O'Toole, G.; Kaplan, H. B.; Kolter, R., Biofilm formation as microbial development. *Annu Rev Microbiol* **2000,** *54*, 49-79.

25. Dunne, W. M., Jr., Bacterial adhesion: seen any good biofilms lately? *Clinical microbiology reviews* **2002,** *15* (2), 155-166.

26. Banin, E.; Vasil, M. L.; Greenberg, E. P., Iron and Pseudomonas aeruginosa biofilm formation. *Proc Natl Acad Sci U S A* **2005,** *102* (31), 11076-81.

27. Wu, Y.; Outten, F. W., IscR controls iron-dependent biofilm formation in Escherichia coli by regulating type I fimbria expression. *J Bacteriol* **2009,** *191* (4), 1248-1257.

28. Mattick, J. S., Type IV Pili and Twitching Motility. **2002,** *56* (1), 289-314.

29. O'Toole, G.; Kaplan, H. B.; Kolter, R., Biofilm Formation as Microbial Development. **2000,** *54* (1), 49-79.

30. O'Toole, G. A.; Kolter, R., Flagellar and twitching motility are necessary for Pseudomonas aeruginosa biofilm development. *Mol Microbiol* **1998,** *30* (2), 295-304.

31. Gerke, C.; Kraft, A.; Sussmuth, R.; Schweitzer, O.; Gotz, F., Characterization of the N-acetylglucosaminyltransferase activity involved in the biosynthesis of the Staphylococcus epidermidis polysaccharide intercellular adhesin. *J Biol Chem* **1998,** *273* (29), 18586-93.

32. Huang, R.; Li, M.; Gregory, R. L., Bacterial interactions in dental biofilm. *Virulence* **2011,** *2* (5), 435-444.

33. P. Stoodley; K. Sauer; D. G. Davies; Costerton, J. W., Biofilms as Complex Differentiated Communities. **2002,** *56* (1), 187-209.

34. Kostakioti, M.; Hadjifrangiskou, M.; Hultgren, S. J., Bacterial biofilms: development, dispersal, and therapeutic strategies in the dawn of the postantibiotic era. *Cold Spring Harb Perspect Med* **2013,** *3* (4), a010306.

35. Beloin, C.; Roux, A.; Ghigo, J. M., Escherichia coli biofilms. *Current topics in microbiology and immunology* **2008,** *322*, 249-289.

36. Hunt, S. M.; Werner, E. M.; Huang, B.; Hamilton, M. A.; Stewart, P. S., Hypothesis

for the role of nutrient starvation in biofilm detachment. *Applied and environmental microbiology* **2004,** *70* (12), 7418-7425.

37. Santin, G. C.; Oliveira, D. S. B.; Galo, R.; Borsatto, M. C.; Corona, S. A. M., Antimicrobial photodynamic therapy and dental plaque: a systematic review of the literature. *TheScientificWorldJournal* **2014,** *2014*, 824538-824538.

38. SOCRANSKY, S. S.; HAFFAJEE, A. D., Dental biofilms: difficult therapeutic targets. **2002,** *28* (1), 12-55.

39. Elasri, M. O.; Miller, R. V., Study of the response of a biofilm bacterial community to UV radiation. *Applied and environmental microbiology* **1999,** *65* (5), 2025-2031.

40. Algburi, A.; Comito, N.; Kashtanov, D.; Dicks, L. M. T.; Chikindas, M. L., Control of Biofilm Formation: Antibiotics and Beyond. *Applied and environmental microbiology* **2017,** *83* (3), e02508-16.

41. Liu, Y.; Tay, J. H., The essential role of hydrodynamic shear force in the formation of biofilm and granular sludge. *Water research* **2002,** *36* (7), 1653-65.

42. Stoodley, P.; Jacobsen, A.; Dunsmore, B. C.; Purevdorj, B.; Wilson, S.; Lappin-Scott, H. M.; Costerton, J. W., The influence of fluid shear and AICI3 on the material properties of Pseudomonas aeruginosa PAO1 and Desulfovibrio sp. EX265 biofilms. *Water science and technology : a journal of the International Association on Water Pollution Research* **2001,** *43* (6), 113-20.

43. Nealson, K. H.; Platt, T.; Hastings, J. W., Cellular control of the synthesis and activity of the bacterial luminescent system. *Journal of bacteriology* **1970,** *104* (1), 313-322.

44. Li, Y. H.; Tian, X., Quorum sensing and bacterial social interactions in biofilms. *Sensors (Basel)* **2012,** *12* (3), 2519-38.

45. Xavier, J. B., Social interaction in synthetic and natural microbial communities. *Mol Syst Biol* **2011,** *7*, 483.

46. Berlanga, M.; Guerrero, R., Living together in biofilms: the microbial cell factory and its biotechnological implications. *Microb Cell Fact* **2016,** *15* (1), 165-165.

47. Li, Z.; Nair, S. K., Quorum sensing: how bacteria can coordinate activity and

synchronize their response to external signals? *Protein science : a publication of the Protein Society* **2012,** *21* (10), 1403-1417.

48. Ng, W.-L.; Bassler, B. L., Bacterial quorum-sensing network architectures. *Annual review of genetics* **2009,** *43*, 197-222.

49. Blanchard, A. E.; Lu, T., Bacterial social interactions drive the emergence of differential spatial colony structures. *BMC Syst Biol* **2015,** *9*, 59.

50. D'Souza, G.; Shitut, S.; Preussger, D.; Yousif, G.; Waschina, S.; Kost, C., Ecology and evolution of metabolic cross-feeding interactions in bacteria. *Natural Product Reports* **2018,** *35* (5), 455-488.

51. Faust, K.; Raes, J., Microbial interactions: from networks to models. *Nat Rev Microbiol* **2012,** *10* (8), 538-50.

52. Hibbing, M. E.; Fuqua, C.; Parsek, M. R.; Peterson, S. B., Bacterial competition: surviving and thriving in the microbial jungle. *Nat Rev Microbiol* **2010,** *8* (1), 15-25.

53. Kreth, J.; Merritt, J.; Shi, W. Y.; Qi, F. X., Competition and coexistence between Streptococcus mutans and Streptococcus sanguinis in the dental biofilm. *Journal of Bacteriology* **2005,** *187* (21), 7193-7203.

54. Moons, P.; Michiels, C. W.; Aertsen, A., Bacterial interactions in biofilms. *Critical Reviews in Microbiology* **2009,** *35* (3), 157-168.

55. Celiker, H.; Gore, J., Cellular cooperation: insights from microbes. *Trends Cell Biol* **2013,** *23* (1), 9-15.

56. Mee, M. T.; Collins, J. J.; Church, G. M.; Wang, H. H., Syntrophic exchange in synthetic microbial communities. *Proc Natl Acad Sci U S A* **2014,** *111* (20), E2149-56.

57. Ponomarova, O.; Patil, K. R., Metabolic interactions in microbial communities: untangling the Gordian knot. *Current Opinion in Microbiology* **2015,** *27*, 37-44.

58. Wintermute, E. H.; Silver, P. A., Emergent cooperation in microbial metabolism. *Mol Syst Biol* **2010,** *6*, 407.

59. Kim, H. J.; Boedicker, J. Q.; Choi, J. W.; Ismagilov, R. F., Defined spatial structure stabilizes a synthetic multispecies bacterial community. *Proc Natl Acad Sci U S A* **2008,** *105*

(47), 18188-93.

60. Rozen, D. E.; Philippe, N.; Arjan de Visser, J.; Lenski, R. E.; Schneider, D., Death and cannibalism in a seasonal environment facilitate bacterial coexistence. *Ecology letters* **2009,** *12* (1), 34-44.

61. Hillesland, K. L.; Stahl, D. A., Rapid evolution of stability and productivity at the origin of a microbial mutualism. *Proc Natl Acad Sci U S A* **2010,** *107* (5), 2124-9.

62. Shou, W.; Ram, S.; Vilar, J. M. G., Synthetic cooperation in engineered yeast populations. *Proceedings of the National Academy of Sciences* **2007,** *104* (6), 1877-1882.

63. Kim, H. J.; Boedicker, J. Q.; Choi, J. W.; Ismagilov, R. F., Defined spatial structure stabilizes a synthetic multispecies bacterial community. *Proceedings of the National Academy of Sciences* **2008,** *105* (47), 18188-18193.

64. Hol, F. J.; Galajda, P.; Nagy, K.; Woolthuis, R. G.; Dekker, C.; Keymer, J. E., Spatial structure facilitates cooperation in a social dilemma: empirical evidence from a bacterial community. *PLoS One* **2013,** *8* (10), e77042.

65. Allen, B.; Gore, J.; Nowak, M. A., Spatial dilemmas of diffusible public goods. *eLife* **2013,** *2*, e01169.

66. Agapakis, C. M.; Boyle, P. M.; Silver, P. A., Natural strategies for the spatial optimization of metabolism in synthetic biology. *Nature Chemical Biology* **2012,** *8*, 527.

67. Balagadde, F. K.; Song, H.; Ozaki, J.; Collins, C. H.; Barnet, M.; Arnold, F. H.; Quake, S. R.; You, L., A synthetic Escherichia coli predator-prey ecosystem. *Mol Syst Biol* **2008,** *4*, 187.

68. Hansen, S. K.; Rainey, P. B.; Haagensen, J. A. J.; Molin, S., Evolution of species interactions in a biofilm community. *Nature* **2007,** *445*, 533.

69. McCarty, N. S.; Ledesma-Amaro, R., Synthetic Biology Tools to Engineer Microbial Communities for Biotechnology. *Trends Biotechnol* **2019,** *37* (2), 181-197.

70. Blanchard, A. E.; Lu, T., Bacterial social interactions drive the emergence of differential spatial colony structures. *BMC systems biology* **2015,** *9*, 59-59.

71. Katsikogianni, M.; Missirlis, Y. F., Concise review of mechanisms of bacterial

adhesion to biomaterials and of techniques used in estimating bacteria-material interactions. *European cells & materials* **2004,** *8*, 37-57.

72. Renner, L. D.; Weibel, D. B., Physicochemical regulation of biofilm formation. *Mrs Bull* **2011,** *36* (5), 347-355.

73. Tuson, H. H.; Weibel, D. B., Bacteria-surface interactions. *Soft Matter* **2013,** *9* (18), 4368-4380.

74. Yuan, Y.; Hays, M. P.; Hardwidge, P. R.; Kim, J., Surface characteristics influencing bacterial adhesion to polymeric substrates. *Rsc Adv* **2017,** *7* (23), 14254-14261.

75. Grace, J. L.; Huang, J. X.; Cheah, S.-E.; Truong, N. P.; Cooper, M. A.; Li, J.; Davis, T. P.; Quinn, J. F.; Velkov, T.; Whittaker, M. R., Antibacterial Low Molecular Weight Cationic Polymers: Dissecting the Contribution of Hydrophobicity, Chain Length and Charge to Activity. *Rsc Adv* **2016,** *6* (19), 15469-15477.

76. Murata, H.; Koepsel, R. R.; Matyjaszewski, K.; Russell, A. J., Permanent, non-leaching antibacterial surfaces—2: How high density cationic surfaces kill bacterial cells. *Biomaterials* **2007,** *28* (32), 4870-4879.

77. Harkes, G.; Feijen, J.; Dankert, J., Adhesion of Escherichia coli on to a series of poly(methacrylates) differing in charge and hydrophobicity. *Biomaterials* **1991,** *12* (9), 853-860.

78. Halan, B.; Buehler, K.; Schmid, A., Biofilms as living catalysts in continuous chemical syntheses. *Trends in Biotechnology* **2012,** *30* (9), 453-465.

79. Berne, C.; Ellison, C. K.; Ducret, A.; Brun, Y. V., Bacterial adhesion at the single-cell level. *Nature Reviews Microbiology* **2018,** *16* (10), 616-627.

80. Absolom, D. R.; Lamberti, F. V.; Policova, Z.; Zingg, W.; van Oss, C. J.; Neumann, A. W., Surface thermodynamics of bacterial adhesion. *Appl Environ Microbiol* **1983,** *46* (1), 90-7.

81. Chung, K. K.; Schumacher, J. F.; Sampson, E. M.; Burne, R. A.; Antonelli, P. J.; Brennana, A. B., Impact of engineered surface microtopography on biofilm formation of Staphylococcus aureus. *Biointerphases* **2007,** *2* (2), 89-94.

82. Hsu, L. C.; Fang, J.; Borca-Tasciuc, D. A.; Worobo, R. W.; Moraru, C. I., Effect of micro- and nanoscale topography on the adhesion of bacterial cells to solid surfaces. *Appl Environ Microbiol* **2013,** *79* (8), 2703-12.

83. Friedlander, R. S.; Vlamakis, H.; Kim, P.; Khan, M.; Kolter, R.; Aizenberg, J., Bacterial flagella explore microscale hummocks and hollows to increase adhesion. *Proc Natl Acad Sci U S A* **2013,** *110* (14), 5624-9.

84. Feng, G.; Cheng, Y.; Wang, S. Y.; Hsu, L. C.; Feliz, Y.; Borca-Tasciuc, D. A.; Worobo, R. W.; Moraru, C. I., Alumina surfaces with nanoscale topography reduce attachment and biofilm formation by Escherichia coli and Listeria spp. *Biofouling* **2014,** *30* (10), 1253-68.

85. Cheng, Y.; Feng, G.; Moraru, C. I., Micro- and Nanotopography Sensitive Bacterial Attachment Mechanisms: A Review. *Frontiers in microbiology* **2019,** *10*, 191-191.

86. Perera-Costa, D.; Bruque, J. M.; González-Martín, M. L.; Gómez-García, A. C.; Vadillo-Rodríguez, V., Studying the Influence of Surface Topography on Bacterial Adhesion using Spatially Organized Microtopographic Surface Patterns. *Langmuir : the ACS journal of surfaces and colloids* **2014,** *30* (16), 4633-4641.

87. Hochbaum, A. I.; Aizenberg, J., Bacteria Pattern Spontaneously on Periodic Nanostructure Arrays. *Nano Letters* **2010,** *10* (9), 3717-3721.

88. Senaratne, W.; Andruzzi, L.; Ober, C. K., Self-assembled monolayers and polymer brushes in biotechnology: current applications and future perspectives. *Biomacromolecules* **2005,** *6* (5), 2427-48.

89. Berne, C.; Ducret, A.; Hardy, G. G.; Brun, Y. V., Adhesins Involved in Attachment to Abiotic Surfaces by Gram-Negative Bacteria. *Microbiology spectrum* **2015,** *3* (4), 10.1128/microbiolspec.MB-0018-2015.

90. Busscher, H. J.; Weerkamp, A. H., Specific and non-specific interactions in bacterial adhesion to solid substrata. *Fems Microbiol Rev* **1987,** *3* (2), 165-173.

91. Van Houdt, R.; Michiels, C. W., Role of bacterial cell surface structures in Escherichia coli biofilm formation. *Research in microbiology* **2005,** *156* (5-6), 626-33.

92. Krogfelt, K. A.; Bergmans, H.; Klemm, P., Direct evidence that the FimH protein is the mannose-specific adhesin of Escherichia coli type 1 fimbriae. *Infection and immunity* **1990,** *58* (6), 1995-8.

93. Lillington, J.; Geibel, S.; Waksman, G., Biogenesis and adhesion of type 1 and P pili. *Biochimica et biophysica acta* **2014,** *1840* (9), 2783-93.

94. Bouckaert, J.; Mackenzie, J.; De Paz, J. L.; Chipwaza, B.; Choudhury, D.; Zavialov, A.; Mannerstedt, K.; Anderson, J.; Piérard, D.; Wyns, L.; Seeberger, P. H.; Oscarson, S.; De Greve, H.; Knight, S. D., The affinity of the FimH fimbrial adhesin is receptor-driven and quasi-independent of Escherichia coli pathotypes. *Mol Microbiol* **2006,** *61* (6), 1556-1568.

95. Pieters, R. J., Intervention with bacterial adhesion by multivalent carbohydrates. *Medicinal research reviews* **2007,** *27* (6), 796-816.

96. Disney, M. D.; Seeberger, P. H., The Use of Carbohydrate Microarrays to Study Carbohydrate-Cell Interactions and to Detect Pathogens. *Chemistry & Biology* **2004,** *11* (12), 1701-1707.

97. Hsu, K.-L.; Mahal, L. K., A lectin microarray approach for the rapid analysis of bacterial glycans. *Nature Protocols* **2006,** *1*, 543.

98. Hsu, K.-L.; Pilobello, K. T.; Mahal, L. K., Analyzing the dynamic bacterial glycome with a lectin microarray approach. *Nature Chemical Biology* **2006,** *2* (3), 153-157.

99. Sankaran, S.; Kiren, M. C.; Jonkheijm, P., Incorporating Bacteria as a Living Component in Supramolecular Self-Assembled Monolayers through Dynamic Nanoscale Interactions. *ACS Nano* **2015,** *9* (4), 3579-86.

100. Elahipanah, S.; Radmanesh, P.; Luo, W.; O'Brien, P. J.; Rogozhnikov, D.; Yousaf, M. N., Rewiring Gram-Negative Bacteria Cell Surfaces with Bio-Orthogonal Chemistry via Liposome Fusion. *Bioconjugate Chem* **2016,** *27* (4), 1082-1089.

101. Weber, T.; Chandrasekaran, V.; Stamer, I.; Thygesen, M. B.; Terfort, A.; Lindhorst, T. K., Switching of Bacterial Adhesion to a Glycosylated Surface by Reversible Reorientation of the Carbohydrate Ligand. *Angewandte Chemie International Edition* **2014,** *53* (52), 14583-14586.

102. Weber, T.; Chandrasekaran, V.; Stamer, I.; Thygesen, M. B.; Terfort, A.; Lindhorst, T. K., Switching of Bacterial Adhesion to a Glycosylated Surface by Reversible Reorientation of the Carbohydrate Ligand. *Angew Chem Int Edit* **2014,** *53* (52), 14583-14586.

103. Weber, T.; Chandrasekaran, V.; Stamer, I.; Thygesen, M. B.; Terfort, A.; Lindhorst, T. K., Switching of bacterial adhesion to a glycosylated surface by reversible reorientation of the carbohydrate ligand. *Angew Chem Int Ed Engl* **2014,** *53* (52), 14583-6.

104. Sankaran, S.; van Weerd, J.; Voskuhl, J.; Karperien, M.; Jonkheijm, P., Photoresponsive Cucurbit[8]uril-Mediated Adhesion of Bacteria on Supported Lipid Bilayers. *Small* **2015,** *11* (46), 6187-96.

105. Voskuhl, J.; Sankaran, S.; Jonkheijm, P., Optical control over bioactive ligands at supramolecular surfaces. *Chem Commun (Camb)* **2014,** *50* (96), 15144-7.

106. Sankaran, S.; van Weerd, J.; Voskuhl, J.; Karperien, M.; Jonkheijm, P., Photoresponsive Cucurbit[8]uril-Mediated Adhesion of Bacteria on Supported Lipid Bilayers. *Small* **2015,** *11* (46), 6187-6196.

107. Nakanishi, J.; Kikuchi, Y.; Takarada, T.; Nakayama, H.; Yamaguchi, K.; Maeda, M., Photoactivation of a Substrate for Cell Adhesion under Standard Fluorescence Microscopes. *Journal of the American Chemical Society* **2004,** *126* (50), 16314-16315.

108. Rolli, C. G.; Nakayama, H.; Yamaguchi, K.; Spatz, J. P.; Kemkemer, R.; Nakanishi, J., Switchable adhesive substrates: Revealing geometry dependence in collective cell behavior. *Biomaterials* **2012,** *33* (8), 2409-2418.

109. Petersen, S.; Alonso, J. M.; Specht, A.; Duodu, P.; Goeldner, M.; del Campo, A., Phototriggering of Cell Adhesion by Caged Cyclic RGD Peptides. *Angewandte Chemie International Edition* **2008,** *47* (17), 3192-3195.

110. Jin, X. F.; Riedel-Kruse, I. H., Biofilm Lithography enables high-resolution cell patterning via optogenetic adhesin expression. *P Natl Acad Sci USA* **2018,** *115* (14), 3698-3703.

111. Huang, Y. J.; Xia, A. G.; Yang, G.; Jin, F., Bioprinting Living Biofilms through Optogenetic Manipulation. *Acs Synth Biol* **2018,** *7* (5), 1195-1200.

112. Yazdi, S.; Ardekani, A. M., Bacterial aggregation and biofilm formation in a vortical flow. *Biomicrofluidics* **2012,** *6* (4), 44114-44114.

113. van der Woude, M. W.; Henderson, I. R., Regulation and function of Ag43 (flu). *Annu Rev Microbiol* **2008,** *62*, 153-69.

114. Ulett, G. C.; Webb, R. I.; Schembri, M. A., Antigen-43-mediated autoaggregation impairs motility in Escherichia coli. *Microbiology (Reading, England)* **2006,** *152* (Pt 7), 2101-10.

115. Laganenka, L.; Colin, R.; Sourjik, V., Chemotaxis towards autoinducer 2 mediates autoaggregation in Escherichia coli. *Nat Commun* **2016,** *7*, 12984.

116. Woodward, D. E.; Tyson, R.; Myerscough, M. R.; Murray, J. D.; Budrene, E. O.; Berg, H. C., Spatio-temporal patterns generated by Salmonella typhimurium. *Biophys J* **1995,** *68* (5), 2181-2189.

117. Budrene, E. O.; Berg, H. C., Complex patterns formed by motile cells of Escherichia coli. *Nature* **1991,** *349* (6310), 630-633.

118. Budrene, E. O.; Berg, H. C., Dynamics of formation of symmetrical patterns by chemotactic bacteria. *Nature* **1995,** *376* (6535), 49-53.

119. Bernardi, A.; Jimenez-Barbero, J.; Casnati, A.; De Castro, C.; Darbre, T.; Fieschi, F.; Finne, J.; Funken, H.; Jaeger, K. E.; Lahmann, M.; Lindhorst, T. K.; Marradi, M.; Messner, P.; Molinaro, A.; Murphy, P. V.; Nativi, C.; Oscarson, S.; Penades, S.; Peri, F.; Pieters, R. J.; Renaudet, O.; Reymond, J. L.; Richichi, B.; Rojo, J.; Sansone, F.; Schaffer, C.; Turnbull, W. B.; Velasco-Torrijos, T.; Vidal, S.; Vincent, S.; Wennekes, T.; Zuilhof, H.; Imberty, A., Multivalent glycoconjugates as anti-pathogenic agents. *Chem Soc Rev* **2013,** *42* (11), 4709-4727.

120. Wei, T.; Tang, Z.; Yu, Q.; Chen, H., Smart Antibacterial Surfaces with Switchable Bacteria-Killing and Bacteria-Releasing Capabilities. *ACS Applied Materials & Interfaces* **2017,** *9* (43), 37511-37523.

121. Leire, E.; Amaral, S. P.; Louzao, I.; Winzer, K.; Alexander, C.; Fernandez-Megia, E.; Fernandez-Trillo, F., Dendrimer mediated clustering of bacteria: improved aggregation

and evaluation of bacterial response and viability. *Biomater Sci-Uk* **2016,** *4* (6), 998-1006.

122. Gupta, A.; Landis, R. F.; Rotello, V. M., Nanoparticle-Based Antimicrobials: Surface Functionality is Critical. *F1000Research* **2016,** *5*, F1000 Faculty Rev-364.

123. Schmidt, B.; Sankaran, S.; Stegemann, L.; Strassert, C. A.; Jonkheijm, P.; Voskuhl, J., Agglutination of bacteria using polyvalent nanoparticles of aggregation-induced emissive thiophthalonitrile dyes. *J Mater Chem B* **2016,** *4* (27), 4732-4738.

124. Disney, M. D.; Zheng, J.; Swager, T. M.; Seeberger, P. H., Detection of Bacteria with Carbohydrate-Functionalized Fluorescent Polymers. *Journal of the American Chemical Society* **2004,** *126* (41), 13343-13346.

125. Mintzer, M. A.; Dane, E. L.; O'Toole, G. A.; Grinstaff, M. W., Exploiting dendrimer multivalency to combat emerging and re-emerging infectious diseases. *Molecular pharmaceutics* **2012,** *9* (3), 342-354.

126. Lui, L. T.; Xue, X.; Sui, C.; Brown, A.; Pritchard, D. I.; Halliday, N.; Winzer, K.; Howdle, S. M.; Fernandez-Trillo, F.; Krasnogor, N.; Alexander, C., Bacteria clustering by polymers induces the expression of quorum-sensing-controlled phenotypes. *Nat Chem* **2013,** *5* (12), 1058-65.

127. Xue, X.; Pasparakis, G.; Halliday, N.; Winzer, K.; Howdle, S. M.; Cramphorn, C. J.; Cameron, N. R.; Gardner, P. M.; Davis, B. G.; Fernández-Trillo, F.; Alexander, C., Synthetic Polymers for Simultaneous Bacterial Sequestration and Quorum Sense Interference. *Angewandte Chemie International Edition* **2011,** *50* (42), 9852-9856.

128. Perez-Soto, N.; Creese, O.; Fernandez-Trillo, F.; Krachler, A. M., Aggregation of Vibrio cholerae by Cationic Polymers Enhances Quorum Sensing but Overrides Biofilm Dissipation in Response to Autoinduction. *ACS Chem Biol* **2018,** *13* (10), 3021-3029.

129. Almant, M.; Moreau, V.; Kovensky, J.; Bouckaert, J.; Gouin, S. G., Clustering of Escherichia coli Type-1 Fimbrial Adhesins by Using Multimeric Heptyl α-D-Mannoside Probes with a Carbohydrate Core. *Chemistry – A European Journal* **2011,** *17* (36), 10029-10038.

130. Pasparakis, G.; Cockayne, A.; Alexander, C., Control of bacterial aggregation by

thermoresponsive glycopolymers. *Journal of the American Chemical Society* **2007,** *129* (36), 11014-+.

131. Glass, D. S.; Riedel-Kruse, I. H., A Synthetic Bacterial Cell-Cell Adhesion Toolbox for Programming Multicellular Morphologies and Patterns. *Cell* **2018,** *174* (3), 649-658 e16.

132. Muhlhauser, W. W.; Fischer, A.; Weber, W.; Radziwill, G., Optogenetics - Bringing light into the darkness of mammalian signal transduction. *Biochimica et biophysica acta. Molecular cell research* **2017,** *1864* (2), 280-292.

133. Baaske, J.; Gonschorek, P.; Engesser, R.; Dominguez-Monedero, A.; Raute, K.; Fischbach, P.; Müller, K.; Cachat, E.; Schamel, W. W. A.; Minguet, S.; Davies, J. A.; Timmer, J.; Weber, W.; Zurbriggen, M. D., Dual-controlled optogenetic system for the rapid down-regulation of protein levels in mammalian cells. *Sci Rep-Uk* **2018,** *8* (1), 15024-15024.

134. Müller, K.; Weber, W., Optogenetic tools for mammalian systems. *Molecular bioSystems* **2013,** *9* (4), 596--608.

135. Tischer, D.; Weiner, O. D., Illuminating cell signalling with optogenetic tools. *Nature Reviews Molecular Cell Biology* **2014,** *15* (8), 551-558.

136. Deisseroth, K., Optogenetics. *Nat Methods* **2010,** *8*, 26.

137. Muller, K.; Weber, W., Optogenetic tools for mammalian systems. *Mol Biosyst* **2013,** *9* (4), 596-608.

138. Zoltowski, B. D.; Schwerdtfeger, C.; Widom, J.; Loros, J. J.; Bilwes, A. M.; Dunlap, J. C.; Crane, B. R., Conformational Switching in the Fungal Light Sensor Vivid. *Science* **2007,** *316* (5827), 1054-1057.

139. Zoltowski, B. D.; Vaccaro, B.; Crane, B. R., Mechanism-based tuning of a LOV domain photoreceptor. *Nat Chem Biol* **2009,** *5* (11), 827-34.

140. Pudasaini, A.; El-Arab, K. K.; Zoltowski, B. D., LOV-based optogenetic devices: light-driven modules to impart photoregulated control of cellular signaling. *Frontiers in molecular biosciences* **2015,** *2*, 18.

141. Lungu, O. I.; Hallett, R. A.; Choi, E. J.; Aiken, M. J.; Hahn, K. M.; Kuhlman, B., Designing photoswitchable peptides using the AsLOV2 domain. *Chem Biol* **2012,** *19* (4),

507-17.

142. Guntas, G.; Hallett, R. A.; Zimmerman, S. P.; Williams, T.; Yumerefendi, H.; Bear, J. E.; Kuhlman, B., Engineering an improved light-induced dimer (iLID) for controlling the localization and activity of signaling proteins. *Proc Natl Acad Sci U S A* **2015,** *112* (1), 112-7.

143. Kawano, F.; Suzuki, H.; Furuya, A.; Sato, M., Engineered pairs of distinct photoswitches for optogenetic control of cellular proteins. *Nat Commun* **2015,** *6*, 6256.

144. Nihongaki, Y.; Kawano, F.; Nakajima, T.; Sato, M., Photoactivatable CRISPR-Cas9 for optogenetic genome editing. *Nature biotechnology* **2015,** *33* (7), 755-60.

145. Kawano, F.; Okazaki, R.; Yazawa, M.; Sato, M., A photoactivatable Cre-loxP recombination system for optogenetic genome engineering. *Nat Chem Biol* **2016,** *12* (12), 1059-1064.

146. Nihongaki, Y.; Furuhata, Y.; Otabe, T.; Hasegawa, S.; Yoshimoto, K.; Sato, M., CRISPR–Cas9-based photoactivatable transcription systems to induce neuronal differentiation. *Nat Methods* **2017,** *14*, 963.

147. Furuya, A.; Kawano, F.; Nakajima, T.; Ueda, Y.; Sato, M., Assembly Domain-Based Optogenetic System for the Efficient Control of Cellular Signaling. *Acs Synth Biol* **2017,** *6* (6), 1086-1095.

148. Yu, G.; Onodera, H.; Aono, Y.; Kawano, F.; Ueda, Y.; Furuya, A.; Suzuki, H.; Sato, M., Optical manipulation of the alpha subunits of heterotrimeric G proteins using photoswitchable dimerization systems. *Sci Rep* **2016,** *6*, 35777.

149. Chervyachkova, E.; Wegner, S. V., Reversible Social Self-Sorting of Colloidal Cell-Mimics with Blue Light Switchable Proteins. *Acs Synth Biol* **2018,** *7* (7), 1817-1824.

150. Flemming, H. C.; Wingender, J.; Szewzyk, U.; Steinberg, P.; Rice, S. A.; Kjelleberg, S., Biofilms: an emergent form of bacterial life. *Nat Rev Microbiol* **2016,** *14* (9), 563-75.

151. Davies, D., Understanding biofilm resistance to antibacterial agents. *Nat Rev Drug Discov* **2003,** *2* (2), 114-22.

152. Stacy, A.; McNally, L.; Darch, S. E.; Brown, S. P.; Whiteley, M., The biogeography of polymicrobial infection. *Nat Rev Microbiol* **2016,** *14* (2), 93-105.

153. Nadell, C. D.; Drescher, K.; Foster, K. R., Spatial structure, cooperation and competition in biofilms. *Nat Rev Microbiol* **2016,** *14* (9), 589-600.

154. Epstein, A. K.; Wong, T.-S.; Belisle, R. A.; Boggs, E. M.; Aizenberg, J., Liquid-infused structured surfaces with exceptional anti-biofouling performance. *Proceedings of the National Academy of Sciences* **2012,** *109* (33), 13182-13187.

155. Tsoligkas, A. N.; Winn, M.; Bowen, J.; Overton, T. W.; Simmons, M. J. H.; Goss, R. J. M., Engineering Biofilms for Biocatalysis. *ChemBioChem* **2011,** *12* (9), 1391-1395.

156. Burlage, R. S.; Kuo, C. T., Living biosensors for the management and manipulation of microbial consortia. *Annu Rev Microbiol* **1994,** *48*, 291-309.

157. Iqbal, M.; Nazir, A.; Abbas, M.; Kanwal, Q.; Iqbal, D. N., Bioremediation: A Green, Sustainable and Eco-Friendly Technique for the Remediation of Pollutants. In *Advanced Materials for Wastewater Treatment*, John Wiley & Sons, Inc.: 2017; pp 263-311.

158. Jensen, H.; Biggs, C. A.; Karunakaran, E., The importance of sewer biofilms. **2016,** *3* (4), 487-494.

159. Terada, A.; Hibiya, K.; Nagai, J.; Tsuneda, S.; Hirata, A., Nitrogen removal characteristics and biofilm analysis of a membrane-aerated biofilm reactor applicable to high-strength nitrogenous wastewater treatment. *J Biosci Bioeng* **2003,** *95* (2), 170-8.

160. Volke, D. C.; Nikel, P. I., Getting Bacteria in Shape: Synthetic Morphology Approaches for the Design of Efficient Microbial Cell Factories. *Adv Biosyst* **2018,** *2* (11), 1800111.

161. Wang, X.; Zhu, H.; Yang, F.; Yang, X., Biofilm-Engineered Nanostructures. *Advanced Materials* **2009,** *21* (27), 2815-2818.

162. Xu, L.; Robert, L.; Ouyang, Q.; Taddei, F.; Chen, Y.; Lindner, A. B.; Baigl, D., Microcontact printing of living bacteria arrays with cellular resolution. *Nano Lett* **2007,** *7* (7), 2068-72.

163. Merrin, J.; Leibler, S.; Chuang, J. S., Printing multistrain bacterial patterns with a piezoelectric inkjet printer. *PLoS One* **2007,** *2* (7), e663.

164. Connell, J. L.; Ritschdorff, E. T.; Whiteley, M.; Shear, J. B., 3D printing of

microscopic bacterial communities. *Proc Natl Acad Sci U S A* **2013,** *110* (46), 18380-5.

165. Chen, F.; Wegner, S. V., Blue Light Switchable Bacterial Adhesion as a Key Step toward the Design of Biofilms. *Acs Synth Biol* **2017,** *6* (12), 2170-2174.

166. Huang, Y.; Xia, A.; Yang, G.; Jin, F., Bioprinting Living Biofilms through Optogenetic Manipulation. *ACS Synthetic Biology* **2018,** *7* (5), 1195-1200.

167. Jin, X.; Riedel-Kruse, I. H., Biofilm Lithography enables high-resolution cell patterning via optogenetic adhesin expression. **2018,** *115* (14), 3698-3703.

168. Voskuhl, J.; Sankaran, S.; Jonkheijm, P., Optical control over bioactive ligands at supramolecular surfaces. *Chem Commun* **2014,** *50* (96), 15144-15147.

169. Grabosch, C.; Kolbe, K.; Lindhorst, T. K., Glycoarrays by a New Tandem Noncovalent–Covalent Modification of Polystyrene Microtiter Plates and their Interrogation with Live Cells. *ChemBioChem* **2012,** *13* (13), 1874-1879.

170. Kau, A. L.; Hunstad, D. A.; Hultgren, S. J., Interaction of uropathogenic Escherichia coli with host uroepithelium. *Curr Opin Microbiol* **2005,** *8* (1), 54-9.

171. Liu, X.; Yuk, H.; Lin, S.; Parada, G. A.; Tang, T. C.; Tham, E.; de la Fuente-Nunez, C.; Lu, T. K.; Zhao, X., 3D Printing of Living Responsive Materials and Devices. *Adv Mater* **2018,** *30* (4).

172. Wegner, S. V.; Senturk, O. I.; Spatz, J. P., Photocleavable linker for the patterning of bioactive molecules. *Sci Rep* **2015,** *5*, 18309.

173. Schenk, F. C.; Boehm, H.; Spatz, J. P.; Wegner, S. V., Dual-functionalized nanostructured biointerfaces by click chemistry. *Langmuir* **2014,** *30* (23), 6897-905.

174. Schweighauser, L.; Wegner, H. A., Chemical Talking with Living Systems: Molecular Switches Steer Quorum Sensing in Bacteria. **2015,** *16* (12), 1709-1711.

175. Laganenka, L.; Colin, R.; Sourjik, V., Chemotaxis towards autoinducer 2 mediates autoaggregation in Escherichia coli. *Nature Communications* **2016,** *7*, 12984.

176. Liu, W.; Roder, H. L.; Madsen, J. S.; Bjarnsholt, T.; Sorensen, S. J.; Burmolle, M., Interspecific Bacterial Interactions are Reflected in Multispecies Biofilm Spatial Organization. *Front Microbiol* **2016,** *7*, 1366.

177. Zhou, M. H.; Wang, H. Y.; Hassett, D. J.; Gu, T. Y., Recent advances in microbial fuel cells (MFCs) and microbial electrolysis cells (MECs) for wastewater treatment, bioenergy and bioproducts. *J Chem Technol Biot* **2013,** *88* (4), 508-518.

178. Jensen, H.; Biggs, C. A.; Karunakaran, E., The importance of sewer biofilms. *Wires-Water* **2016,** *3* (4), 487-494.

179. Swartjes, J. J. T. M.; Das, T.; Sharifi, S.; Subbiahdoss, G.; Sharma, P. K.; Krom, B. P.; Busscher, H. J.; van der Mei, H. C., A Functional DNase I Coating to Prevent Adhesion of Bacteria and the Formation of Biofilm. *Advanced Functional Materials* **2013,** *23* (22), 2843-2849.

180. Mee, M. T.; Collins, J. J.; Church, G. M.; Wang, H. H., Syntrophic exchange in synthetic microbial communities. *Proceedings of the National Academy of Sciences of the United States of America* **2014,** *111* (20), E2149-E2156.

181. Song, H.; Ding, M. Z.; Jia, X. Q.; Ma, Q.; Yuan, Y. J., Synthetic microbial consortia: from systematic analysis to construction and applications. *Chemical Society Reviews* **2014,** *43* (20), 6954-6981.

182. Elahipanah, S.; Radmanesh, P.; Luo, W.; O'Brien, P. J.; Rogozhnikov, D.; Yousaf, M. N., Rewiring Gram-Negative Bacteria Cell Surfaces with Bio-Orthogonal Chemistry via Liposome Fusion. *Bioconjug Chem* **2016,** *27* (4), 1082-9.

183. Peschke, T.; Rabe, K. S.; Niemeyer, C. M., Orthogonal Surface Tags for Whole-Cell Biocatalysis. *Angewandte Chemie International Edition* **2017**.

184. Zhang, R.; Heyde, K. C.; Scott, F. Y.; Paek, S. H.; Ruder, W. C., Programming Surface Chemistry with Engineered Cells. *ACS Synth Biol* **2016,** *5* (9), 936-41.

185. Rozhok, S.; Shen, C. K.; Littler, P. L.; Fan, Z.; Liu, C.; Mirkin, C. A.; Holz, R. C., Methods for fabricating microarrays of motile bacteria. *Small* **2005,** *1* (4), 445-51.

186. Poortinga, A. T.; Bos, R.; Busscher, H. J., Controlled electrophoretic deposition of bacteria to surfaces for the design of biofilms. *Biotechnol Bioeng* **2000,** *67* (1), 117-20.

187. Mockl, L.; Muller, A.; Brauchle, C.; Lindhorst, T. K., Switching first contact: photocontrol of E. coli adhesion to human cells. *Chem Commun (Camb)* **2016,** *52* (6), 1254-7.

188. Hu, Y.; Zou, W.; Julita, V.; Ramanathan, R.; Tabor, R. F.; Nixon-Luke, R.; Bryant, G.; Bansal, V.; Wilkinson, B. L., Photomodulation of bacterial growth and biofilm formation using carbohydrate-based surfactants. *Chem. Sci.* **2016,** *7* (11), 6628-6634.

189. Velema, W. A.; van der Berg, J. P.; Hansen, M. J.; Szymanski, W.; Driessen, A. J.; Feringa, B. L., Optical control of antibacterial activity. *Nat Chem* **2013,** *5* (11), 924-8.

190. Van der Berg, J. P.; Velema, W. A.; Szymanski, W.; Driessen, A. J. M.; Feringa, B. L., Controlling the activity of quorum sensing autoinducers with light. *Chem. Sci.* **2015,** *6* (6), 3593-3598.

191. Rice, J. J.; Daugherty, P. S., Directed evolution of a biterminal bacterial display scaffold enhances the display of diverse peptides. *Protein Eng Des Sel* **2008,** *21* (7), 435-42.

192. Hall-Stoodley, L.; Costerton, J. W.; Stoodley, P., Bacterial biofilms: from the natural environment to infectious diseases. *Nat Rev Microbiol* **2004,** *2* (2), 95-108.

193. Peschke, T.; Rabe, K. S.; Niemeyer, C. M., Orthogonal Surface Tags for Whole-Cell Biocatalysis. *Angewandte Chemie (International ed. in English)* **2017,** *56* (8), 2183-2186.

194. Brenner, K.; You, L.; Arnold, F. H., Engineering microbial consortia: a new frontier in synthetic biology. *Trends Biotechnol* **2008,** *26* (9), 483-9.

195. Wood, T. K.; Hong, S. H.; Ma, Q., Engineering biofilm formation and dispersal. *Trends Biotechnol* **2011,** *29* (2), 87-94.

196. Gao, M.; Zheng, H.; Ren, Y.; Lou, R.; Wu, F.; Yu, W.; Liu, X.; Ma, X., A crucial role for spatial distribution in bacterial quorum sensing. *Sci Rep* **2016,** *6*, 34695.

197. Mitri, S.; Foster, K. R., The genotypic view of social interactions in microbial communities. *Annu Rev Genet* **2013,** *47*, 247-73.

198. Song, H.; Payne, S.; Gray, M.; You, L., Spatiotemporal modulation of biodiversity in a synthetic chemical-mediated ecosystem. *Nat Chem Biol* **2009,** *5* (12), 929-35.

199. Liu, C.; Fu, X.; Liu, L.; Ren, X.; Chau, C. K.; Li, S.; Xiang, L.; Zeng, H.; Chen, G.; Tang, L. H.; Lenz, P.; Cui, X.; Huang, W.; Hwa, T.; Huang, J. D., Sequential establishment of stripe patterns in an expanding cell population. *Science* **2011,** *334* (6053), 238-41.

200. Pasparakis, G.; Cockayne, A.; Alexander, C., Control of bacterial aggregation by thermoresponsive glycopolymers. *J Am Chem Soc* **2007,** *129* (36), 11014-5.

201. Sankaran, S.; Zhao, S.; Muth, C.; Paez, J.; Del Campo, A., Toward Light-Regulated Living Biomaterials. *Adv Sci (Weinh)* **2018,** *5* (8), 1800383.

202. Au - Jin, X.; Au - Riedel-Kruse, I. H., High-resolution Patterned Biofilm Deposition Using pDawn-Ag43. *JoVE* **2018,** (140), e58625.

203. Sankaran, S.; del Campo, A., Optoregulated Protein Release from an Engineered Living Material. *Advanced Biosystems* **2019,** *3* (2), 1800312.

204. Chen, F.; Ricken, J.; Xu, D.; Wegner, S. V., Bacterial Photolithography: Patterning Escherichia coli Biofilms with High Spatial Control Using Photocleavable Adhesion Molecules. *Advanced Biosystems* **2019,** *3* (3), 1800269.

205. Mukherjee, M.; Hu, Y.; Tan, C. H.; Rice, S. A.; Cao, B., Engineering a light-responsive, quorum quenching biofilm to mitigate biofouling on water purification membranes. *Science Advances* **2018,** *4* (12), eaau1459.

206. Benedetti, L.; Barentine, A. E. S.; Messa, M.; Wheeler, H.; Bewersdorf, J.; De Camilli, P., Light-activated protein interaction with high spatial subcellular confinement. *Proc Natl Acad Sci U S A* **2018,** *115* (10), E2238-E2245.

207. Whiteley, M.; Diggle, S. P.; Greenberg, E. P., Progress in and promise of bacterial quorum sensing research. *Nature* **2017,** *551* (7680), 313-320.

208. Connell, J. L.; Kim, J.; Shear, J. B.; Bard, A. J.; Whiteley, M., Real-time monitoring of quorum sensing in 3D-printed bacterial aggregates using scanning electrochemical microscopy. *P Natl Acad Sci USA* **2014,** *111* (51), 18255-18260.

209. Seth, E. C.; Taga, M. E., Nutrient cross-feeding in the microbial world. *Front Microbiol* **2014,** *5*, 350.

210. Ponomarova, O.; Patil, K. R., Metabolic interactions in microbial communities: untangling the Gordian knot. *Curr Opin Microbiol* **2015,** *27*, 37-44.

211. Kreis, C. T.; Le Blay, M.; Linne, C.; Makowski, M. M.; Baumchen, O., Adhesion of Chlamydomonas microalgae to surfaces is switchable by light. *Nat Phys* **2018,** *14* (1), 45-49.

212. Purcell, E. B.; Siegal-Gaskins, D.; Rawling, D. C.; Fiebig, A.; Crosson, S., A photosensory two-component system regulates bacterial cell attachment. *Proceedings of the National Academy of Sciences* **2007,** *104* (46), 18241.

213. Iwasaki, T.; Fukazawa, R.; Miyajima-Nakano, Y.; Baldansuren, A.; Matsushita, S.; Lin, M. T.; Gennis, R. B.; Hasegawa, K.; Kumasaka, T.; Dikanov, S. A., Dissection of hydrogen bond interaction network around an iron-sulfur cluster by site-specific isotope labeling of hyperthermophilic archaeal Rieske-type ferredoxin. *J Am Chem Soc* **2012,** *134* (48), 19731-8.

Appendix

Nucleotide and amino acid sequences of optogenetic proteins

nMagHigh

Nucleotide sequence:

ATGCACACACTATATGCTCCCGGAGGGTATGATATAATGGGATACCTAGATCAAATA
GGCAACCGTCCGAACCCGCAAGTGGAGCTGGGCCCGGTGGACACCAGCTGCGCG
CTGATCCTGTGCGACCTGAAGCAGAAAGATACCCCGATTGTGTACGCGAGCGAGG
CGTTCCTGTACATGACCGGTTATAGCAACGCGGAAGTTCTGGGCCGTAACTGCCGT
TTTCTGCAAAGCCCGGATGGTATGGTGAAGCCGAAAAGCACCCGTAAGTATGTTG
ACAGCAACACCATCAACACCATTCGTAAAGCGATCGATCGTAACGCGGAAGTGCA
GGTTGAAGTGGTTAACTTCAAGAAAAACGGCCAACGTTTCGTGAACTTTCTGACC
ATCATTCCGGTTCGTGATGAGACCGGCGAATATCGTTATAGCATGGGTTTTCAATGC
GAGACCGAAGGCGGTAGC

Amino acid sequence:

MHTLYAPGGYDIMGYLDQIGNRPNPQVELGPVDTSCALILCDLKQKDTPIVYASEAFL
YMTGYSNAEVLGRNCRFLQSPDGMVKPKSTRKYVDSNTINTIRKAIDRNAEVQVEV
VNFKKNGQRFVNFLTIIPVRDETGEYRYSMGFQCETEGGS-

pMagHigh

Nucleotide sequence:

ATGCACACACTATATGCTCCCGGAGGGTATGATATAATGGGATACCTACGTCAAATA
CGCAACCGTCCGAACCCGCAAGTGGAGCTGGGCCCGGTGGACACCAGCTGCGCG
CTGATCCTGTGCGACCTGAAGCAGAAAGATACCCCGATTGTGTACGCGAGCGAGG
CGTTCCTGTACATGACCGGTTATAGCAACGCGGAAGTTCTGGGCCGTAACTGCCGT

TTTCTGCAAAGCCCGGATGGTATGGTGAAGCCGAAAAGCACCCGTAAGTATGTTG
ACAGCAACACCATCAACACCATTCGTAAAGCGATCGATCGTAACGCGGAAGTGCA
GGTTGAAGTGGTTAACTTCAAGAAAAACGGCCAACGTTTCGTGAACTTTCTGACC
ATCATTCCGGTTCGTGATGAGACCGGCGAATATCGTTATAGCATGGGTTTTCAATGC
GAGACCGAAGGCGGTAGC

Amino acid sequence:

MHTLYAPGGYDIMGYLRQIRNRPNPQVELGPVDTSCALILCDLKQKDTPIVYASEAFL
YMTGYSNAEVLGRNCRFLQSPDGMVKPKSTRKYVDSNTINTIRKAIDRNAEVQVEV
VNFKKNGQRFVNFLTIIPVRDETGEYRYSMGFQCETEGGS-

pMag

Nucleotide sequence:

ATGCACACACTATATGCTCCCGGAGGGTATGATATAATGGGATACCTACGTCAAATA
CGCAACCGTCCGAACCCGCAAGTGGAGCTGGGCCCGGTGGACACCAGCTGCGCG
CTGATCCTGTGCGACCTGAAGCAGAAAGATACCCCGATTGTGTACGCGAGCGAGG
CGTTCCTGTACATGACCGGTTATAGCAACGCGGAAGTTCTGGGCCGTAACTGCCGT
TTTCTGCAAAGCCCGGATGGTATGGTGAAGCCGAAAAGCACCCGTAAGTATGTTG
ACAGCAACACCATCAACACCAGTCGTAAAGCGATCGATCGTAACGCGGAAGTGCA
GGTTGAAGTGGTTAACTTCAAGAAAAACGGCCAACGTTTCGTGAACTTTCTGACC
ATGATTCCGGTTCGTGATGAGACCGGCGAATATCGTTATAGCATGGGTTTTCAATGC
GAGACCGAAGGCGGTAGC

Amino acid sequence:

MHTLYAPGGYDIMGYLRQIRNRPNPQVELGPVDTSCALILCDLKQKDTPIVYASEAFL
YMTGYSNAEVLGRNCRFLQSPDGMVKPKSTRKYVDSNTINTSRKAIDRNAEVQVEV
VNFKKNGQRFVNFLTMIPVRDETGEYRYSMGFQCETEGGS-

pMagFast1

Nucleotide sequence:

ATGCACACACTATATGCTCCCGGAGGGTATGATATAATGGGATACCTACGTCAAATA
CGCAACCGTCCGAACCCGCAAGTGGAGCTGGGCCCGGTGGACACCAGCTGCGCG
CTGATCCTGTGCGACCTGAAGCAGAAAGATACCCCGGTTGTGTACGCGAGCGAGG
CGTTCCTGTACATGACCGGTTATAGCAACGCGGAAGTTCTGGGCCGTAACTGCCGT
TTTCTGCAAAGCCCGGATGGTATGGTGAAGCCGAAAAGCACCCGTAAGTATGTTG
ACAGCAACACCATCAACACCATGCGTAAAGCGATCGATCGTAACGCGGAAGTGCA
GGTTGAAGTGGTTAACTTCAAGAAAAACGGCCAACGTTTCGTGAACTTTCTGACC
ATGATTCCGGTTCGTGATGAGACCGGCGAATATCGTTATAGCATGGGTTTTCAATGC
GAGACCGAAGGCGGTAGC

Amino acid sequence:

MH T L Y A P G G Y D I Met G Y L R Q I R N R P N P Q V E L G P V D T S C A L I L C D
L K Q K D T P V V Y A S E A F L Y Met T G Y S N A E V L G R N C R F L Q S P D G Met
V K P K S T R K Y V D S N T I N T Met R K A I D R N A E V Q V E V V N F K K N G Q
R F V N F L T Met I P V R D E T G E Y R Y S Met G F Q C E T E G G S-